8-1-2012

Scorpion Phylogeography in the North American Aridlands

Matthew Ryan Graham
University of Nevada, Las Vegas, graham40@unlv.nevada.edu

SCORPION PHYLOGEOGRAPHY IN THE NORTH AMERICAN ARIDLANDS

by

Matthew Ryan Graham

Bachelor of Science
Marshall University
2004

Master of Science
Marshall University
2007

A dissertation submitted in partial fulfillment of
the requirements for the

Doctor of Philosophy in Biological Sciences

School of Life Sciences
College of Sciences
The Graduate College

University of Nevada, Las Vegas
August 2012

THE GRADUATE COLLEGE

We recommend the thesis prepared under our supervision by

Matthew R. Graham

entitled

Scorpion Phylogeography in the North American Aridlands

be accepted in partial fulfillment of the requirements for the degree of

Doctor of Philosophy in Biological Sciences
School of Life Sciences

Brett Riddle, Ph.D., Committee Co-Chair

Jef Jaeger, Ph.D., Committee Co-Chair

Allen Gibbs, Ph.D., Committee Member

Matthew Lachniet, Ph.D., Graduate College Representative

Tom Piechota, Ph.D., Interim Vice President for Research &
Dean of the Graduate College

August 2012

ABSTRACT

Scorpion Phylogeography in the North American Aridlands

by

Matthew Ryan Graham

Dr. Brett R. Riddle, Examination Committee Co-Chair
Professor
University of Nevada, Las Vegas

Dr. Jef R. Jaeger, Examination Committee Co-Chair
Research Assistant Professor
University of Nevada, Las Vegas

Understanding the geographic, geologic, and climatic forces responsible for generating current patterns of biodiversity has been a central objective of phylogeography. To develop a better understanding of these processes in the North American aridlands, I used DNA sequence data and species distribution modeling to conduct three phylogeographic assessments incorporating four species of arid-adapted scorpions: *Hadrurus arizonensis*, *H. jedediah*, *H. spadix*, and *Paruroctonus becki*. In an assessment of *H. arizonensis,* phylogeographic patterns indicate that Pleistocene climate cycles and associated glacial refugia played a central role in structuring the genetic diversity of this species in the Mojave and Sonoran deserts, mostly supporting predictions from a recent model of historical biotic assembly for these regions. However, the phylogeography of *H. arizonensis* also revealed a potential glacial refugium along the Lower Colorado River Valley that had not been considered in

previous evaluations. To assess the impact that Pleistocene climate fluctuations had in other North American aridlands, I then compared phylogeographic patterns from *H. jedediah* and *H. spadix*, to those from *H. arizonensis*. Since these three species are closely related and morphologically similar, effects from phylogenetic signal and divergent phenotypes should have been minimal, so differences in phylogeographic patterns should reflect the relative influence of Pleistocene climates in different regions. Under this assumption, comparative phylogeography of these three species suggest that the impact of glacial climates was most pronounced for the biotas of the Great Basin and Snake River Plain, over those in the Colorado Plateau, and Mohave and Sonoran deserts. Finally, I conducted a phylogeography of *P. becki*, an unrelated species that spans the Mojave Desert and western Great Basin. Phylogenetic analyses identified five mitochondrial lineages in *P. becki*. The timing and geographic arrangement of these lineages supports a vicariant origin associated with the tectonically dynamic Eastern California Shear Zone. In association with these deeper patterns, demographic analyses indicated that a lineage in the Great Basin had undergone a recent post-glacial expansion, which according to predictions from climate-based models and a landscape interpolation of genetic distances, probably occurred from refugial areas in the northwest Great Basin. In general, phylogeographic assessments of North American aridland scorpions support phylogeographic inferences from co-distributed organisms, but add a novel glacial refugium in the Mojave Desert and a unique pattern of post-glacial expansions from an area within the Great Basin.

ACKNOWLEDGEMENTS

First, I thank my wife, Jessica Graham, for her continuous support of my sometimes crazy ambitions. Jessica and I have shared many grand adventures together and I look forward to many more; it is fun to be married to someone I also consider my best friend. I owe colossal thanks my parents, George and Penny Graham, who have been incredibly supportive, to the point that they accompanied me on numerous collecting trips in often harsh and downright miserable desert conditions. The following people deserve thanks for their willingness to stumble through the desert under the haze of purple lights in search of venomous arachnids: Joshua Ingoldt, Melinda Graham, Stephen Parks, Jef Jaeger, Tereza Jezkova, Michael Webber, Joshua Greenwood, Rebeca Rivera, Mallory Eckstut, Adam Leland, and Ryan Valverde.

I thank Tereza Jezkova, my friend and unofficial mentor, for always being there to help in any way possible, even though it usually came with a good dose of sarcasm. I thank Michael Webber for her dedication to helping others and for being a great friend, despite claiming to hate systematics (we all know that she really loves it). I owe thanks to Robert Bryson Jr. for his encouragement and motivation, and for showing me how to "kick ass and take names". Victor Fet, Rich Ayrey, Robert Bryson Jr., and Michael Wall kindly donated specimens. I thank Viktória Oláh-Hemmings for teaching me valuable skills in the lab, for help with analyses, and for showing the rest of us how to stay organized. Lisa Hancock kindly assisted with georeferencing. Victor Fet deserves many thanks for his guidance over the years and for his enthusiasm towards anything related

to scorpions; he is a constant reminder that science should be fun and rewarding. Michael Wall at SDNHM and Vince Lee, Anthea Carmichael, Stan Williams, and Charles Griswold at CAS provided assistance accessing museum collections. Lorenzo Prendini graciously provided important specimens and encouragement.

I am grateful to everyone who has served on my advisory committee: Jef Jaeger, Brett Riddle, Matthew Lachniet, Allen Gibbs, Victor Fet, and Kathy Longshore. In particular, I thank Jef Jaeger and Brett Riddle for serving as my co-chairs and for their enormous contributions to my development as a scientist. Brett has been a constant role model and source of inspiration. His success is no doubt linked to his affable personality, enthusiasm for science, and his ability to completely change your scientific perceptions with a single sentence. I owe thanks to Jef for putting up with me over the years, for his good humor, support in and out of academia, and for showing me by example that you can achieve great things if you are willing to quit whining and do the work. Samples collected from Death Valley National Park were collected under permits issued by the National Park Service. A portion of this research was conducted under a task agreement with the National Park Service (J8R07080009) administered through the Great Basin Cooperative Ecosystem Studies Unit.

TABLE OF CONTENTS

LIST OF TABLES

LIST OF FIGURES

CHAPTER 1

INTRODUCTION

Over two decades ago, John Avise and others introduced a field known as 'phylogeography'. At the time, the principle aim of phylogeography was to better understand micro- and macro-evolutionary processes by forming a bridge between phylogenetics and population genetics. The field of phylogeography has since flourished, and is now largely integrative, with the focus progressing toward comparisons of phylogeographic patterns among multiple taxa. In the next three chapters, I use phylogeography to study the evolutionary history of four species of scorpions distributed throughout the North American aridlands.

I begin in Chapter 2 with a fine-scale phylogeographic analysis of the largest and perhaps most renowned scorpion in North America, the Arizona hairy scorpion (*Hadrurus arizonensis* Ewing). This species occurs in low to mid-elevation habitats throughout the Mojave and Sonoran deserts where it is often abundant, particularly in sandy habitats like desert washes. By collecting several hundred specimens throughout the range of *H. arizonensis*, I conducted a comprehensive genetic assessment of this scorpion species. Analysis of mitochondrial sequence data, along with species distribution modeling, suggest that glacial climates caused *H. arizonensis* to fragment into at least six refugia, from which populations expanded as climates warmed following the last glacial maximum. Of these refugia, an area along the northern portion of the Lower Colorado River appears be a novel refugium that had not been specifically considered in previous phylogeographic evaluations of co-distributed taxa.

In Chapter 3, I explored phylogeographic patterns in two additional *Hadrurus* species; the black hairy scorpion (*Hadrurus spadix* Stahnke) from the Colorado Plateau and a new species that my colleagues and I are currently describing from the Mojave and Great Basin deserts (*Hadrurus jedediah* Prendini et al. [in prep]). By comparing the phylogeographic patterns of these three species, I assessed the influence of Pleistocene climate fluctuations on scorpion populations from different North American aridlands. Since all three species are closely related and morphologically similar, I discuss the results under the assumption that differences among their phylogeographic patterns are not strongly influenced by phylogenetic signal or major differences in phenotypes. Genetic data, along with species distribution models, suggest that all three species were indeed influenced by glacial climates, highlighting the pervasive impact of historical climate change on the North American aridlands. However, scorpions in the Great Basin and Snake River Plain appear to have been most severely impacted. Like several co-distributed taxa, the phylogeography of *H. jedediah* suggest that it only recently colonized these northern regions from more stable areas in the south, probably as climates warmed following the last glacial maximum. Therefore, in relation to nearby arid regions, the Great Basin and Snake River Plain biotas may have been the most sensitive to historical changes in climate.

In Chapter 4, I further explore the sensitivity of the Great Basin Desert by using mitochondrial and nuclear markers, as well as species distribution models, to reconstruct the phylogeography of the Beck desert scorpion, *Paruroctonus becki* (Gertsch and Allred). Although distantly related, the current distribution of *P. becki* is

similar to that of *H. jedediah,* occurring throughout the Mojave Desert and western sections of the Great Basin. Interestingly, I detected five geographically structured mitochondrial DNA lineages that closely correspond with the location and timing of Pliocene geologic events in the tectonically dynamic Eastern California Shear Zone. In addition, phylogeographic patterns suggest that a lineage in the western Great Basin colonized the region following the last glacial maximum, and may have endured glacial conditions in another previously undetected small refugium within the northwest Great Basin. Landscape interpolations of genetic distances suggest that *P. becki* may have expanded south and east from this glacial refugium, establishing a larger distribution in the Great Basin as climates warmed.

In summary, the phylogeography of four North American scorpions generally supports predictions made by similar assessments of co-distributed terrestrial organisms. I expand on the descriptions of glacial refugia for arid-adapted organisms in the Mojave Desert specifying an additional refugium along the northern reach of the Lower Colorado River Valley. I also identify an area within the Lahontan Trough of the northwestern Great Basin where one desert-adapted scorpion species appears to have persisted during glacial periods. Both regions are within basins known to have retained somewhat warmer conditions than surrounding regions during glacial periods, and should be incorporated into future models of biotic assembly in the Mojave Desert and Great Basin. Furthermore, phylogeographic patterns from scorpions underscore the instability of the northernmost aridlands, as organisms in the Great Basin and Snake River Plain appear be particularly sensitive to climate change.

CHAPTER 2

PHYLOGEOGRAPHY OF THE ARIZONA HAIRY SCORPION (*HADRURUS ARIZONENSIS*) SUPPORTS A MODEL OF BIOTIC ASSEMBLY IN THE MOJAVE DESERT AND ADDS A NEW PLEISTOCENE REFUGIUM

Abstract

With increasing phylogeographic data from North American deserts, multi-taxon biogeographic syntheses of individual desert regions are beginning to emerge. One such synthesis, which I call the 'Mojave Assembly Model', compares phylogeographic patterns from predominantly vertebrate taxa to provide a preliminary model for the assembly of the Mojave Desert biota. Here, I tested predictions made by the Mojave Assembly Model by examining the phylogeographic history of *Hadrurus arizonensis*, a notably large scorpion distributed throughout the Mojave and Sonoran deserts. I reconstructed the maternal history of *H. arizonensis* using mitochondrial sequence data and used occurrence records to generate climate-based species distribution models. Phylogenetic and structure analyses revealed a maternal genealogy that splits basally into a southern clade along the coast of Sonora and a northern clade that includes a minimum of six geographic lineages (groups) throughout the northern Sonoran and the Mojave deserts. Molecular dating suggested that the two basal clades diverged between the late Pliocene and early Pleistocene, whereas lineages within each clade diverged between the middle and late Pleistocene. The timing and location of genetic differentiation, in combination with results from demographic analyses and species

distribution models, suggest that Pleistocene climate cycles and associated glacial refugia played an important role in structuring genetic diversity within *H. arizonensis*. These results are generally consistent with predictions of Pleistocene refugia from studies of vertebrates, but also reveal an area along the northern portion of the Lower Colorado River Valley that may have acted as an additional refugium for arid-adapted taxa during Pleistocene glacial cycles.

Introduction

The deserts landscapes of southwestern North America were shaped by a complex history of landscape evolution through the Neogene due to tectonic activity associated with the junction of the Pacific and North American plate boundaries (e.g. Flesch et al. 2000). Species inhabiting these deserts through this time not only endured physical changes in the earth's surface, such as formation of basins and mountain ranges due to extensions of the lithosphere, but coped with repeated changes in climate, especially during the Pleistocene (Riddle and Hafner 2006). As a result, the biodiversity and endemism of the North American deserts is high in relation to other natural ecosystems in North America (Mittermeier et al. 2003), most likely elevated by vicariance and adaption in a topographically dynamic landscape.

Biogeographic studies of North American deserts indicate that many desert organisms exhibit similar histories associated with the evolution of regional deserts, and with new datasets continuing to emerge, our understanding of the histories of North American desert biotas continues to improve (Hafner and Riddle 2011). While many

early biogeographic studies focused on broad-scale, interspecific relationships within and between the North American deserts (e.g. Riddle & Honeycutt 1990; Riddle 1995), increasing phylogeographic information from multiple taxa provides prospects for addressing more intricate biogeographic histories within individual regions. Recently, Bell et al. (2010) conducted one such synthesis by comparing phylogeographic data from two species of *Xerospermophilus* Merriam (round-tailed ground squirrels) to similar studies of co-occurring taxa in the Mojave and Sonoran deserts. Their model (hereafter referred to as the 'Mojave Assembly Model') outlines a preliminary hypothesis for the historical assembly of the Mojave Desert biota (as well as part of the adjacent Sonoran Desert), which can be summarized as a history of geologically and climatically induced vicariant events between the late Neogene and Quaternary, followed by postglacial expansion and secondary contact (see Fig. 2.1 for a visual overview).

In short, the Mojave Assembly Model begins with diversification associated with the development of the Colorado River and an aquatic incursion of the Colorado and Gila rivers called the 'Bouse Formation' between the Late Miocene and early Pliocene (reviewed in Mulcahy et al. 2006). During the late Pliocene, orogenesis of the Sierra Nevada and Transverse ranges (Wakabayashi and Sawyer 2001; Jones et al. 2004; Warrick and Mertes 2009; but see Henry 2009 for a review of alternative geologic reconstructions), as well as uplift of the western Mojave Desert (Cox et al. 2003), may have then left some arid-adapted forms isolated in rain-shadowed basins where they diverged in allopatry. Climatic conditions during Pleistocene glacial periods are thought to have fragmented arid habitats even further, facilitating additional lineage formation

associated with isolated desert basins, drainages, and other isolated regions of suitable climate. Following the last glacial maximum (LGM), arid-adapted organisms then expanded their ranges out of the basins, with southern populations generally spreading northward.

Support for the Mojave Assembly Model comes mostly from phylogeographic studies of terrestrial vertebrate taxa, and with the exception of *Homalonychus* Marx spiders, patterns proposed by the model have not been adequately assessed with terrestrial invertebrates. Herein I contribute a detailed phylogeographic investigation of *Hadrurus arizonensis* Ewing, an arid-adapted scorpion distributed throughout low to mid elevations of the Mojave and Sonoran deserts. This scorpion is most common in sandy areas such as dune systems and washes (Williams, 1970) where it can construct elaborate burrows up to 2 meters in depth (Stahnke 1966; Anderson 1975). Also known as the Arizona hairy scorpion, *H. arizonensis* is the largest scorpion in North America (up to 127 mm in length). The species has considerable morphological variation, potentially indicative of geographic structuring of populations. Two formerly recognized subspecies: *H. arizonensis arizonensis* Ewing, *H. arizonensis pallidus* Williams and *H. arizonensis austrinus* Williams were synonymized when mitochondrial data did not support morphological interpretations (Fet et al. 2001).

Using mitochondrial sequence data from *H. arizonensis* samples collected from throughout its distribution for genetic assessment, my goal was to explore the phylogeography of *H. arizonensis*, with particular reference to the Mojave Assembly Model, but also including the species' distribution in the Sonoran Desert. In addition, I

used species distribution modeling (Elith and Leathwick 2009) to investigate changes in the distribution of climate suitable for *H. arizonensis* since the LGM (~21 Ka). If *H. arizonensis* was influenced by the events outlined by the Mojave Assembly Model, then I would expect this ground-dwelling invertebrate to yield phylogeographic patterns similar to those recovered from co-distributed vertebrate species. Furthermore, if climatic conditions during Pleistocene glacial periods caused *H. arizonensis* to fragment into allopatric refugia, as predicted by the Mojave Assembly Model, species distribution models should depict a fragmented distribution during the LGM and genetic data should reveal evidence of lineage formation in areas where climates remained suitable.

Materials and Methods

Sampling

I obtained 256 samples representing 84 unique localities from throughout the distribution of *H. arizonensis*. Representative voucher specimens have been preserved at the American Museum of Natural History (AMNH) and the San Diego Natural History Museum (SDNHM), with those collected from Death Valley National Park on a long-term loan to SDNHM. I pooled localities less than 10 km apart and without obvious intervening biogeographic barriers for analyses, resulting in 64 general sites (Fig. 2.2; Table 2.1). Phylogeography, as often currently practiced, incorporates elements of phylogenetics, population genetics, and demographic approaches (e.g. Althoff and Pellmyr 2002), and these methods require different sampling strategies. For phylogenetic analyses that did not require large sample sizes per site – the haplotype

network and Mantel test – I used all 256 individual samples. To calculate nucleotide diversity (π), haplotype diversity (h) and frequency of private haplotypes, I limited assessments to sites with sample sizes ≥ 8, resulting in 14 sites containing a total of 135 samples. In order to characterize population structure (SAMOVA, see below), I used sites with samples sizes ≥ 4 (27 sites), but in a separate assessment used only sites with sample sizes ≥ 8 (14 sites) to ensure that sample size did not produce substantially different results (see below).

For species distribution modeling, I used 267 occurrence points, representing the 84 unique sampling localities and 183 additional locations from georeferenced museum specimens (AMNH, SDNH, Smithsonian Institution, and California Academy of Sciences). I visually verified species designations of each museum specimen. The majority of museum records lacked coordinates, so I used GOOGLE EARTH (http://earth.google.com) to estimate latitude and longitude from information on voucher labels using standard georeferencing techniques. I excluded records with georeferencing errors greater than five kilometers so that the input records matched the spatial resolution of the modeling rasters (2.5 arc-minutes).

Molecular Techniques

I sequenced a 1029 base pair (bp) portion of the mitochondrial gene for cytochrome *c* oxidase subunit I (*cox1*), a marker that has been useful for phylogeographic assessments of insects (Zhang and Hewitt 1997) and arachnids (e.g. Prendini et al. 2003, 2005; Thomas and Hedin 2008; Wang et al. 2008, Graham et al.

2012). First, I isolated total genomic DNA from leg tissue using a standard phenol-chloroform extraction or DNeasy Extraction Kit (Qiagen Inc., Valencia, CA, USA). I then amplified the targeted gene by polymerase chain reaction using ExTaq Polymerase Premix (Takara Mirus Bio Inc., Madison, WI, USA) and different combinations of external primers listed in Table 2.2. All combinations of external primers successfully amplified sequences at annealing temperatures ranging between 54°C and 60°C. Since two regions of single nucleotide repeats (8-10 bp) caused signal strength at the 3' end to weaken, I used internal primers to verify nucleotide calls in regions with weak signal by sequencing within the region amplified by the external primers. I conducted cycle sequencing using BigDye Terminator Cycle Sequencing Ready Reaction Kit v. 3.1 (Qiagen Inc., Valencia, CA, USA). For electrophoresis and visualization, I used an ABI 3130 automated sequencer (Applied Biosystems Inc., Foster City, CA, USA). I aligned sequences using SEQUENCHER v. 4.6 (Gene Codes Corp Inc., Ann Arbor, MI, USA) and verified alignments against those of *Uroctonus mordax* Thorell (GenBank No. EU523756.1).

Phylogenetic Analyses and Population Structure

I assessed the *cox1* phylogeny of *H. arizonensis* under the criterion of bayesian inference (BI) implemented in MRBAYES v. 3.1.2 (Ronquist and Huelsenbeck 2003), conducting the analyses through the Cyberinfrastructure for Phylogenetic Research cluster (CIPRES Gateway v 3.1) at the San Diego Supercomputer Center. First, I used the program COLLAPSE v. 1.2 (available at http://darwin.uvigo.es) to remove redundant

haplotypes. I then calculated best-fit models of nucleotide substitution for the haplotype data under several codon partitioning schemes (separately, positions 1+2 combined and 3 separate, and unpartitioned) using JMODELTEST v. 0.1.1 and the Akaike information criterion (AIC; Posada 2008). For the BI runs, I unlinked model parameters across character partitions and left the Metropolis-coupled Markov Chain Monte Carlo (MCMC) on default (3 hot, 1 cold chain), except I set the heating parameter to 0.01 in order to keep state swap frequencies between 10% and 70%. I ran each partitioning scheme for 10 million generations, sampling trees every 1000 generations and discarding the first 25% as burn-in. All analyses were run twice, and after confirming that the duplicate Markov chains converged on similar mean likelihoods in TRACER v. 1.5 (Rambaut and Drummond 2007) and the program AWTY (Are We There Yet; Nylander et al. 2008), I inferred the best-fit partitioning scheme using bayes factors (Nylander et al. 2004). I based final interpretations on the 50% majority-rule consensus tree and associated posterior probabilities from the two runs of the best model.

Much of the structure in the resulting BI phylogeny was shallow (see Results), so I used the program NETWORK v. 4.5.1.6 (Fluxus Technology Ltd 2004) to construct median-joining networks of the mtDNA haplotypes (Bandelt et al. 1999). I first constructed preliminary networks and explored the effect of different transition/transversion weighting schemes (all assessments produced nearly identical topologies). I constructed a final network with transitions/transversions weighted 3 to 1 and used the maximum parsimony option to remove excessive links (Polzin and Daneshmand 2003).

To identify genetically distinct geographic groups without *a priori* groupings, I used SAMOVA v. 1.0 (Dupanloup et al. 2002) to conduct a spatial analysis of molecular variance (SAMOVA). Using 500 iterations for each run, I conducted assessments with partitions (*k* values) rising from 2 to 13 (the maximum number of groupings given the 14 sites) for the ≥ 8 dataset and 2 to 20 (the maximum number of groupings program will allow) for the ≥ 4 dataset. I evaluated trends in F_{CT}, a measure of the degree of differentiation between groups, to determine which number of partitions (*k* value) best represents groupings that are maximally differentiated and geographically homogenous. As the interpretation of SAMOVA may be affected by isolation by distance (Dupanloup et al. 2002), I used ALLELES IN SPACE v. 3.11 (Miller 2005) to perform a Mantel test (Mantel 1967) to evaluate correlation between geographic Euclidean distances and uncorrected *p*-distances (using 1000 randomizations).

Demographic History

I used ARLEQUIN v. 3.11 (Excoffier et al. 2005) to estimate several genetic indices for groups that were indicated by the BI tree, haplotype network, and SAMOVA. I estimated nucleotide diversity (π) and haplotype diversity (*h*), because in a comparative context these diversity indices can reveal patterns of past demographic expansion or constriction (Grant and Bowen 1998; see Results). I also calculated Fu's F (Fu 1997) and mismatch analyses (Rogers 1995) to test for demographic or spatial expansion within predefined groups.

I constructed Bayesian skyline plots, implemented in BEAST v. 1.5.4 (Drummond & Rambaut 2007) to estimate the shape of population growth through time for each group. This assessment required estimation of best-fit substitution models for each group (as above), followed by BEAST runs of 20 million generations for each group except one (group I; see Results), which required 2 independent runs of 60 million generations in order to reach an ESS greater than 200. Demographic plots were visualized using TRACER.

Molecular Dating

I used BEAST on a reduced dataset consisting of eight exemplar samples, selected to capture the deeper genetic structure within *H. arizonensis*, to estimate divergence dates between mtDNA groups. For this analysis, I estimated a best-fit substitution model for the unpartitioned sequences using JMODELTEST. I used an uncorrelated lognormal clock model and a mutation rate of 0.007 substitutions/site/million years, which was based on geological calibrations for the separation of island and mainland populations of a scorpion species (*Mesobuthus gibbosus* Brullé) from the Aegean region in the eastern Mediterranean (Gantenbein et al. 2005). I selected a standard deviation of 0.003, thereby encompassing an alternative mutation rate based on 16S rDNA in scorpions (Gantenbein and Largiadèr 2002) which is thought to evolve at a similar rate as *cox1* (Gantenbein et al. 2005; also see Chapter 4). I ran BEAST for 40 million generations with a Yule tree prior and retained samples every 1,000 generations. I again used Tracer to confirm stationarity of the MCMC chain, as

well as to determine the adequacy of the effective sample sizes (ESS > 200 for each estimated parameter).

Because the BEAST topology derived from the eight exemplar samples was different at the more recent nodes than that resulting from the BI analysis of the entire dataset (see Results), I also used BSPs to estimate time to most recent common ancestor (TMRCA) for the groups identified by SAMOVA. I again used TRACER to ensure stationarity and to obtain TMRCA estimates.

Species Distribution Models

I constructed species distribution models using the program MAXENT v. 3.3.2 (Phillips et al. 2006), known to perform well in comparisons with other modeling approaches (Elith et al. 2006). I screened 19 bioclimatic predictor layers representing current climatic trends, seasonality, and extremes of temperature and precipitation (Hijmans et al. 2005), to avoid over-fitting and improve model transferability (Peterson et al. 2007), by assessing correlations among the different layers based on values from grid cells containing occurrence records. I selected among the correlated layers (Pearson's correlation coefficient > 0.75), retaining layers representing quarter climates rather than monthly climates, and precipitation during the coldest quarter rather than precipitation during the wettest quarter. The final predictor layers comprised the following 10 bioclimatic layers: Bio2, mean diurnal range; Bio3, isothermality; Bio6, minimum temperature of the coldest month; Bio7, temperature annual range; Bio8, mean temperature of the wettest quarter; Bio10, mean temperature of warmest

quarter; Bio11, mean temperature of coldest quarter; Bio15, precipitation seasonality; Bio17, precipitation of the driest quarter; Bio18, precipitation of the warmest quarter; Bio19, precipitation of the coldest quarter. I masked (clipped) the bioclimatic layers to ecoregions (Olson et al. 2001) that contain occurrence records (Mojave Basin and Range, Sonoran Desert, Arizona/New Mexico Mountains, Sinaloa Coastal Plain, Baja Californian Desert) to improve model accuracy and reduce problems with extrapolation (Pearson et al. 2002; Thuiller et al. 2004; Randin et al. 2006),

I ran MAXENT using logistic output with default settings and random seeding. I tested the robustness of the models by cross-validation, dividing presence points into five groups and running five iterations while using a different group for each run. Thus, 20% of the presence points were used as test points and 80% were used for model training (Nogués-Bravo 2009). I relied on the default method available in MAXENT for determining the area under the receiver operating characteristic curve (AUC) to assess model performance.

I projected the models onto simulated climates for the LGM derived from the Community Climate System Model (CCSM; Otto-Bliesner et al. 2006) and the Model for Interdisciplinary Research on Climate (MIROC; Hasumi and Emori 2004) to explore the distribution of suitable habitat for *H. arizonensis* during glacial periods. Climatic suitability was displayed in ARCGIS by converting continuous MAXENT outputs into binary grids using the maximum training sensitivity plus specificity threshold. This threshold balances errors of omission (sensitivity) with the fraction of the study area predicted as suitable habitat, which is used as a proxy for commission error (specificity),

and has performed well in comparisons of various threshold criteria (Liu et al. 2005; Jiménez-Valverde 2007).

Results

Phylogenetic Analyses and Population Structure

The 256 *cox1* sequences obtained for *H. arizonensis* yielded 141 unique haplotypes containing 149 variable sites, 103 of which were parsimony-informative. Uncorrected *p*-distances ranged from 0.0% to 4.1%, with an average of 1.1%. Examination of chromatograms revealed no evidence of double peaks, indels, frameshifts, or premature stop codons that would indicate co-amplification of nuclear mitochondrial pseudogenes (Bertheau et al. 2011).

Bayes factors indicated that partitioning by each codon position provided the best fit, and substitution models selected under the AIC were as follows: first = HKY+G, second = HKY+G, third = HKY+I+G. The resulting majority-rule consensus tree exhibited two strongly supported deeper nodes (Fig. 2.3) that formed geographically cohesive clades – a northern clade representing the majority of the samples distributed throughout the northern half of the range, and a southern clade along the coast of Sonora. The uncorrected *p*-distances between samples within the southern clade ranged from 0.8% to 2.4%, with an average of 1.6%; and up to 2.5% in the northern clade, with an average of 1.1%. Average uncorrected *p*-distance between the northern and southern clades was 3.35%.Both clades contained considerable phylogeographic structure, with numerous subclades (groups) strongly supported within the northern

clade (identified as groups I – VI; Fig. 2.3). There was no statistical support for relationships between most groups, with the exception of groups II and III (Fig. 2.3).

The median-joining haplotype network (Fig. 2.4) revealed sub-networks, or groups, that mostly correspond to the clades and groups identified in the BI analyses. As in the BI analysis, the southern samples form a distinct group of haplotypes, separated from the large group of northern haplotypes by 19 mutational steps. Similarly, the southernmost sample is removed from the southern group by 17 steps. The remaining samples comprise the northern clade in the BI tree and are highly structured. The largest group within the northern clade (group I) occupies a central position within the haplotype network and is distributed across the center of the range, extending from the northern coast of the Gulf of California, north along the Lower Colorado River Valley to the northernmost sites in Nevada and Utah. Several long branches within this group were further labeled as groups A-D.

The SAMOVA results using different samples sizes yielded similar F_{CT} values and groupings, so for ease of presentation I limit results to the ≥ 4 dataset because it includes more sites and represents a more thorough geographic sampling. SAMOVA indicated a high degree of geographic structuring in the northern clade, as F_{CT} values continued to increase over the range of possible groups (Table 2.3). An asymptote was reached at about five groups (k = 5), which corroborated four of six groups identified within the northern clade in BI and network analyses (Fig. 2.5a). At k = 6, SAMOVA identified a group from north of the Gila River near Phoenix, AZ (Site 38 – Piute Valley, NV) that was strongly supported by both BI and network analyses (Fig. 2.5b). At k = 7, a

group in the western Anza-Borrego Desert region (Salton Trough) was identified, which was also supported by the haplotype network (Fig. 2.4 – group A), but the distinctiveness of this group was not supported by the BI analysis (Fig. 2.3).

The Mantel test revealed a correlation between geographic and genetic distances (Fig. 2.6; $r = 0.49$, $p > 0.01$), indicating the potential for isolation by distance (IBD). In the presence of IBD, SAMOVA results can be skewed, as they are expected to identify partitions that fall between the most widely spaced populations or the middle of the sampling areas (Dupanloup et al. 2002). Instead of conforming to a pattern expected under IBD, all groups identified partitions (as *k* increased until F_{CT} values reached an asymptote) representing geographically cohesive lineages supported by the BI and network analyses. Although one partition was identified near the middle of the sampling area (group III), all samples in the group are narrowly restricted to a small area along the Lower Colorado River Valley and represent a strongly supported monophyletic group.

Demographic History

Each of the groups within the northern clade contained π values ranging from 0.836 to 1.0 and values of *h* ranging from 0.002 to 0.007 (Table 2.4), although the larger values are influenced by a single site containing individuals from two different haplogroups (Site 38 – Surprise, AZ). All Fu's F values were negative (Table 2.4), indicating deviations from mutation-drift equilibrium, as would be expected for populations that have undergone recent expansion or selection (Fu 1997). Mismatch

distributions were unimodal for groups I–IV, indicating recent demographic expansion or selection (Rogers and Harpending 1992). Distribution curves were multimodal for groups V and VI, signifying that the populations may be at equilibrium, although sample sizes were low for both groups. Similarly, parametric bootstraps resulted in sum of squares deviations (SSD) that were all low, but many fold lower for groups I–IV. Raggedness values (r) were not significant for either the sudden expansion or spatial expansion mismatch models (Table 2.4), meaning the data are a good fit for either model of expansion.

For group I, a history of moderate population growth during the late Pleistocene was depicted by the BSP (Fig. 2.7). This growth apparently ceased about 100,000 thousand years ago when the population underwent a brief decline, followed by a period of rapid population growth and subsequent stability during the last 50 Ka. For all other groups, BSPs portray relatively stable population sizes through the late Pleistocene and Holocene.

Divergence Dating

Molecular dating (Fig. 2.8) estimated the divergence between the northern and southern clades to have occurred between the late Pliocene to mid Pleistocene (3.08--1.79 Ma), with a mean estimate at the start of the Pleistocene (2.44 Ma). Divergence within the southern clade is estimated to have occurred between the early (2.4 Ma) and mid (1.03 Ma) Pleistocene. The TMRCA for each group in the northern clade (Table 2.4) was estimated to be between the Pleistocene (1.43 Ma) and the Holocene (6 Ka).

Species Distribution Models

The species distribution models yielded high AUC scores for both training and testing data (both > 0.95), indicating that the models performed significantly better than random (Raes and ter Steege 2007). The species distribution model under current climatic conditions (Fig. 2.9a) depicted largely contiguous suitable climate across the majority of the Mojave Desert and northern portions of the Sonoran Desert. Unsuitable areas were predicted in the mountainous regions of the Mojave Desert. In the south, climate is predicted to be suitable in a narrow region along the Mexican coastlines of Sonora and Baja California. This model appears to somewhat underestimate the distribution of suitable areas in Sonora, as two occurrence records in Sonora fall outside of the predicted area.

LGM models based on different climatic scenarios (MIROC and CCSM) were similar (Figs. 2.10b, c), but incongruent along a northern portion of the Lower Colorado River Valley extending upriver to the mouth of the western Grand Canyon. Examination of multivariate similarity surfaces (MESS) show slightly negative values for both models in this region (Fig. 2.10), so the discrepancy could be due to 'novel' environments where at least one variable has a value that is outside the reference (current) range (Elith et al. 2010). An area of even lower (more negative) MESS values occurs along the northern Sonora coast in the CCSM models, mostly driven by a variable representing average diurnal temperature range (Bio2). The CCSM models also predicted suitable but highly

disjunct areas along the southern coast of Sonora and the northern coast of Baja California Sur, whereas the MIROC model does not.

Both models highlight a minimum of two general areas that may have contained suitable climate during the LGM, one in the western Mojave and one along the southern portion of the Colorado River. Although the degree of connectivity varied between models, both predicted suitable climate within low-elevation valleys of the western and northwestern Mojave Desert. In the CCSM model, fragmented areas with suitable climates were predicted within Saline, Death, and Panamint valleys; although these valleys were mostly filled in by Pleistocene lakes (Grayson 1993). In contrast, the MIROC model predicted larger areas of suitable climate in these regions, indicating that areas surrounding the Pleistocene lakes (which probably contained sandy habitat along shorelines) may have been suitable as well. Southern areas predicted by both LGM models were similar, but extended further south in the MIROC model. The LGM models both highlighted southern portions of the California Central Valley, an area currently occupied by the related species *Hadrurus obscurus* Williams.

Discussion

Phylogeography of *Hadrurus arizonensis*

Mitochondrial sequence data suggest that the phylogeography of *H. arizonensis* has been shaped by a history of fragmentation, reduced gene flow, and demographic expansion since the late Pliocene. My assessments of phylogenetic and population structure (Figs. 2.3, 2.4, and 2.5) all indicate that the species consists of two main clades;

a southern clade narrowly distributed along the coast of Sonora, Mexico, and a widespread northern clade comprising the remainder of the distribution in the Sonoran and Mojave deserts. Divergence between these two clades appears to have occurred between the mid Pliocene and early Pleistocene, a timeframe too recent to be explained by Neogene vicariant events such as the extensions of the Sea of Cortez (the Bouse Embayment) and development of the Colorado River (Fig. 2.1; reviewed in Wood et al. 2008). Instead, divergence between northern and southern clades could have been associated with contemporaneous uplift of the Transverse and Peninsular ranges, which created isolated rain-shadow deserts (Axelrod 1979) where arid-adapted taxa are thought to have diverged in allopatry (Bell et al. 2010). According to the Mojave Assembly Model, the first of these isolated basins developed during the Pliocene (between 4 and 2 Ma); one located in the western Mojave Desert and another along the Lower Colorado River Valley (Fig. 2.1b). However, based on their distributions, the split between the northern and southern clades probably occurred somewhere along the coast of Sonora, so isolation within these basins was probably not responsible for the initial north and south divergence of *H. arizonensis*. More likely, the clades diverged during the early Pleistocene, a timeframe during which desert taxa fragmented into additional desert basins (Bell et al. 2010), including one along the coast of Sonora (Fig. 2.1c).

Although my sampling of the southern clade was sparse, levels of genetic differentiation between southern specimens was high, as the southernmost population was 2.4% divergent (uncorrected *p*-distance) from the nearest coastal sample 200 km to

the northwest. Molecular dating places this level of divergence between the early and mid Pleistocene. Accordingly, vicariance within the southern clade could be attributed to an increased influence of the Río Yaqui (indicated in Fig. 2.4a). This river, like other rivers to the south, runs west from the Sierra Madre Occidental and has been postulated as the cause of genetic divergences in other taxa (Hafner and Riddle 2011). The CCSM model proposes that LGM climates may have been suitable in a disjunct area on the southern Sonora coast (Fig. 2.9b). Persistence in this area during the LGM would explain the high genetic diversity in the southern clade if individuals from this area have retained a genetic signal of earlier divergence. Following the LGM, habitat may have become available along the rest of the Sonoran coast, allowing haplotypes north of the Río Yaqui to freely colonized new areas, following the coastline northward. This scenario contradicts predictions from the MIROC model, which portrays no suitable climate along the southern and central coast of Sonora (Fig. 2.9c). Instead, suitable climate is depicted along the Lower Colorado River Valley and in fragmented patches that are currently within the Sea of Cortez, but were terrestrial during the LGM. If the MIROC model more accurately depicts the LGM distribution, then the Southern Clade could have diversified in these areas, followed by expansion along the coast of Sonora during the current interglacial. Additional genetic sampling, however, would be needed to test these alternative hypotheses.

Phylogeographic patterns within the northern clade appear to have been shaped during the Pleistocene. Six geographically structured groups (Fig. 2.5b), representing monophyletic maternal lineages were recovered by the phylogenetic and structure

analyses (Figs. 2.3–2.5), and molecular dating estimates place the TMRCA for these groups in the mid Pleistocene to early Holocene. The distributions of these groups mostly correspond to the same basins and drainages where other organisms are thought to have persisted during Pleistocene glacial periods. Based on these results, the fluctuating climates of the Pleistocene most likely isolated northern clade populations within several allopatric refugia long enough to establish reciprocally monophyletic mtDNA lineages.

Most of the mtDNA lineages within the northern clade of *H. arizonensis* are geographically congruent with glacial refugia predicted by the Mojave Assembly Model. There is also demographic evidence that populations of these scorpions have undergone recent spatial expansions, as would be expected for arid-adapted taxa expanding their ranges as the climate became warmer. The evidence of expansion is particularly strong for groups I-IV (Table 2.4, Fig. 2.7). Additional tests of demographic expansion conducted by comparing within group values of π and *h*, based on the method employed by Grant and Bowen (1998), provide further evidence of expansion. Groups II–VI all have low π and high *h,* containing few highly divergent haplotypes. Such a genetic pattern would be expected under a hypothesis of Pleistocene fragmentation where populations underwent bottlenecks (such as contraction into glacial refugia), followed by rapid population growth and accumulation of novel mutations (Grant and Bowen 1998). Genetic patterns within Groups I and V show high π and high *h*, and appear to have had more stable population sizes through time.

These results provide convincing evidence that the phylogeography of *H. arizonensis*, like co-occurring vertebrate species, was influenced by climatic fluctuations during the Pleistocene. As predicted by the Mojave Assembly Model, climatic conditions during glacial periods appear to have forced the distribution *H. arizonensis* to fragment into several isolated regions mostly associated with desert basins and drainages. The only pattern that conflicts with the Mojave Assembly Model is that of an additional refugium along the northern section of the Lower Colorado River Valley, which I discuss below.

Northern Lower Colorado River Valley Refugium (NLCR)

The phylogeography of *H. arizonensis* highlights an additional potential refugium that may have existed along a northern portion of the Lower Colorado River Valley (hereafter referred to as the NLCR). Evidence for this refugium comes both from the presence of a geographically cohesive mtDNA lineage of *H. arizonensis* (Group III) in the area (Figs. 2.1–2.3), and from one of the species distribution models which predicts that climate within the area was suitable for *H. arizonensis* during the LGM (Fig. 2.9c). The Group III haplotypes cluster within the center of the area predicted by the model, but peripheral localities on the east and west of the predicted area also contain haplotypes from Group I. Furthermore, only Group I haplotypes were found in the northern portion of the area predicted by the model, so the NLCR might have been contained within a smaller region than predicted. The CCSM model does not depict suitable climate in this region at all, so neither model may be entirely accurate in this region.

Group I haplotypes found in sympatry with and north of the Group III haplotypes exhibited low haplotype diversity in relation to Group I haplotypes to the south, suggesting they may have recently expanded northward from a larger refugium (Fig. 2.9c) in the southern section of the Lower Colorado River Valley (hereafter SLCR). This pattern brings up an interesting question; namely, why was the northern Mojave Desert not colonized by postglacial expansion of haplotypes from the NLCR rather than those from the SLCR? Given that Group I and Group III haplotypes in this region occur on both sides of the Colorado River, this landscape feature clearly has not been a consistent barrier (as seen with many other desert organisms). In addition, there are no other obvious topographic barriers between Group I and Group III haplotypes found east of the river in the northern portion of the proposed NLCR. One possibility is that there are fitness differences between these lineages. Given the potential disparity between the sizes of the two refugial areas (Fig. 2.9), the population in the south may have experienced a wider range of ecological conditions than that within the NLCR during glacial periods. As the glacial periods lasted longer than the interglacials, the ecological requirements (fundamental niche) of fragmented populations may have diverged, yielding differential dispersal capabilities across the postglacial landscape.

More intriguing is the possibility that dispersal or fitness differences between these lineages may result from potential hybridization of populations of *H. arizonensis* at sites within the NLCR with *H. spadix,* a closely related species. *Hadrurus spadix* is a generalist and found in a variety of habitats, and prone to occur in rocky habitats and at higher elevations. As currently understood, *H. spadix* is distributed throughout a variety

of mid-elevation habitats within the Mojave Desert and Colorado Plateau, as well as low to mid-elevations in the western and northern Great Basin Desert. However, recent findings suggest that *H. spadix* actually comprises two morphologically similar species (unpublished data); *H. spadix* in the Colorado Plateau, and a new species in the Mojave and Great Basin deserts (Prendini et al. in prep). Provocatively, I found *H. arizonensis* and *H. spadix* in sympatry in the Newberry Mountains of Nevada and the Black Mountains of Arizona, both of which are areas within the NLCR. During sampling, I noted that a few specimens from these sites showed indications of gross morphological intermediacy for patterns in coloration and trichobothria (sensory hairs) ornamentation (data not shown), lending support to the possibility of hybridization. A definitive assessment of whether Group III individuals represent hybrids, however, would best be accomplished through a genetic assessment of nuclear genes.

The presence of a Pleistocene NCLR is supported by phylogeographic patterns in some other taxa occupying the region. For example, the relict leopard frog (*Rana [Lithobates] onca* Cope) appears to have diverged from its closest relative, the lowland leopard frog (*Rana [Lithobates] yavapiensis* Platz and Frost), in this region during the Pleistocene, rendering the former narrowly distributed along river drainages within the NCLR and the latter distributed more broadly across the Sonoran Desert (Oláh-Hemmings et al. 2009). Species distribution models constructed for a related scorpion species, *Hadrurus spadix* Stahnke from the Mojave and Great Basin deserts (potentially a new species as discussed above) predict little suitable habitat in the Great Basin during the LGM, but suitable climate within the Mojave Desert includes a patch which

encompasses the NLCR (Chapter 3). Furthermore, species distribution models for the chisel-toothed kangaroo rat (*Dipodomys microps* Merriam), a rodent species endemic to the Great Basin Desert, predicted that LGM climates were suitable in an area very closely matching that of the NLCR (Jezkova et al. 2011, their Fig. 4b). Therefore, the NLCR might represent an area where several Mojave and Great Basin desert species were able to persist during Pleistocene glacials.

Testing the Mojave Assembly Model

With the exception of the NLCR, phylogeographic patterns in *H. arizonensis* are mostly congruent with patterns predicted by late Pliocene through Holocene portions of the Mojave Assembly Model. During the late Pliocene to early Pleistocene, the Mojave Assembly Model predicts lineage formation in the western Mojave Desert as regional uplift forced desert organisms into basin refugia in the rain shadow of the Transverse Ranges. Although I recovered a unique lineage of *H. arizonensis* in this area (Group II), the molecular clock estimate placed the TMRCA for this group in the middle to late Pleistocene (0.25–0.93 Ma). During the Pleistocene, the Mojave Assembly Model posits that continued block-faulting formed the modern basin topography which, along with more mesic conditions, may have fragmented populations into basins associated with the Mojave River, Amargosa River, Salton Sea, and Lower Colorado River (Fig. 2.1c). The distributions of groups I, II, and IV from the northern clade suggest that *H. arizonensis* may also have occupied these areas during glacial periods. The center of the distribution of Group I, the largest group, extends along the Lower Colorado River Valley and, as

mentioned earlier, may have recently expanded from the southern portion of this region (the SLCR). Group II is distributed throughout the western Mojave Desert, whereas the distribution of Group IV circumscribes the Amargosa River and Death Valley regions. Demographic analyses suggest that these latter two groups underwent recent expansions (Table 2.4, Fig. 2.7), perhaps expanding their ranges from two small glacial refugia in the northwestern Mojave Desert, as predicted by the Mojave Assembly Model.

Bell et al. (2010) attribute these refugia to the Mojave and Amargosa River drainages. Species distribution models for *H. arizonensis*, however, do not predict suitable climate along the Amargosa River during the LGM, but adjacent low-elevations of Death Valley are predicted as suitable (Fig. 2.9). During pluvial periods, Death Valley was filled with a large body of water known as Lake Manly, so while climate may have been suitable, much of the predicted habitat almost certainly was not. Even so, the MIROC model predicted suitable LGM climate in an area larger than high stand estimates for Lake Manly, so populations of *H. arizonensis* in Death Valley could have persisted in areas distributed around the lake, especially in sandy lakeshore habitats.

The Mojave Assembly Model states that Pleistocene climates may have also facilitated vicariance among desert organisms near the Gila River in Arizona. Although my sampling in this area was limited, unique groups of *H. arizonensis* haplotypes (Groups V and VI) from the eastern portion of its range also appear to be divided north and south of the Gila River. Given the relatively small size and ephemeral nature of this river, its significance as a biogeographic barrier is hard to imagine, but distinct groups of

haplotypes have also been found on opposite sides of the river in *Phrynosoma platyrhinos* Girard (desert horned lizards; Jones 1995; Jezkova 2010) and *Chaetodipus penicillatus* Woodhouse (desert pocket mice; Jezkova et al. 2009). Jones (1995) attributed divergence in the *P. platyrhinos* to a Pliocene inundation of the Colorado and Gila Rivers during the Bouse Embayment (see Fig. 2.1a). However, Jezkova et al. (2009) estimated the genetic divergence in *C. penicillatus* to have occurred more recently during the Pleistocene, possibly by fragmentation of habitat in the Gila River area by climatic fluctuations, and not directly by the river itself. A similar situation could have occurred in *H. arizonensis*, as molecular date estimates also suggest that groups across the Gila River diverged during the Pleistocene (Fig. 2.8).

The evidence of substantial genetic structure within the eastern portion of the *H. arizonensis* distribution indicates the potential for some degree of persistence within this region, certainly during the LGM. This is in conflict with the species distribution models that do not depict any suitable climate in the area during the LGM, instead suggesting that the nearest habitat was along the Lower Colorado River Valley. If the species distribution models are not grossly inaccurate in this region and *H. arizonensis* did persist in these eastern areas during the LGM, as evidenced by genetic patterns, then populations there must have endured climate conditions outside of the current realized niche, and perhaps underwent 'niche drifting' (Jezkova et al. 2011).

In summary, the phylogeography of *H. arizonensis* lends support to the predictions of the Mojave Assembly Model during the Pleistocene. Genetic diversity within *H. arizonensis* appears to have been influenced by climate-induced fragmentation and

contraction into glacial refugia, which appears to have caused autochthonous lineage formation within specific regions throughout the Mojave and Sonoran deserts. Furthermore, an additional glacial refugium along the northern portions of the Lower Colorado River (the NLCR) should be incorporated into future models for the historical assembly of the Mojave and Sonoran desert biotas.

Table 2.1. Location and voucher information for genetic samples used in this study. Site numbers correspond with localities portrayed in Fig. 2.1. Coordinates only represent the general sample area.

Site	State	Locality	Lat.	Long.	*n*	Voucher Numbers
1	UT	SNOW CANYON	37.173	-113.649	8	MG0151, MG0152, MG0155, MG0156, MG0980-MG0983
2	NV	COYOTE SPRINGS	36.992	-114.987	8	MG0777-MG0781, MG1146-MG1148
3	NV	VIRGIN RIVER	36.739	-114.186	1	MG0969
4	NV	BIG DUNE	36.638	-116.544	9	MG0997, MG0999-MG1006
5	CA	DOLOMITE ROAD	36.574	-117.978	7	MG0291-MG0297
6	CA	PANAMINT VALLEY	36.433	-117.432	10	MG0551-MG0560
7	NV	MUDDY MOUNTAINS	36.406	-114.766	1	MG1149
8	CA	DEATH VALLEY	36.227	-116.880	7	MG0766-MG0770, MG0772, LP4974
9	CA	WEST SIDE ROAD	35.937	-116.713	3	MG0438-MG0440
10	CA	IBEX DUNES	35.739	-116.383	2	MG0773, MG0774
11	AZ	GREGG'S HIDEOUT	35.905	-114.169	1	MG0792
12	NV	EL DORADO VALLEY	35.887	-114.952	10	MG1133-MG1142
13	AZ	TEMPLE BAR	35.864	-114.481	3	MG1143-MG1145
14	NV	MESQUITE VALLEY	35.762	-115.580	10	MG0230-MG0239
15	CA	TRONA PINNACLES	35.617	-117.370	1	LP1638
16	NV	PIUTE VALLEY	35.269	-114.925	4	MG0101, MG0103, MG0104, MG0105
17	AZ	E OF LAUGHLIN	35.215	-114.430	1	MG0571
18	CA	CALIFORNIA CITY	35.200	-118.058	11	MG0755-MG0764, LP3191
19	NV	NEWBERRY MOUNTAINS	35.174	-114.684	5	MG0467-MG0470, LP8490
20	AZ	WILLOW CREEK	35.141	-113.548	4	MG0717, MG0718, MG0720, MG0721
21	AZ	SITGREAVES PASS	35.046	-114.360	11	MG1069-MG1077, LP2962, LP8997
22	CA	AFTON CANYON	35.040	-116.381	4	MG0742-MG0745
23	AZ	BUCKEYE STATION	34.720	-114.242	7	LP7174, LP7206, MG0088-MG0092
24	AZ	WARM SPRINGS	34.748	-114.482	2	LP7190, LP7211
25	CA	PARK MOABI	34.710	-114.517	1	LP7200
26	AZ	HAVASU QUARRY	34.605	-114.353	2	MG0791, LP7134
27	CA	PEARBLOSSOM	34.602	-117.908	1	LP3190
28	CA	SIDEWINDER MOUNTAINS	34.598	-117.143	1	MG0466
29	CA	CADIZ DUNES	34.403	-115.417	10	MG0970-MG0979
30	CA	SHEEPHOLE MOUNTAINS	34.254	-115.717	4	MG1033-1036
31	CA	PARKER DAM ROAD	34.254	-114.174	1	LP7098
32	AZ	PARKER	34.146	-114.196	7	MG0782-MG0786, LP7189, LP7204

Table 2.1. Location and voucher information continued.

Site	State	Locality	Lat.	Long.	*n*	Voucher Numbers
33	CA	TWENTYNINE PALMS	34.091	-115.608	1	LP7113
34	CA	RICE ROAD	34.083	-115.128	2	LP8959, LP8960
35	CA	WHITE WATER	33.971	-116.653	2	LP3192, LP3421
36	AZ	UTTING	33.840	-113.884	2	MG0572, MG0573
37	CA	INDIO	33.743	-116.170	5	MG1029-1032, LP7218
38	AZ	SURPRISE	33.717	-112.378	10	MG0654-MG0663
39	AZ	QUARTSZITE	33.599	-114.311	5	MG1037-MG1041
40	AZ	EHRENBERG	33.596	-114.500	1	MG0699
41	CA	WILEY'S WELL	33.542	-114.883	9	MG0682-MG0690
42	AZ	SALT RIVER	33.499	-111.788	1	LP8489
43	CA	SALTON CITY	33.288	-116.021	5	MG1024-MG1028
44	CA	BORREGO SPRING	33.214	-116.375	1	LP5045
45	AZ	MARICOPA	32.990	-112.075	1	MG0753
46	CA	VALLECITO	32.972	-116.384	9	MG0118-0122, MG1119-MG1121, MG1123
47	AZ	GILA BEND	32.945	-112.723	1	VF0076
48	AZ	DATELAND	32.807	-113.553	1	VF0046
49	CA	LOS ALGODONES	32.724	-114.728	2	LP4452, VF0077
50	CA	HEBER DUNES	32.723	-115.388	1	LP10553
51	AZ	FORTUNA WASH	32.665	-114.382	5	MG0607-MG0610, LP1813
52	BC	LAGUNA SALADA	32.575	-115.743	1	LP3470
53	AZ	MARANA	32.475	-111.187	10	MG0637-MRG0646
54	AZ	AJO	32.351	-112.830	10	MG0624-MG0633
55	SO	CERRA PRIETA	32.234	-114.067	1	LP4458
56	AZ	BOPP ROAD	32.177	-111.066	1	LP3047
57	SO	SONOYTA	32.103	-113.785	3	LP4460, LP5087, LP5088
58	SO	CEDO DUNES	31.292	-113.498	1	LP2168
59	BC	SAN FELIPE	30.955	-114.796	1	LP4456
60	BC	PUNTA BUFEO	29.857	-114.442	2	LP3469, LP4457
61	BC	PUNTA CALAMAJUE	29.685	-114.163	1	LP8730
62	SO	BAY NEW KINO	28.921	-112.043	1	LP6328
63	SO	SAN CARLOS	27.952	-111.094	2	MG0787, MG0788
64	SO	HUATABAMPITO	26.697	-109.606	1	LP9971

Table 2.2. Primers used for amplification or sequencing of a 1029 bp portion of the mitochondrial gene for cytochrome oxidase subunit I (*cox1*).

Name	Direction	Position	Sequence (5' to 3')
C1_HAD1_L	Forward	External	CGTGCTGARATTGGAAGTCCTGG
LCO	Forward	External	GGTCAACAAATCATAAAGATATTGG
C1_2776_MOD	Reverse	External	GGATAATCAGAATAHCGAGG
HCOoutout	Reverse	External	GTAAATATATGRTGDGCTC
Hariz_Int_F	Forward	Internal	GCTATTACTATGTTGTTGACGG
LE1r	Reverse	Internal	GTAGCAGCAGTAAARTARGCYCGAGTATC
Cruzr	Reverse	Internal	CATACCCAAAGARCCAAAAGG

Table 2.3. Results from spatial analyses of molecular variance (SAMOVA) with different pre-defined number of groups (K) with samples sizes ≥ 4. Numbers in partitions reference sites identified in Figure 2.5. Abbreviations for fixation indices as follows: F_{SC} = proportion of genetic variation between populations within groups; F_{ST} = proportion of genetic variation between populations and groups overall; F_{CT} = proportion of among group genetic variation.

K	F_{SC}	F_{ST}	F_{CT}	Partition
2	0.6041	0.7619	0.3985	(1, 2, 4, 8, 12, 14, 16, 19, 20, 21, 23, 29, 30, 32, 37, 38, 39, 41, 43, 46, 51, 53, 54)(5, 6, 18, 22)
3	0.5693	0.7589	0.4402	(1, 2, 4, 8, 12, 14, 16, 19, 20, 23, 29, 30, 32, 37, 38, 39, 41, 43, 46, 51, 53, 54)(5, 6, 18, 22)(21)
4	0.5299	0.7550	0.4789	(1, 2, 4, 8, 12, 14, 16, 19, 20, 23, 29, 30, 32, 37, 38, 39, 41, 43, 46, 51, 54)(5, 6, 18, 22)(21)(53)
5	0.4332	0.7363	0.5348	(1, 2, 12, 16, 19, 20, 23, 29, 30, 32, 37, 38, 39, 41, 43, 46, 51, 54)(4, 8, 14)(5, 6, 18, 22)(21)(53)
6	0.4022	0.7270	0.5433	(1, 2, 12, 16, 19, 20, 23, 29, 30, 32, 37, 39, 41, 43, 46, 51, 54)(4, 8, 14)(5, 6, 18, 22)(21)(38)(53)
7	0.3667	0.7197	0.5573	(1, 2, 12, 16, 19, 20, 23, 29, 30, 32, 37, 39, 41, 43, 51, 54)(4, 8, 14)(5, 6, 18, 22)(21)(38)(46)(53)
8	0.3395	0.7161	0.5701	(1, 2, 12, 16, 19, 20, 23, 29, 30, 32, 39, 41, 43, 51, 54)(4, 8, 14)(5, 6, 18, 22)(21)(37)(38)(46)(53)
9	0.3240	0.7098	0.5708	(1, 2, 12, 16, 19, 20, 29, 30, 32, 39, 41, 43, 51, 54)(4, 8, 14)(5, 6, 18, 22)(21)(23)(37)(38)(46)(53)
10	0.2623	0.6894	0.5790	(1, 2)(4, 8, 14)(5, 6, 18, 22)(12, 16, 19, 20, 29, 30, 32, 39, 41, 43, 51, 54)(21)(23)(37)(38)(46)(53)

Table 2.4. Nucleotide diversity (π), haplotype diversity (h), and results of Fu's F (F), mismatch analyses, and estimated time to most recent common ancestor (TMRCA; in Ma) for groups in the northern clade (see text). Asterisks indicate values with associated p-values of <0.02 for Fu's F (threshold value corresponding to $\alpha = 0.05$). Graphs of mismatch distributions are displayed in Fig. 2.7.

					Sudden Expansion		Spatial Expansion			
Group Number	***N***	***π***	***h***	***F***	***SSD***	***r***	***SSD***	***r***	**Distribution Curve**	**TMRCA (95% HPD)**
I	146	0.007	0.982	-24.799*	0.001	0.007	0.001	0.007	unimodal	1.02 (0.64–1.43)
II	32	0.002	0.841	-3.764*	0.008	0.057	0.008	0.057	unimodal	0.58 (0.25–0.93)
III	21	0.003	0.910	-3.463*	0.004	0.017	0.006	0.017	unimodal	0.31 (0.13–0.54)
IV	33	0.002	0.867	-4.630*	0.008	0.072	0.008	0.072	unimodal	0.20 (0.006–0.39)
V	7	0.005	1.000	-2.987*	0.063	0.091	0.036	0.091	multimodal	0.59 (0.27–0.96)
VI	11	0.003	0.836	-0.321	0.032	0.101	0.034	0.101	multimodal	0.35 (0.12–0.63)

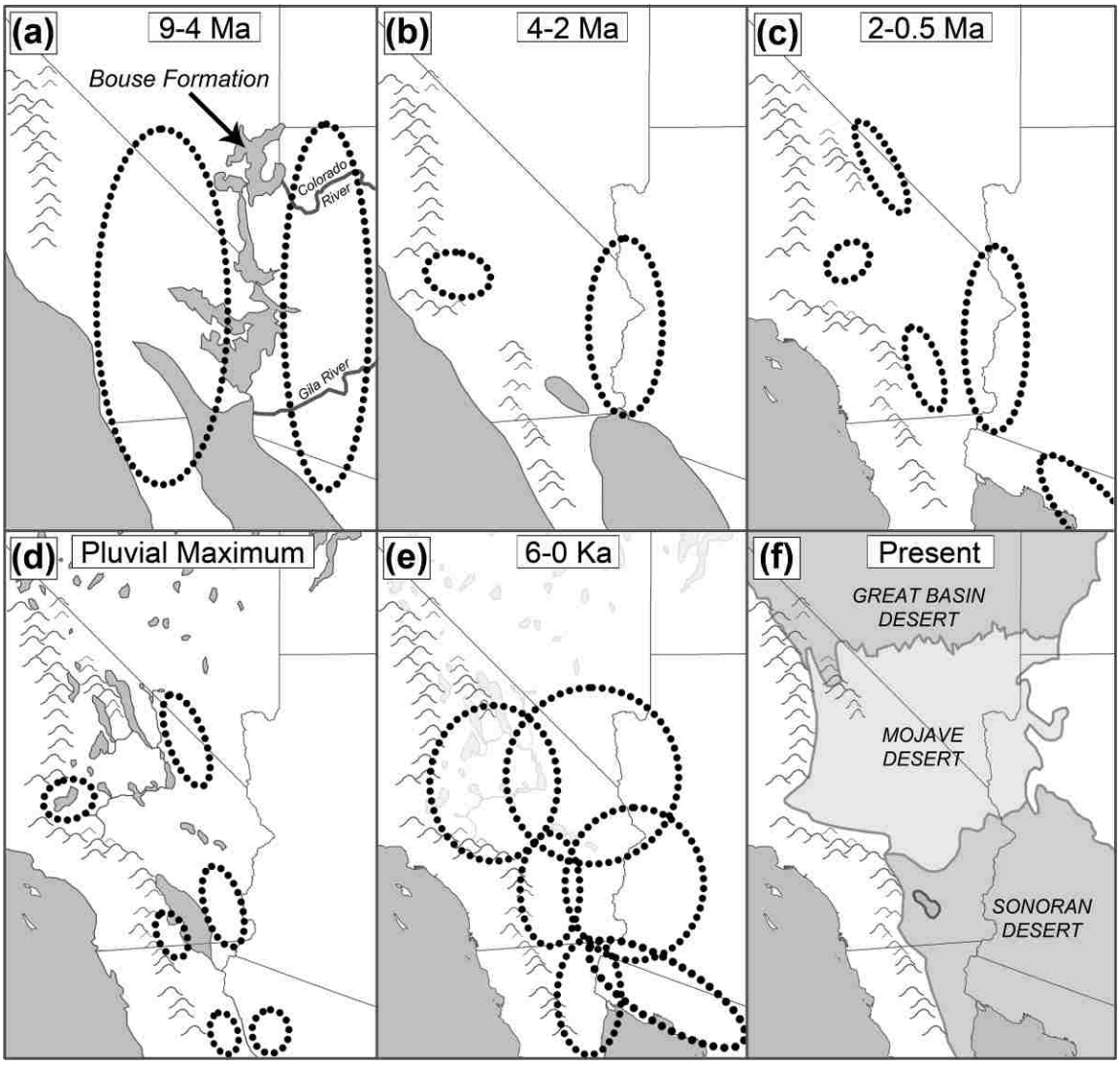

Figure 2.1. The 'Mojave Assembly Model' of historical assembly for the Mojave Desert biota: (a) distribution of taxa sundered by the Bouse Formation and development of a through-flowing Colorado River between 9 and 4 Ma; (b) distribution of taxa isolated in desert basins in the western Mojave Desert (Antelope and Phelan Peak basins) and along the Lower Colorado River Valley between 4 and 2 Ma; (c) location of taxa isolated in desert basins developing during the Pleistocene; (d) fragmented arid refugia during the last glacial maximum; (e) expansion from arid refugia and secondary contact during the Holocene; (f) current boundaries of the Mojave Desert and adjacent Sonoran and Great Basin deserts. Figure redrawn from Bell et al. (2010).

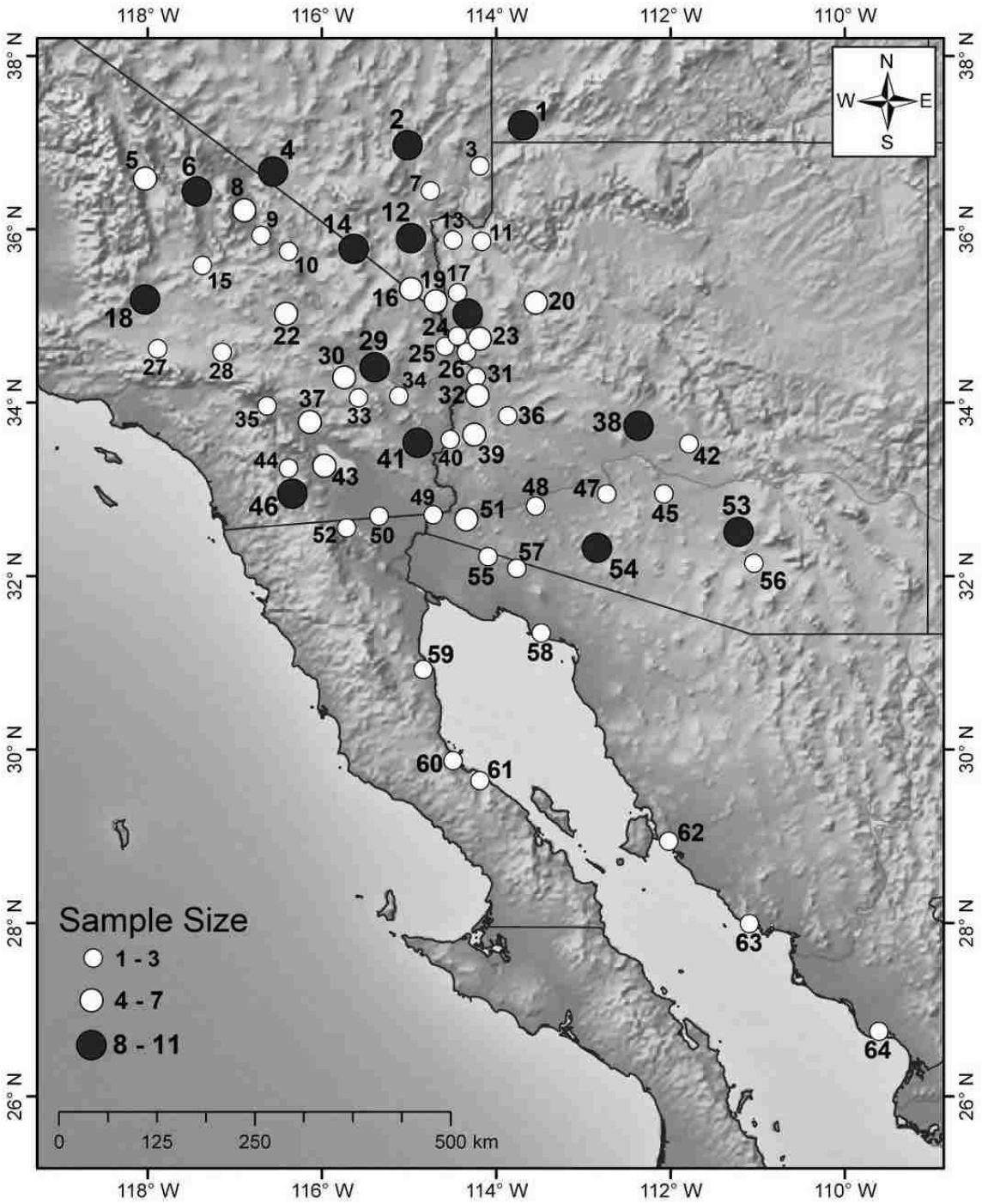

Figure 2.2. Map depicting locations for samples of *Hadrurus arizonensis* Ewing used in genetic analyses. Numbers correspond to location information presented in Table 2.1.

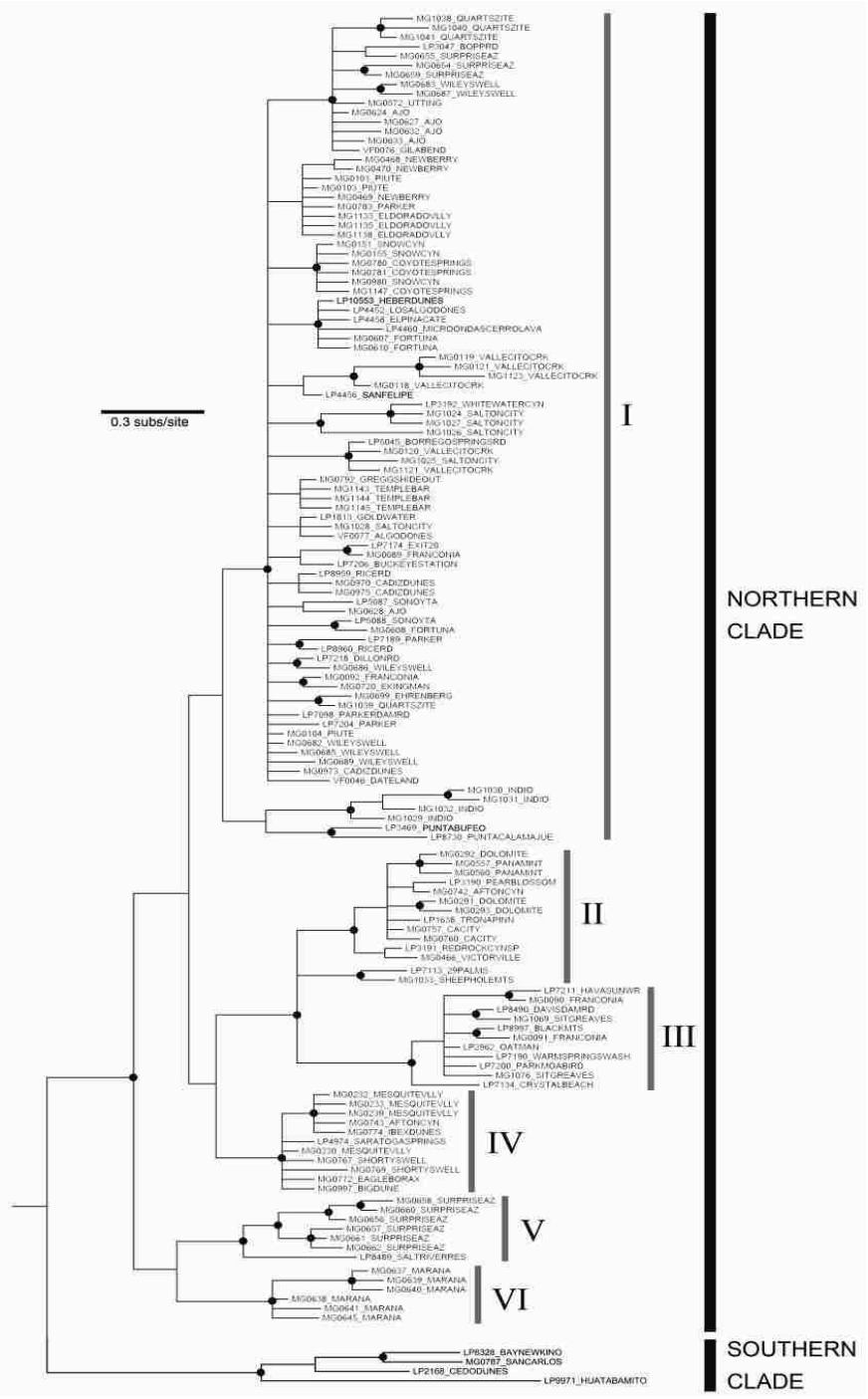

Figure 2.3. Midpoint rooted consensus tree for *Hadrurus arizonensis* Ewing constructed using 1029 bp of *cox1* mtDNA and estimated under a criterion of Bayesian inference. Black circles indicate nodes supported with posterior probabilities of 0.9 or greater. Roman numerals represent groupings indicated by SAMOVA.

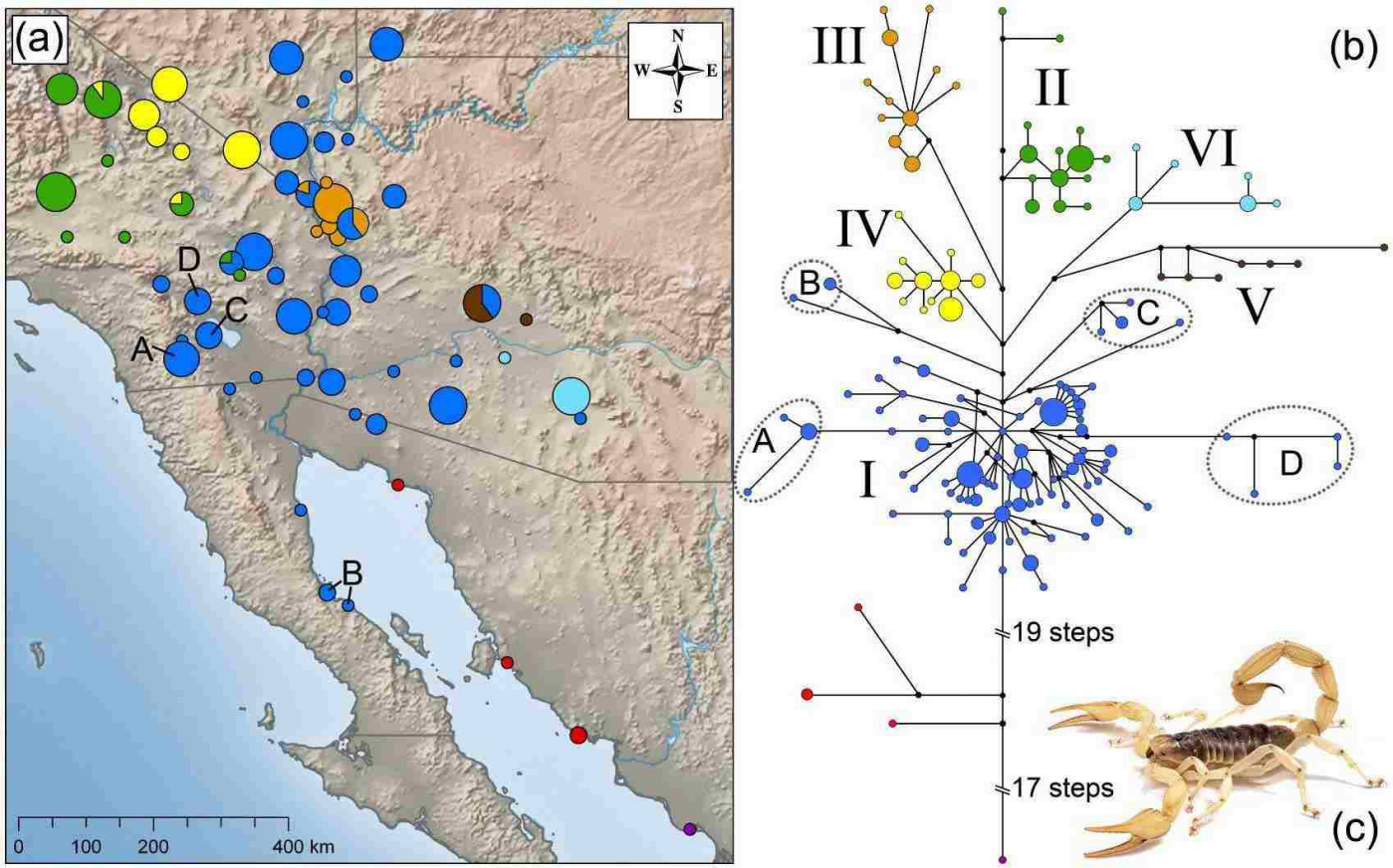

Figure 2.4. Map (a) and network (b) of mtDNA sequence haplotypes of *Hadrurus arizonesis* Ewing (c). Each circle in the network represents one haplotype. Circle size in both the map and network are proportional to sample size. Colors in the map correspond to the colors of each of the groups identified in the haplotype network. Lengths of lines connecting haplotypes in the network are proportional to the number of mutations between the haplotypes, with a transition/transversion ratio of 3:1. Roman numerals represent groupings indicated by SAMOVA.

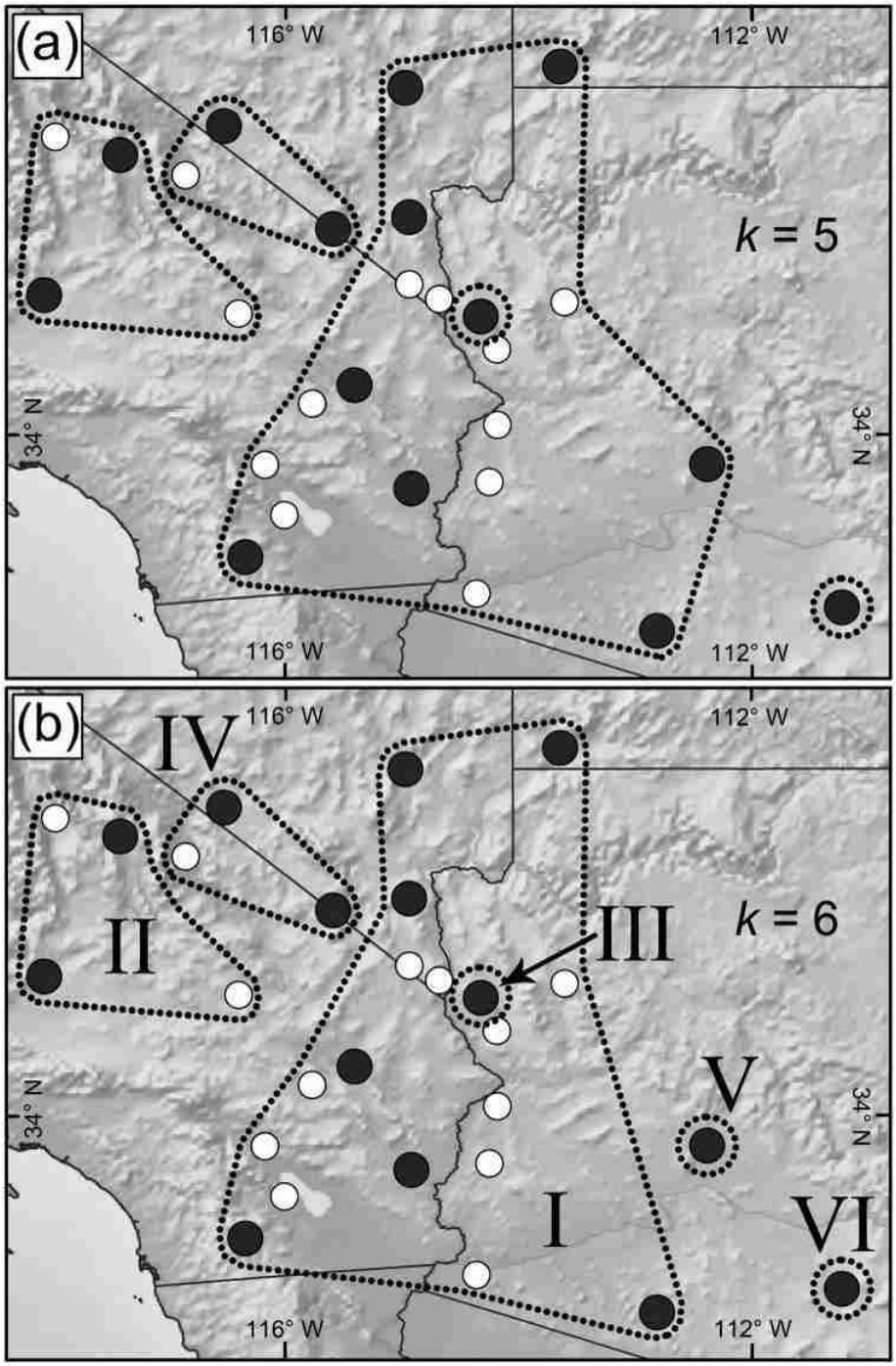

Figure 2.5. Results from SAMOVA with the number of partitions (*k*) set to five (a) and six (b). Dotted lines indicate groups of populations that are geographically homogenous and maximally differentiated. Roman numerals indicate groups also recovered in the network (Fig. 2.4) analyses.

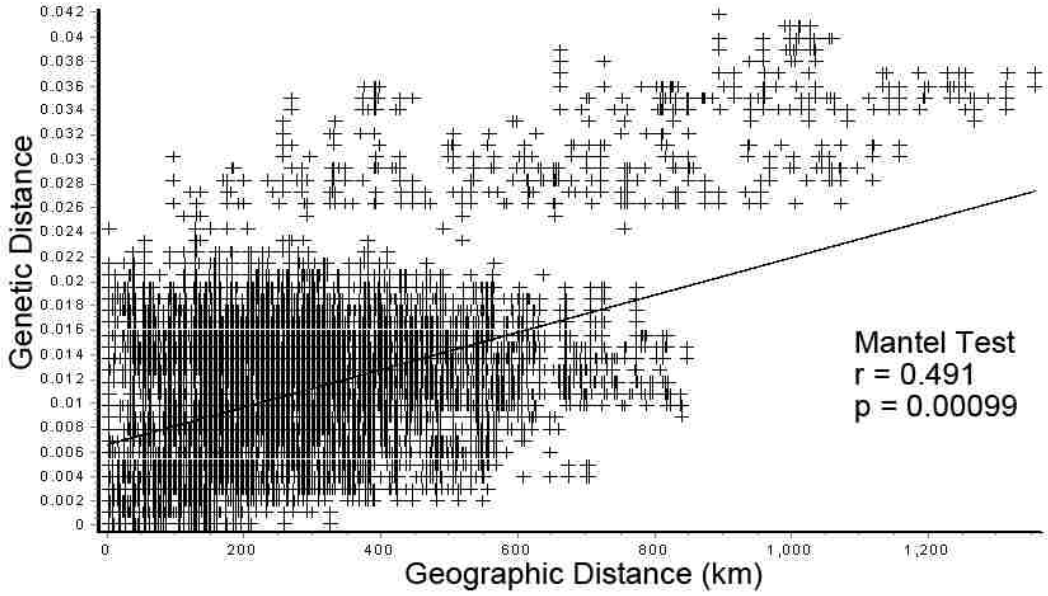

Figure 2.6. Results from a Mantel test of geographic distances (km) and genetic distances (uncorrected p-distance) for *H. arizonensis*.

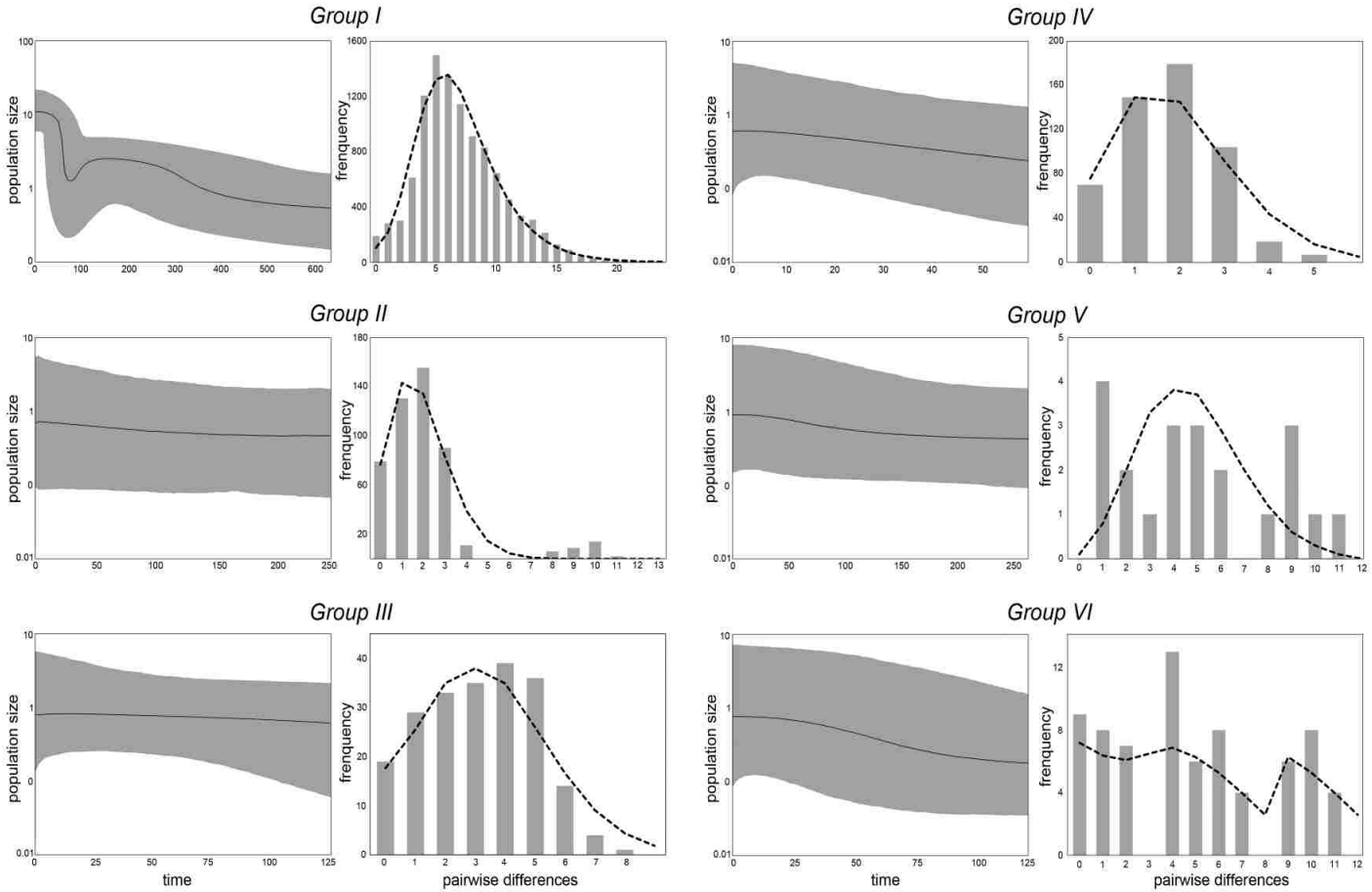

Figure 2.7. Bayesian skyline plots and mismatch distributions for the six mtDNA groups recovered in phylogenetic, network, and spatial analyses. The Bayesian skyline plots depict changes in population size over time, presented in thousands of years (Ka). Dashed lines in mismatch distributions represent the expected distribution if the populations underwent demographic expansion, whereas bars indicate the observed frequency of pairwise differences.

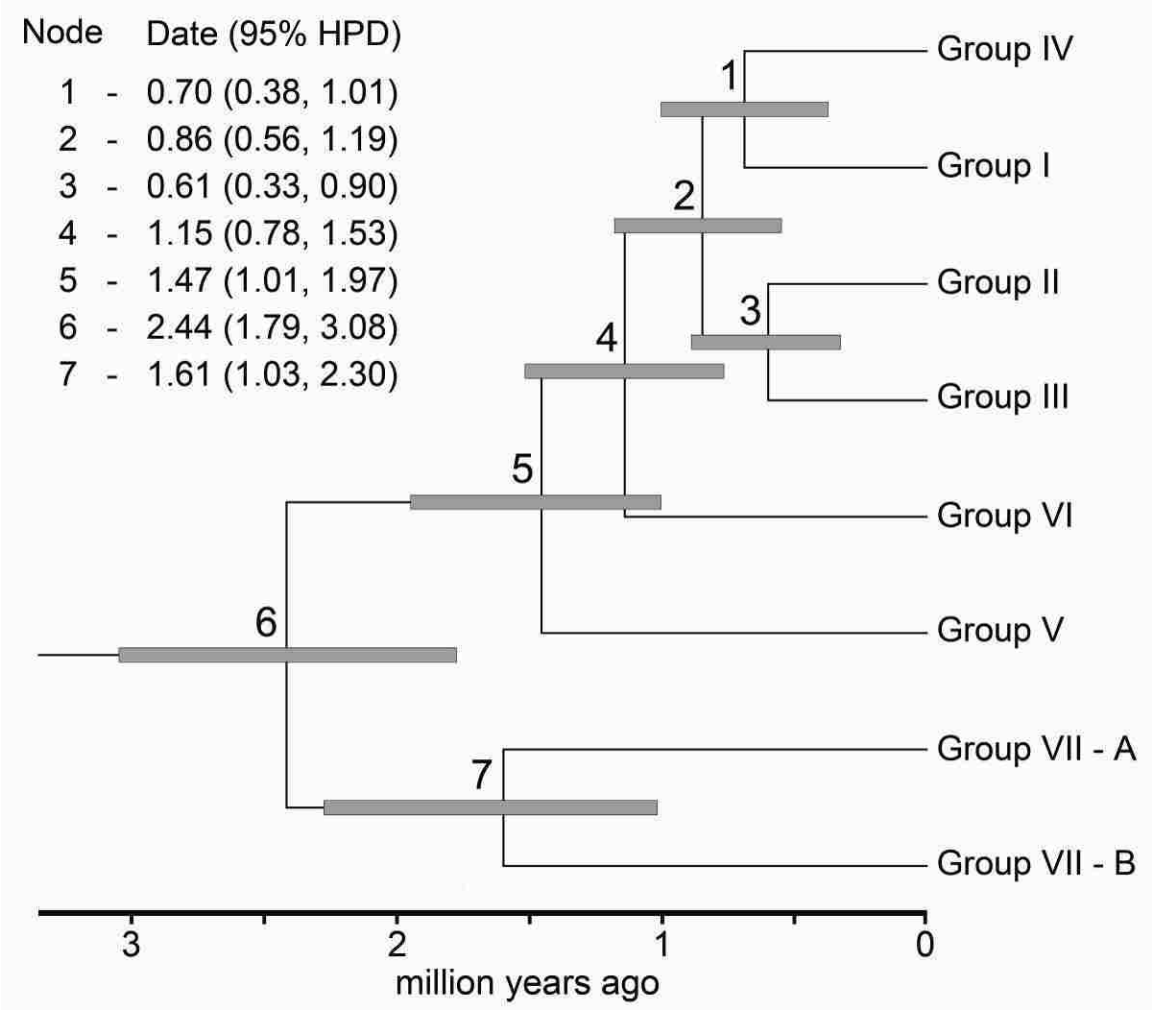

Figure 2.8. Ultrametric tree with the topology and divergence times for major lineages within *Hadrurus arizonensis* Ewing as estimated in BEAST. Divergence times are presented as means and 95% highest posterior densities (HPD).

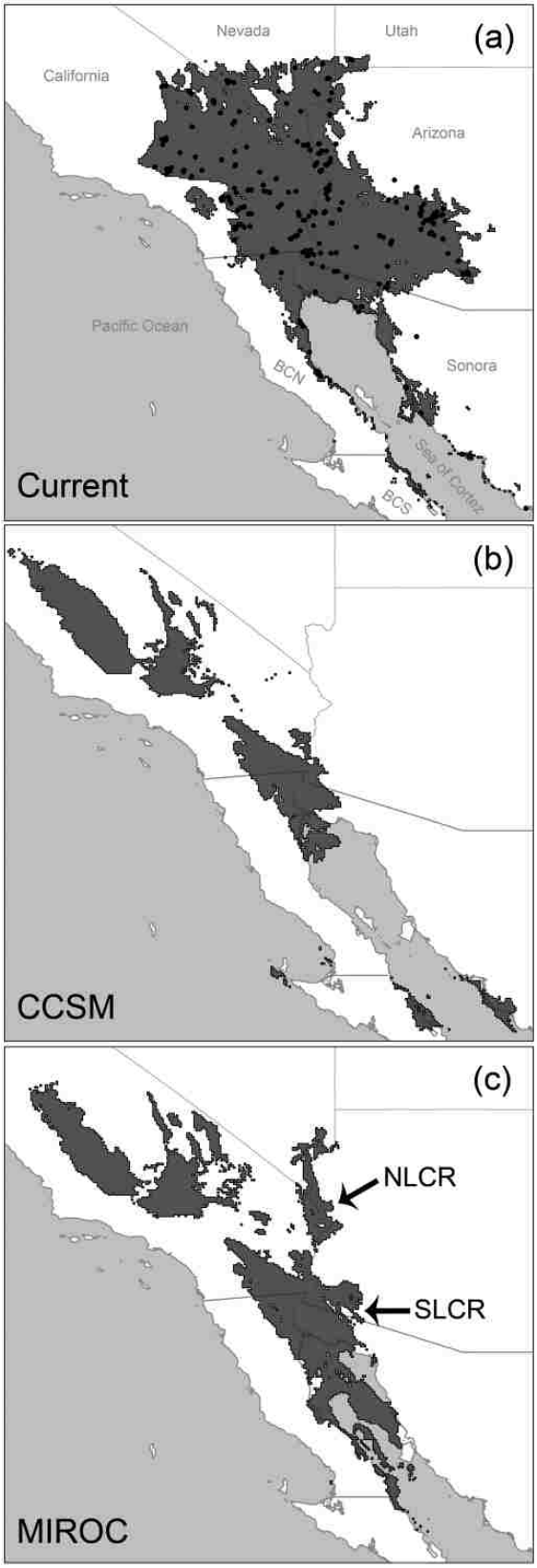

Figure 2.9. Graphical results from species distribution models generated using MAXENT and displayed using the maximum training sensitivity plus specificity threshold. Models represent climate predicted as suitable for *Hadrurus arizonensis* Ewing (dark shading) during current conditions (a) and two LGM conditions estimated from CCSM (b) and MIROC (c) climatic simulations. Black dots (a) represent occurrence records used to generate the models. Arrows indicate postulated glacial refugia discussed in the text. Note that areas predicted as suitable in the Sea of Cortez during the LGM were terrestrial at the time.

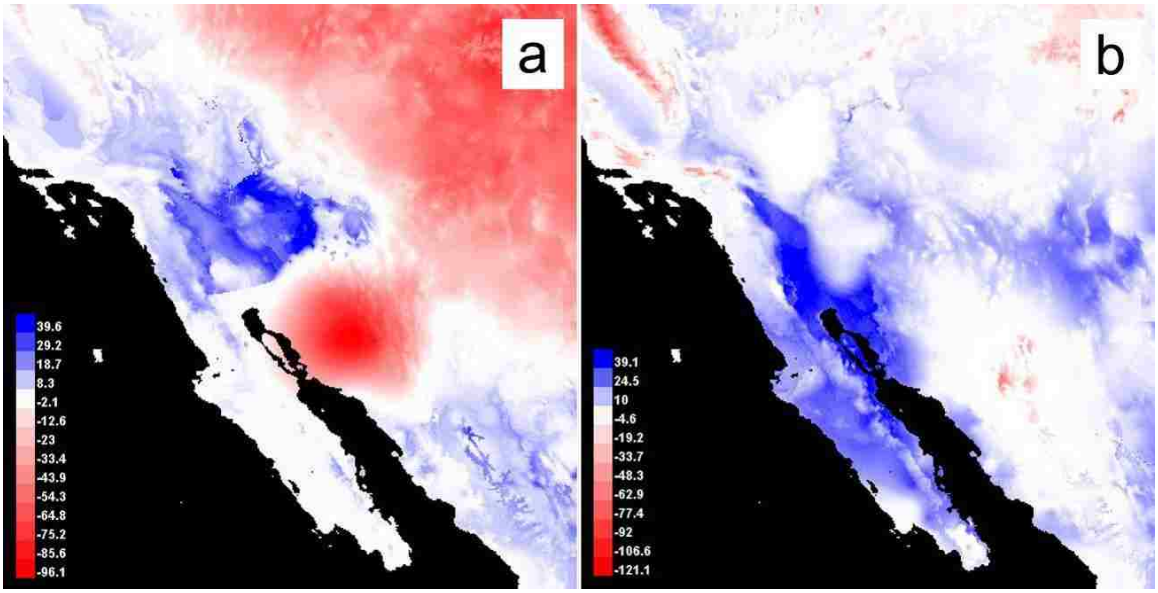

Figure 2.10. Multivariate environmental similarity surfaces (MESS) for projections of LGM climates based on (a) CCSM, and (b) MIROC climate simulations. Negative values (white and red) indicate areas of extrapolation into novel climates.

CHAPTER 3

COMPARATIVE PHYLOGEOGRAPHY OF GIANT HAIRY SCORPIONS (*HADRURUS*) EXPOSES DIFFERENTIAL SENSITIVITES TO HISTORICAL CLIMATE CHANGE AMONG THE NORTH AMERICAN ARIDLANDS

Abstract

A primary goal of comparative phylogeography is to characterize the spatial and demographic responses of different taxa to the same historical events. When distantly related and morphologically dissimilar taxa are compared, however, chances increase that phylogenetic signal and divergent phenotypes will influence patterns and confound interpretations. One way to minimize these effects is to compare closely related species with commensurable phenotypes. I used this approach to assess the influence of Pleistocene climate fluctuations in different North American aridlands by comparing the phylogeographic histories of three closely related and morphologically similar species of giant hairy scorpion (*Hadrurus jedediah, H. spadix, and H. arizonensis*). Phylogeographic analyses of mitochondrial sequence data (*cox1*) and climate-based distribution models suggest that all three species were impacted by glacial climates, but the magnitude of the impact differed substantially among species, presumably influenced by characteristics of the different regions occupied. In the Sonoran and Mojave deserts, *H. arizonensis* appears to have fragmented into at least six glacial refugia, with stronger bottleneck effects in the north. On the Colorado Plateau, *H. spadix* may have

fragmented into three glacial refugia, and demographic assessments predict stable population sizes in the west and a bottleneck in the east. In Mojave Desert, *H. jedediah* appears to have fragmented into three glacial refugia, but only recently colonized the Great Basin and Snake River Plain from the south. With effects from phylogenetic signal and phenotypic differences minimized, comparative phylogeography of giant hairy scorpions provides support to a hypothesis that the biotas of the Great Basin and Snake River Plain were the most sensitive of the North American aridland biotas to historical changes in climate.

Introduction

As emphasized by Darwin (1859), phenotypic traits of related species are often derived from common ancestors and thus not independent. Instead, related species tend to resemble one another more than they resemble species drawn at random from a phylogeny, a phenomenon referred to as 'phylogenetic signal' (Blomberg and Garland 2002; Losos 2008). In comparative studies, phylogenetic signal can be problematic (Burt 1989; Harvey and Pagel 1991), making it difficult to distinguish between differences among patterns that are adaptive versus those that are products of common ancestry (Ricklefs 1996). Phylogenetic signal could also confound comparative phylogeographic studies aimed at determining if different taxa underwent similar responses to the same historical events (Gutiérrez-García and Vázquez-Domínguez 2011; for an early example see Riddle et al. 2000). In particular, when the taxa being compared are distributed in different biogeographic regions, it becomes hard to distinguish between responses that

may be unique to the respective areas versus responses driven by phylogenetic signal. This could complicate interpretations for researchers interested in understanding and comparing the biogeographic histories of areas or regions. Although there are statistical methods to correct for phylogenetic signal (such as phylogenetic independent contrasts), such methods generally increase error variances and weaken interpretations (Felsenstein 1985), and have generally not yet been adapted for use in comparative phylogeography.

An alternative to controlling for phylogeny, and thus minimizing effects from phylogenetic signal, is to compare taxa that are closely related and have shallow phylogenetic histories (MacDougall-Shackleton and Ball 1999); a technique that could easily be applied to comparative phylogeography. By controlling for phylogeny, differences or similarities in spatial and demographic responses to the same historical events (such as Pleistocene climate fluctuations) would more likely be driven by factors inherent to the system or region, such as topography, rather than idiosyncrasies among the study organisms. Taking taxon selection one step further, comparative phylogeography of related taxa that are morphologically similar, such as different species of 'living-fossils', would add an additional constraint on effects from phenotypic differences (although this many not control for physiological changes). Therefore, in a comparative phylogeographic context, related species of morphologically similar taxa, such as the 'living fossils', could be useful for addressing the influence that specific historical events have had on different regions.

Dating to the Carboniferous (Jeram 1994; Coddington et al. 2004), scorpions (Order Scorpiones) are a textbook example of living fossils, so they could hold promise for such a comparative phylogeography. Herein, I compare the phylogeographic histories of three closely related, but differentially distributed, species of giant hairy scorpions (*Hadrurus*). All species of *Hadrurus* are similarly large (up to 127 mm), hirsute, and morphologically similar (Williams 1970), which has complicated taxonomic classifications and estimates of phylogeny (e.g. Williams 1970; Soleglad 1976; Fet and Soleglad 2008; Francke and Prendini 2008). The three species in this study are estimated to have diverged in the Miocene, but the phylogeographic histories within each species appear to be rooted in the Quaternary Period (unpublished data), a time when global climates are known to have undergone profound fluctuations that radically impacted many organisms (Hewitt 2000).

My objective was to assess the influence of Pleistocene climate fluctuations on organisms inhabiting different North American aridlands. To accomplish this, I conducted a comparative phylogeography by investigating the phylogeographic histories of *Hadrurus jedediah* Prendini et al. (in prep) and *Hadrurus spadix* Stahnke, and reanalyzing phylogeographic data for *H. arizonensis* (Ewing) (Chapter 2). Until recently, *H. jedediah* was considered synonymous with *H. spadix*, but the species is currently being described as a distinct species based on genetic patterns and subtle morphological differences (Prendini et al. in prep). The distribution of *H. jedediah* is predominately within the Great Basin and Mojave deserts, whereas *H. arizonensis* occurs throughout

the Mojave Deserts and southward into the Sonoran Desert. *Hadrurus spadix* is endemic to the Colorado Plateau.

Using mitochondrial sequence data from samples collected throughout the ranges of these scorpions, I assessed patterns of genetic diversity using methods from landscape and population genetics. In order to evaluate potential range shifts caused by historical fluctuations in climate, I also developed climate-based species distribution models (SDMs) for each species and projected (hindcasted) the predictions onto estimates of climate conditions during the last glacial maximum (LGM) (approach reviewed in Nogués-Bravo 2009). Earlier Pleistocene glacial periods are expected to have experienced climates similar to that of the LGM (Webb and Bartlein 1992; Bintanja et al. 2005), so I evaluated SDMs under the assumption that such modeling can provide insight into general climatic trends during Late Pleistocene glacial periods. Since the focal species are closely related and morphologically similar, I compared their phylogeographic histories under the assumption that patterns were not largely influenced by phylogenetic signal and divergent phenotypes, and instead represent the differential influence that Pleistocene climate cycles had in the aridlands.

Materials and Methods

Taxon Sampling

I sequenced 141 samples of *H. jedediah* from 56 localities and 43 samples *H. spadix* from 13 localities (Fig. 3.1, Appendices 3, 4). I also used data from 256 samples representing 64 sites from my recent phylogeographic study of *H. arizonensis* (Chapter

2). I identified species based on the locations where samples were collected, and by a combination of diagnostic morphological features (Prendini et al. in prep). All samples were processed as voucher specimens and preserved in the American Museum of Natural History and the San Diego Natural History Museum.

Species Distribution Models

I constructed SDMs using a total of 152 occurrence points for *H. jedediah* and 36 points for *H. spadix*, representing a combination of the sampling localities and additional locations from museum specimens. I compiled occurrence records from museum collections (San Diego Natural History Museum, Smithsonian, California Academy of Sciences, and American Museum of Natural History) and from GPS coordinates associated with my field collections. As above, I identified the museum specimens to species by visually assessing a combination of morphological characters. The majority of museum records lacked coordinate data, so I used GOOGLE EARTH (http://earth.google.com) to estimate latitude and longitude from information on voucher labels. I excluded records with errors greater than five kilometers so that the occurrence data matched the spatial resolution of the modeling rasters (2.5 arc-minutes).

For species distribution modeling, I used MAXENT v. 3.3.2 (Phillips et al. 2006) which has been shown to perform better than other modeling software (Elith et al. 2006). Additional input data included a unique subset of data layers for each species, chosen from the 19 bioclimatic layers used in Chapter 2. For *H. arizonensis,* I used the

same models that were constructed for Chapter 2. For *H. jedediah* and *H. spadix*, I chose subsets of bioclimatic layers by removing highly correlated layers following Chapter 2, except that I used quarter climates over monthly climates and precipitation during the coldest quarter over precipitation during the wettest quarter. Final subsets comprised 11 bioclimatic layers for *H. jedediah* and 9 layers for *H. spadix*. For *H. jedediah*, I used the following layers: Bio2, mean diurnal range; Bio3, isothermality; Bio4, temperature seasonality; Bio5, maximum temperature of the warmest month; Bio6, minimum temperature of the coldest month; Bio8, mean temperature of the wettest quarter; Bio9, mean temperature of the driest quarter; Bio15, precipitation seasonality; Bio16, precipitation of the wettest quarter; Bio17, precipitation of the driest quarter; Bio18, precipitation of the warmest quarter. For *H. spadix* I used: Bio2; Bio3; Bio7, temperature annual range; Bio8; Bio9; Bio11, mean temperature of coldest quarter; Bio14, precipitation of the driest month; Bio15; Bio18. Final subsets were masked (clipped) to the ecoregions that contained occurrence records (Arizona/New Mexico Plateau, Central Basin and Range, Northern Basin and Range, Mojave Basin and Range, Colorado Plateau, Snake River Plain; Olson et al. 2001).

I ran MAXENT using logistic output with default settings except for random seeding. I then projected final models onto CCSM (Otto-Bliesner et al. 2006) and MIROC (Hasumi and Emori 2004) simulations of climatic conditions during the LGM. Model robustness was assessed following procedures outlined in Chapter 2.

Molecular Techniques

As done with *H. arizonensis* (Chapter 2), I isolated total genomic DNA from leg tissues of *H. jedediah* and *H. spadix* using a standard phenol-chloroform extraction and DNeasy Extraction Kit (Qiagen Inc., Valencia, CA, USA). I sequenced a portion of the mitochondrial gene for cytochrome oxidase subunit I (*cox1*) for *H. jedediah* and *H. spadix* samples using procedures identical to those used for *H. arizonensis* (Chapter 2). To align sequences, I used SEQUENCHER v. 4.6 (Gene Codes Corp Inc., Ann Arbor, MI, USA) and verified alignments against those from the *H. arizonensis* dataset.

Phylogeographic Analyses

I used NETWORK v. 4.5.1.6 (Fluxus Technology Ltd 2004) to construct median-joining networks (Bandelt et al. 1999) of the *cox1* haplotypes for each species. Unlike tree-based approaches, networks do not assume that ancestral haplotypes are extinct, allowing for better estimates of relationships among sequences when genetic structure is shallow (Crandall and Templeton 1996). I first constructed preliminary networks for each species to explore the effect of different transition/transversion weighting schemes, although changing these parameters made little difference to network topologies. I constructed final networks with transitions and transversions weighted 3 to 1, and used the maximum parsimony option to remove excessive links (Polzin and Daneshmand 2003).

I used ARLEQUIN v. 3.11 (Excoffier et al. 2009) to estimate nucleotide diversity (π) and haplotype diversity (h) for each species, and for all but one of the haplogroups within *H. jedediah* and *H. spadix* that were inferred from the haplotype network (one

group was not assessed due to an insufficient sample size; see Results). In a comparative context, these diversity indices have been shown to reveal patterns of past population expansion or contraction (Grant and Bowen 1998; Kerdelhue et al. 2009). As an additional test of demographic expansions, I used ARLEQUIN to calculate Fu's *F* (Fu 1997) statistics for each species and each haplogroup.

To visually assess the distribution of genetic diversity for each species, I constructed landscape interpolations of nucleotide and haplotype diversity. First, I pooled localities for each species within 10 km from each other and without obvious intervening biogeographic barriers. Using ARLEQUIN, I then calculated nucleotide and haplotype diversity for individual sites with sample sizes of ≥4 for *H. jedediah* (due to sampling limitations in the eastern Mojave Desert), and ≥8 for *H. spadix* and *H. arizonensis*. I then interpolated each of these values across the areas of currently suitable climate for each species (as predicted by SDMs) using the inverse distance weighted interpolation procedure of the spatial analyst package (Watson and Philip 1985) in ARCGIS.

To assess spatial patterns of genetic differentiation within each species, I used ALLELES IN SPACE v. 3.11 (Miller 2005; Miller et al. 2006) to generate pairwise genetic distances from a Delaunay triangulation-based connectivity network (Brouns et al. 2003; Watson 1992). Distance values were calculated as residuals from a regression of genetic and geographic distances, which corrects for autocorrelation between these measures (Miller et al. 2006). Values were then interpolated onto a 50 x 50 grid in ALLELES IN SPACE with the distance weighting parameter set to 0.5.

I used BEAST v. 1.5.4 (Drummond and Rambaut 2007) to estimate time to most recent common ancestor (TMRCA) for each species and each haplogroup with an adequate sample size (>8), using best-fit substitution models calculated using JMODELTEST v. 0.1.1 and the Akaike information criterion (AIC; Posada 2008). Since fossil data are not available, I calibrated the analyses using a *cox1* mutation rate of 0.007 substitutions/site/million years using an uncorrelated lognormal clock model. This rate was estimated for an unrelated group of scorpions (Gantenbein et al. 2005), but has been used in other assessments of scorpions species (e.g. Prendini et al. 2005; Borges et al. 2010; Graham et al. 2012). I set the standard deviation to 0.003, thereby encompassing an alternative mutation rate for scorpions estimated for 16S rDNA (Gantenbein and Largiadèr 2002; see Chapter 2). I ran BEAST for 50 million generations for *H. jedediah* and *H. spadix*, and for each haplogroup, but ran two independent runs for *H. arizonensis* in order to reach ESS values greater than 200. After discarding 10% of the generations as burn-in, I used Tracer to ensure stationarity, to obtain TMRCA estimates, and to draw the Bayesian skyline plots.

Results

Species Distribution Models

The various SDMs yielded high AUC scores for both training and testing data (both > 0.95), indicating that the models performed significantly better than random (Raes and ter Steege 2007). Under current climatic conditions, the SDM for *H. jedediah* indicated that areas of suitable climate encompassed most of the Mojave Desert,

extending north through the low to mid-elevations of the western Great Basin, and into the Snake River Plain of southern Idaho and eastern Oregon (Fig. 3.2a). No regions of suitable climate were predicted in the eastern Great Basin for this species except for a small disjunct low elevation patch in the Bonneville Basin, which was part of Lake Bonneville during pluvial maxima (Grayson 1993).

Models of areas that might be suitable for *H. jedediah* during the LGM were similar under both CCSM and MIROC projections (Figs. 3.2d & 3.2g). Both models suggested that the Great Basin was devoid of suitable climate during the LGM except for small isolated patches in the Lahontan Trough north of Reno, NV, much of which was under water during pluvial maxima (Grayson 1993). Suitable climate was predicted to have remained available during the LGM in parts of the Mojave Desert, Salton Trough, sections of the Lower Colorado River Valley, and along the majority of the California coast, the coastal ranges, and California's Central Valley. The models also highlighted a potentially isolated glacial refugium at the northern end of the Lower Colorado River (see discussion of this region in Chapter 2). The greatest difference between the two LGM models for *H. jedediah* was along the Snake River Plain, which was predicted to have retained suitable climate in the MIROC model (Fig. 3.2g) but not in the CCSM model (Fig. 3.2d).

The SDM for *H. spadix* under current climatic conditions (Fig. 3.2b) indicated suitable climate throughout much of the Colorado Plateau and portions of the southern Great Basin Desert and eastern Mojave Desert. In the eastern portion of this range, the distribution of suitable climate extended into western Colorado and northwestern New

Mexico following the drainages of the Colorado, Delores, and San Juan rivers. During the LGM, Both the CCSM and MIROC models for *H. spadix* suggested that the majority of this area on the Colorado Plateau was not suitable (Figs. 3.2e, h). Both models, however, depicted small patchworks of suitable climate in portions of the Mojave Desert, but the MIROC model also included suitable patches within the northern end of the Lower Colorado River Valley (see Chapter 2). The MIROC model also predicted a large area of suitable climate along the Mogollon Rim in Arizona, the northeast Sonoran Desert, and into the Madrean region of northern Mexico.

Phylogeography

Mitochondrial *cox1* sequences contained 101 variable and 63 parsimony informative sites for *H. jedediah*, and 39 variable and 24 parsimony informative sites for *H. spadix*. From these data, I identified a total of 90 unique halpotypes (70 and 20 respectively). In *H. arizonensis,* I had previously identified 149 variable and 103 parsimony informative sites among 141 haplotypes (Chapter 2). Careful examination of chromatograms revealed no evidence of co-amplification of nuclear mitochondrial pseudogenes in any of the sequences (Bertheau et al. 2011).

The median-joining haplotype network for *H. jedediah* (Fig. 3.3a) revealed three main haplogroups. The largest haplogroup formed the center of the network and consisted of haplotypes distributed throughout the Mojave Desert (Mojave Haplogroup). An additional haplogroup, nine mutational steps removed from the central group, consisted of haplotypes narrowly distributed within the eastern Mojave Desert,

ranging from the Amargosa Valley to the Las Vegas Valley (Southern Nevada Haplogroup). A third haplogroup, also nine steps removed from the central group, consisted of specimens from northern portions of the sampling distribution (Northern Haplogroup). Within this haplogroup, individuals from the northern Great Basin Desert and Snake River Plain formed a star-shaped network (indicated by white circles in Fig. 3.3a), a pattern that can indicate recent demographic expansion (Avise 2000).

The median-joining network for *H. spadix* also consisted of three haplogroups which were separated by a minimum of 8 and 9 mutational steps (Fig. 3.3b). These haplogroups were arranged geographically, with a group in the Grand Canyon and Virgin Mountains (Western Haplogroup), a group in the Grand Canyon and Little Colorado River Valley (Central Haplogroup), and a group from the Canyonlands of southern Utah and northern Arizona (Eastern Haplogroup). Of these, the haplogroup from the Grand Canyon and Virgin Mountains contained the greatest genetic diversity, whereas the haplogroup from the Canyonlands formed a star shape in the network. The number of mutational steps among the four samples in the Grand Canyon and Little Colorado River Valley was greater than those within the haplogroup to the northeast, although sampling was too limited to provide a meaningful assessment of this genetic diversity.

Landscape interpolations of genetic distance values (Fig. 3.4) formed geographic clines of high to low genetic distances for each species. For *H. jedediah*, genetic distances were relatively high in the south, with the highest differentiation occurring as high peaks in the southwest and southeast in the Mojave Desert and southern Great Basin. At approximately 38°N, distance values decreased considerably, with the lowest

values occurring in the low-elevations areas of the Lahontan Trough within the Great Basin. Genetic distance interpolations for *H. spadix* reveal a geographic cline running from the southwest to northeast, with the highest values in the west along the Grand Canyon region, eastern Mojave Desert, and southeast Great Basin. For *H. arizonensis*, genetic distances were greatest in the southeast, gradually decreasing to the northwest. Two troughs of low distance values occurred along this cline, one in the vicinity of Lower Colorado River Valley, and another in the extreme northwest in areas surrounding the Amargosa Valley.

Demographic Analyses

Comparisons of nucleotide and haplotype diversity can reveal patterns of past demographic expansion and/or constriction (Grant and Bowen 1998). Nucleotide diversity values greater than 0.005 and haplotype diversity values greater than 0.5 are considered high, whereas values lower than these thresholds are considered low (Grant and Bowen 1998). Nucleotide and haplotype diversity were high for each species (Table 3.2), indicating significant genetic structuring. For *H. jedediah*, both the Northern Haplogroup and the Southern Nevada Haplogroup contained high haplotype diversity but low nucleotide diversity, a pattern indicative of recent population growth. A similar pattern was present for the Eastern Haplogroup in *H. spadix.* For the Mojave Haplogroup in *H. jedediah* and the Western Haplogroup of *H. spadix* both nucleotide and haplotype diversity were high*,* indicating the potential that these groups maintained larger, and more stable effective population sizes. Values of Fu's *F* were negative for

each species and each haplogroup, which is expected for groups that have undergone expansions (Table 3.2). Although samples sizes were small, the values were not significant for the southern haplogroup in *H. jedediah* and the Western haplogroup *in H. spadix*, indicating that a model of stability could not be rejected for these groups.

For *H. jedediah*, the landscape interpolation of nucleotide diversity, clipped to areas of currently suitable climate, indicated high diversity in the south with decreasing diversity northward (Fig. 3.5a). The interpolation of haplotype diversity is similar (Fig. 3.5d), but with an area of low diversity at the transitional region between the Great Basin and Mojave deserts near the White-Inyo Mountain Range. Furthermore, an area of low nucleotide diversity and high haplotype diversity occurs along the Owens River Valley, which extends north from the Mojave Desert. In combination, these data suggested that populations of *H. jedediah* probably remained stable along the northern Lower Colorado River Valley and in parts of the northern Mojave, but expanded northward into the Great Basin and most recently into the Snake River Plain.

Landscape interpolations of nucleotide diversity for *H. spadix* indicated high diversity in the western portion of the predicted distribution and much lower nucleotide diversity in the east (Fig. 3.5b). The interpolation of haplotype diversity is similar except that values were high in the northeastern areas (Fig. 3.5e) near Moab, Utah (site 51). This pattern is consistent with a bottleneck or founder event, suggesting that populations of *H. spadix* could have remained stable in the western part of its range and undergone a recent demographic expansion to the northeast. Results from interpolations of nucleotide and haplotype diversity in *H. arizonensis* depicted a general

trend of high diversity in the south, especially the southeast, with decreasing diversity northward.

Although confidence intervals are large, Bayesian skyline plots (Fig. 3.6) portrayed similar trend lines for each *H. jedediah* haplogroup, indicating that population sizes for groups of this species appear to have undergone demographic expansion starting about 50 to 100 Ka. For *H. spadix,* the small samples size resulted in little predictive power, although the pattern may indicate that the population remained relatively stable through the late Pleistocene and Holocene. For *H. arizonensis*, BSPs depict population growth during the late Pleistocene, but relatively stable population sizes for Groups II-VI through the late Pleistocene and Holocene (Chapter 2). TMRCA estimates for the groups within these species all fell within the late Pleistocene. Mean estimates of the TMRCA for *H. jedediah* and *H. spadix* were in the mid Pleistocene, with that for *H. arizonensis* in the late Pliocene (Table 3.2).

Discussion

Giant Hairy Scorpion Phylogeography

Climate models for *H. arizonensis* predicted fragmented areas of suitable climate during the LGM, particularly in the Mojave Desert (Figs. 3.2f, 3.2i), and mitochondrial data revealed a minimum of six geographically structured lineages (Fig. 3.3c). Several of the lineages overlap the areas predicted to contain suitable climate during the LGM, so historical fragmentation of suitable climate may have facilitated lineage formation within the species. Genetic diversity was generally higher in the southern distribution of

H. arizonensis, decreasing northward (Figs. 3.4c, 3.5c, f). Under the assumption that earlier Pleistocene glacial periods experienced climates similar to that of the LGM, these results suggest that the phylogeography of *H. arizonensis* was shaped by a history of fragmentation into glacial refugia (Fig. 3.7c) with resultant reduction of population sizes, followed by demographic expansion as climate warmed. Lower diversity within northern populations could reflect stronger bottleneck effects than in areas further south (see Chapter 2 for details).

The majority of the genetic diversity within *H. jedediah* occurs within the Mojave Desert (Figs. 3.4a, 3.5a, d), and a haplotype network revealed three main haplogroups within this species (Fig. 3.3a). All three haplogroups are present in the Mojave Desert, but only one occurs in the Great Basin and Snake River Plain (Fig. 3.7a). Since the western Great Basin and Snake River Plain contain only a subset of haplotypes that are found in the south, *H. jedediah* may have expanded recently from the south into these northern areas following a leading edge model of colonization (Hewitt 1996). Demographic analyses are concordant with this scenario, as genetic patterns within the northern haplogroup of *H. jedediah* are consistent with population expansion (Table 3.2, Fig. 3.6).

The SDMs also support a hypothesis of recent northward expansion by *H. jedediah*. Currently suitable climates in the Great Basin and Snake River Plain were predicted to be mostly unsuitable during the LGM (Fig. 3.2d, g). In the Mojave Desert, however, the SDMs predicted maintenance of suitable climate during the latest glacial period, although in smaller, more fragmented areas than depicted currently (Figs. 3.2d,

g). Interestingly, SDMs also predicted a large area of suitable climate for *H. jedediah* along the California coast and California's Central Valley during the LGM. Although *Hadrurus* have never been documented from the California coast, *Hadurus obscurus* Stahnke, a species closely related to *H. jedediah* and *H. spadix* (Francke and Prendini 2008; unpublished data), is known from California's Central Valley.

To the east, SDMs predicted areas with currently suitable climate for *H. spadix* throughout the Colorado Plateau and in parts of the eastern Mojave Desert and southern Great Basin (Fig. 3.2b). During the LGM, however, no suitable climate was predicted on the Colorado Plateau (Figs. 3.2e, h). Instead, the distribution was predicted to have been shifted to the south and to the west during the LGM, with the most proximal areas of suitable climate found along the Colorado River just west of the Grand Canyon, as well as within the Virgin River Basin. The haplotype network for *H. spadix* revealed three geographically structured haplogroups (Fig. 3.3b), two of which have coalescent times in the late Pleistocene (Table 3.2). During late Pleistocene glacial periods, the climate of the Colorado Plateau was in general much cooler and drier than it is today, and vertical distributions of many plant species were displaced to lower elevations (Betancourt 1990). If *H. spadix* underwent a similar response to glacial climates, then the lack of suitable climate on the Colorado Plateau depicted by the models (Figs. 3.2e, h) could be due to using bioclimatic rasters (layers) that were too coarse to capture fine-scale climate conditions within canyons.

The westernmost haplogroup within *H. spadix* consisted of individuals collected from the western Grand Canyon and the Virgin Mountains. The western Grand Canyon

is essentially a low-elevation corridor of warm desert extending into the Colorado Plateau (Cole 1990), providing an elevational gradient of different microhabitats along which organisms like *H. spadix* could have endured changing climates. This seems particularly true for rocky south-facing slopes and hillsides, which could have retained solar radiation and perhaps remained warmer than adjacent habitats during glacial cycles. Although my sample size was small (12 individuals from 3 sites), demographic analyses suggest that the effective population size of the western haplogroup has remained stable (Table 3.2, Fig. 3.6).

On the eastern Colorado Plateau, I found another haplogroup distributed along the San Juan and Upper Colorado rivers, potentially reflecting another glacial refugium in this area. Although the sample size was small, the star-shaped haplotype network (Fig. 3.3b) and patterns of genetic diversity of this eastern haplogroup (low π and high h - Fig. 3.5) are consistent with a population bottleneck followed by rapid population growth (Grant and Bowen 1998). Haplotype diversity in this group was highest in the northeast (Figs. 3.5e), so *H. spadix* in the eastern Colorado Plateau may have expanded from a glacial refugium along the Upper Colorado River drainage (Fig. 3.7b). Demographic analyses of the eastern haplogroup portray conflicting results, as Fu's F rejected a hypothesis of demographic stability (Table 3.2) but the Bayesian skyline plot indicated a stable effective population size (Fig. 3.6). However, credibility intervals for the estimated effective population size of the Eastern Haplogroup (based on 27 individuals from 3 sites) were large and the coalescent time was recent (Table 3.2), so the sequence data may not have contained enough variation to detect the true

demographic signal. I also detected a haplogroup in *H. spadix* from areas along the drainage of the Little Colorado River in northern Arizona, so the species may have retained populations in this area during glacial periods as well. Unfortunately, my sample size was not large enough for demographic analyses of this group.

The SDMs predicted suitable climate in areas within the eastern Mojave Desert and southern Great Basin (Fig. 3.2b), and although my sampling was limited, I have not documented any records of *H. spadix* from this region. Instead, this area is within the known distribution of *H. jedediah*. Potentially westward expansion of *H. spadix* may be inhibited by competitive or demographic processes associated with its close relative. Alternatively, the current distribution of *H. spadix* might actually reflect ecological conditions (such as sandstone habitats of the Colorado Plateau) that were not reflected in the climatic layers used for modeling. Such factors seem especially prone to influence scorpion distributions since scorpions tend to exhibit strong ecological stenotopy and are known to be influenced by edaphic conditions (Fet et al. 1998; Prendini 2001, 2005).

Comparative Phylogeography: Differential Impact of Pleistocene Climates

Pleistocene climate oscillations appear to have influenced the sizes and distributions of *Hadrurus* scorpions in the Mojave Desert, Sonoran Desert, Great Basin, Colorado Plateau, and Snake River Plain. Demographic responses and the scale and direction of distributional shifts, however, varied considerably among the species and regions. Phylogeographic patterns suggest that the distributions *H. arizonensis, H. jedediah,* and *H. spadix* all deceased in size during the LGM. Of these species, *H.*

arizonensis appears to have experienced the smallest reduction, but the highest degree of fragmentation, as it may have endured glacial conditions in six or more refugia (Chapter 2). This pattern is generally consistent with those from co-distributed organisms in the Mojave and Sonoran Deserts that also appear to have endured glacial periods in isolated desert refugia (Bell et al. 2010). These deserts experience less seasonality than regions to the north, so extreme conditions during glacial periods do not appear to have been as severe as in northern areas. In addition, the Mojave and Sonoran deserts are at lower mean elevations than the adjacent arid regions, so mean temperatures during glacial periods were generally warmer (Grayson 1993).

On the Colorado Plateau, the distribution of *H. spadix* also appears to have decreased in size and became fragmented during the LGM, but potentially with more of a range reduction than *H. arizonensis* and less fragmentation. Genetic data suggest that *H. spadix* endured glacial conditions in at least three refugia and colonized much of the current range on the Colorado Plateau, especially the eastern portion, as climate warmed following the LGM (Fig. 3.7b). Other plants and animals of the Colorado Plateau are thought to have responded similarly. According to data from macrofossils (Bentancourt et al. 1990; Thompson and Anderson 2000), plants currently inhabiting the Colorado Plateau underwent similar responses to glacial climates, as some tree species, such as *Pinus ponderosa* Douglas ex Lawson (ponderosa pine) and *Pinus edulis* Engelmann (Colorado pinyon), were displaced southward during the glacial periods. Phylogeography of some animal taxa on the Colorado Plateau, such as *Bufo punctatus* Baird and Girard (red-spotted toads) and the *Perognathus fasciatus* Wied-Neuwied

species group (silky pocket mice), have indicated close affinities with the Chihuahuan Desert, southern Rocky Mountains, and Great Plains (Jaeger et al. 2005; Neiswenter and Riddle 2011). Phylogeographic patterns from others, such as *Xantusia* Baird (night lizards; Sinclair et al. 2004), *Hypsiglena* Cope (night snakes; Mulcahy 2008), *Crotalus* Linnaeus (rattlesnakes; Pook et al. 2000; Ashton and de Queiroz 2001), and *Sceloporus* Wiegmann (spiny lizards; Orange 1997; Schulte et al. 2006; Leaché and Mulcahy 2007) suggest a western ancestry in the Sonoran and Mojave deserts. Thus, as inferred by Leaché and Mulcahy (2007), the Colorado Plateau has a mixed ancestry, with a modern biota containing a combination of species from surrounding arid regions.

Phylogeographic patterns suggest that *H. jedediah* underwent a severe distributional response to changing climates during glacial cycles. As predicted by SDMs (Fig. 3.2), *H. jedediah* appears to have only recently colonized the entire northern half of its current distribution. Contrary to the Mojave and Sonoran deserts, the northern areas of the Great Basin and Snake River Plain experience greater seasonality and colder mean temperatures due to their more northern latitudes and lower elevations. During the glacial periods, organisms within these regions would have had to either track their climate niche by shifting distributions, or endure extreme climate conditions *in situ* by altering their realized niches. Phylogeographic analyses of Great Basin rodents, *Dipodomys microps* Merriam (chisel-toothed kangaroo rat; Jezkova et al. 2011) and *Microdipodops megacephalus* Merriam (dark kangaroo mouse; Hafner and Upham 2011) suggest that these rodents shifted realized niches and persisted in the Great Basin. Alternatively, genetic patterns from *Phrynosoma platyrhinos* Girard (desert

horned lizard; Jezkova 2010), *Neotoma cinerea* (Ord) (bushy-tailed woodrat; Hornsby and Matocq 2011), and those described herein for *H. jedediah* all indicate that they shifted distributions, and only recently colonized the northern areas since the LGM from more stable regions in the south (but see Chapter 4 for a novel response).

In summary, *H. arizonensis* and *H. spadix* appear to have endured Pleistocene glacial episodes in patches of suitable climate throughout their distributions, but *H. jedediah* may have been more severely impacted, only recently colonizing the western Great Basin and Snake River Plain from glacial refugia to the south. Since *H. arizonensis*, *H. jedediah*, and *H. spadix* are closely related and morphologically similar, these differences should reflect the relative influence of Pleistocene climates and topography in different North American aridlands, rather than resulting from divergent phenotypes or phylogenetic signal. Working under this assumption, the arid biotas of the Mojave Desert, Sonoran Desert, Great Basin, Colorado Plateau, and Snake River Plain all appear to have been impacted to some degree by Pleistocene glacial cycles. The Great Basin and Snake River Plain biotas, however, may have been particularly sensitive, as many of the current species occupying these regions appear to have only recently colonized as glacial conditions retreated and climates warmed.

Table 3.1 Location and voucher information for genetic samples used in this study. Site numbers correspond with localities portrayed in Fig. 3.1. Coordinates only represent the general sample area.

Site	Species	State	Locality	Lat.	Long.	*n*	Voucher Numbers
1	*H. jedediah*	CA	BERDOO CYN	33.8276	-116.1512	3	LP8909, LP8950, LP8506
2	*H. jedediah*	CA	PALMDALE	34.5082	-117.9790	2	MG1110, MG1111
3	*H. jedediah*	CA	PROVIDENCE MTS	34.9148	-115.5457	4	MG1125, MG1126, MG1127, MG1128
4	*H. jedediah*	AZ	OATMAN	35.0087	-114.3880	1	LP2444
5	*H. jedediah*	CA	MOJAVE	35.0689	-118.2410	1	MG0711
6	*H. jedediah*	NV	XMAS TREE PASS	35.2612	-114.7440	5	MG1051, MG1053, MG1054, MG1057, MG1058
7	*H. jedediah*	CA	JAWBONE CYN	35.3175	-118.0810	1	LP7225
8	*H. jedediah*	CA	MORNING STAR MINE	35.3627	-115.4229	1	LP8503
9	*H. jedediah*	CA	AVAWATZ MTS	35.5191	-116.3184	1	LP4396
10	*H. jedediah*	NV	NIPTON RD	35.5197	-115.1400	2	MG0221, MG0222
11	*H. jedediah*	NV	MESQUITE DUNES	35.7622	-115.5797	3	MG0227-MG0229
12	*H. jedediah*	NV	SANDY VALLEY	35.9016	-115.3973	1	LP8512
13	*H. jedediah*	CA	WILD ROSE	36.0926	-117.1327	1	MG0775
14	*H. jedediah*	NV	NELLIS AFB	36.2231	-115.0190	1	MG0793
15	*H. jedediah*	NV	BLUE POINT	36.3928	-114.4425	1	MG0570
16	*H. jedediah*	CA	EMIGRANT CYN	36.4102	-117.1747	2	MG0464, MG0465
17	*H. jedediah*	CA	ECHO CYN	36.5049	-116.7070	2	MG0771, MG0985
18	*H. jedediah*	CA	TUTTLE CREEK	36.5058	-118.1733	8	MG0455-MG0462
19	*H. jedediah*	CA	SALINE VALLEY	36.5599	-117.5870	1	LP5039
20	*H. jedediah*	CA	LONG JOHN CYN	36.6693	-117.9707	8	MG0300, MG0301, MG0303-MG0308
21	*H. jedediah*	CA	MESQUITE SPRINGS	36.9631	-117.3710	1	LP4975
22	*H. jedediah*	NV	SARCOBATUS	37.0400	-116.8157	9	MG0938-MG0946
23	*H. jedediah*	CA	GLACIER LODGE RD	37.0597	-118.2637	1	LP8904
24	*H. jedediah*	CA	EUREKA DUNES	37.1093	-117.6741	6	MG0149, MG0150, MG0566-MG0569
25	*H. jedediah*	NV	N BEATTY	37.2946	-117.0462	1	MG0014
26	*H. jedediah*	CA	DEEP SPRINGS	37.3130	-118.1031	1	MG0317
27	*H. jedediah*	CA	TUNGSTON HILLS	37.3567	-118.5291	6	LP5046, MG0311-MG0315
28	*H. jedediah*	NV	TIKABOO	37.5740	-115.6079	10	MG0908-MG0917

Table 3.1. Location and voucher information continued

Site	Species	State	Locality	Lat.	Long.	*n*	Voucher Numbers
29	*H. jedediah*	NV	MURIETTA	38.2461	-118.3905	1	MG0441
30	*H. jedediah*	NV	LUNAR CRATER	38.3892	-116.0684	1	MG0316
31	*H. jedediah*	NV	BLACK DYKE MT	38.3949	-118.1811	1	LP4777
32	*H. jedediah*	NV	MINA	38.4293	-118.0657	10	MG0415, MG0416, MG0847-MG0854
33	*H. jedediah*	NV	HAWTHORNE	38.6111	-118.7176	1	LP6295
34	*H. jedediah*	NV	BLOW SAND MTS	39.1990	-118.7221	2	MG0443, MG0444
35	*H. jedediah*	NV	KINGSTON	39.2080	-117.0929	2	MG0877, MG0878
36	*H. jedediah*	NV	FERNLEY	39.5073	-119.2175	3	MG0419-MG0421
37	*H. jedediah*	NV	SPARKS	39.8553	-119.6559	1	LP6296
38	*H. jedediah*	NV	HONEY LAKE VALLEY	40.1290	-119.8215	1	MG0442
39	*H. jedediah*	NV	GERLACH	40.6431	-119.3127	2	MG0289, MG0290
40	*H. jedediah*	NV	WINNEMUCCA	41.1256	-117.7631	9	MG0278-MG0285
41	*H. jedediah*	NV	SURPRISE VALLEY	41.1622	-119.9612	2	MG0287, MG0288
42	*H. jedediah*	ID	BRUNEAU CYN	42.7622	-115.7394	2	MG0257, MG0258
43	*H. jedediah*	ID	GLENNS FERRY	43.0174	-115.2463	10	MG0246-MG0255
44	*H. jedediah*	ID	MURPHY	43.2012	-116.5861	9	MG0268-MG0277
45	*H. spadix*	AZ	SUNSET CRATER	35.6053	-111.3684	3	LP7792, MG1016, MG1018,
46	*H. spadix*	AZ	BRIGHT ANGEL	36.0660	-112.1369	2	MG1009, MG1010
47	*H. spadix*	AZ	TOROWEAP	36.2256	-113.2263	1	MG1017
48	*H. spadix*	AZ	VIRGIN MTS	36.6622	-114.0116	10	MG0162, MG0959-MG0967
49	*H. spadix*	AZ	LEE'S FERRY	36.7261	-111.7581	9	MG0182, MG0789, MG0889-MG0894, MG0896
50	*H. spadix*	UT	BLUFF	37.2896	-109.6329	9	MG0201, MG0790, MG0989-MG0995
51	*H. spadix*	UT	MOAB	38.6264	-109.5061	9	LP7277, MG0208-MG0214, MG0219

Table 3.2. Sample size (n), number of haplotypes (*k*), nucleotide diversity (π), haplotype diversity (*h*), results from Fu's F (*F*), and estimated time to most recent common ancestor (TMRCA; in Ma) for species and haplogroups of *Hadrurus* (see text). Asterisks indicate values with associated p-values of <0.02 (the threshold value corresponding to $\alpha = 0.05$ for Fu's *F*). Values for *Hadrurus arizonensis* Ewing and Groups I–VI are repeated from Chapter 2.

Species / haplogroup	**n**	***k***	***π***	***h***	***F* (p-value)**	**TMRCA**
H. jedediah	141	69	0.012	0.917	-24.136*	1.46 (0.99-1.98)
Northern	71	21	0.003	0.707	-7.130*	0.61 (0.29-0.96)
Mojave	56	39	0.006	0.970	-25.224*	0.51 (0.23-0.81)
Southern NV	14	9	0.004	0.879	-1.933	0.61 (0.37-0.88)
H. spadix	43	20	0.008	0.804	-2.650	1.33 (0.75-1.96)
Eastern	27	9	0.001	0.513	-7.990*	0.06 (0.02-0.11)
Western	12	8	0.007	0.924	-0.011	0.73 (0.40-1.08)
H. arizonensis	256	141	0.011	0.989	-23.944*	3.07 (2.12-4.11)
Group I	146	90	0.007	0.982	-24.799*	1.02 (0.64–1.43)
Group II	32	11	0.002	0.841	-3.764*	0.58 (0.25–0.93)
Group III	21	11	0.003	0.910	-3.463*	0.31 (0.13–0.54)
Group IV	33	11	0.002	0.867	-4.630*	0.20 (0.006–0.39)
Group V	7	7	0.005	1.000	-2.987*	0.59 (0.27–0.96)
Group VI	11	6	0.003	0.836	-0.321	0.35 (0.12–0.63)

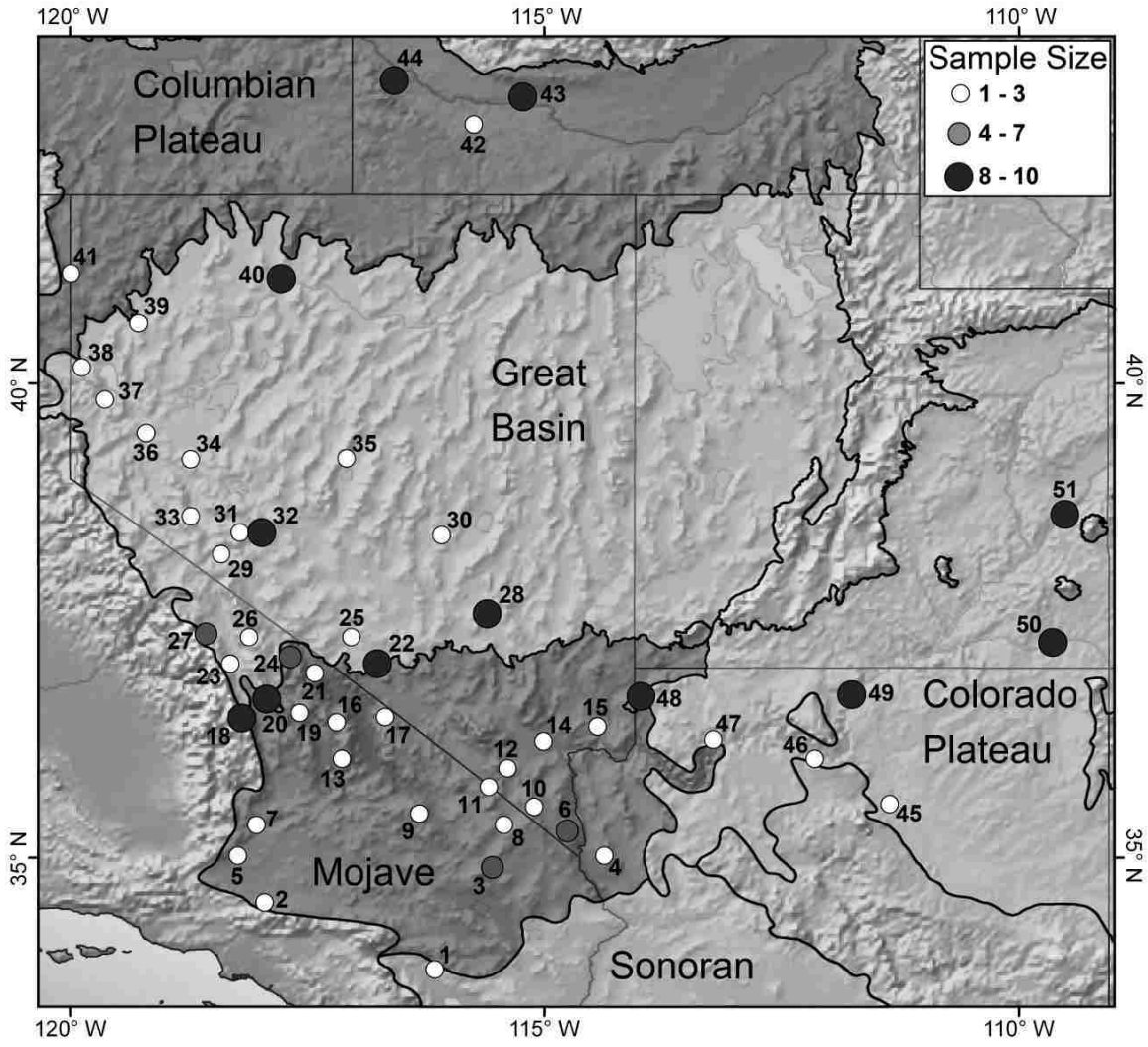

Figure 3.1. Map depicting samples sites for *Hadrurus jedediah* Prendini et al. (in prep) (sites 1-44) and *H. spadix* Stahnke (sites 45–51). Outlines and shading represent ecoregions discussed in the text. Numbers correspond to those in Table 3.1.

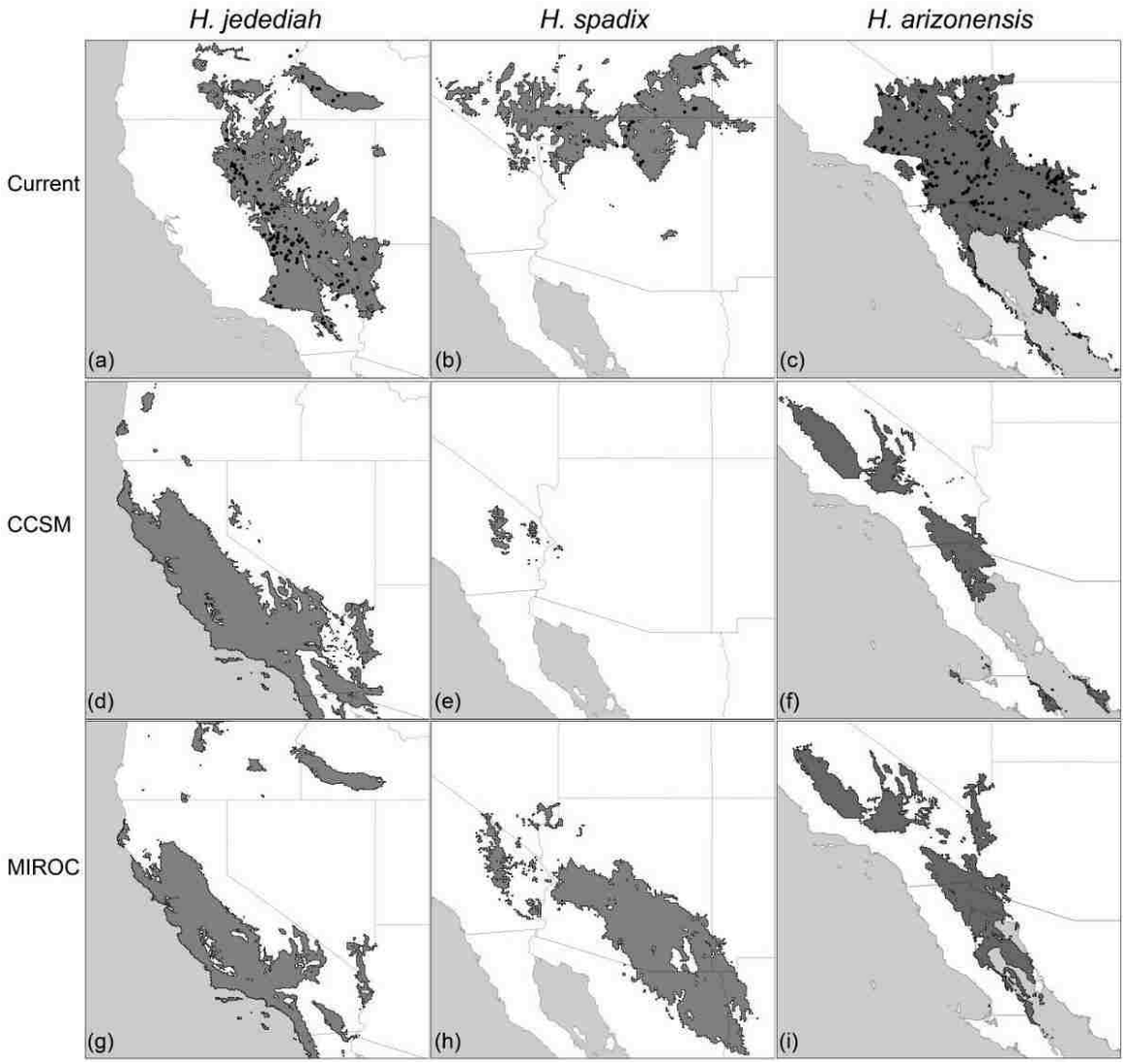

Figure 3.2. Graphical results from species distribution models generated using MAXENT and displayed using the maximum training sensitivity plus specificity threshold for *Hadrurus jedediah* Prendini et al. (in prep) (a, d, g), *Hadrurus spadix* Stahnke (b, e, h), and *Hadrurus arizonensis* Ewing (c, f, i). Models represent climate predicted as suitable (dark shading) during current conditions (a-c) and during the last glacial maximum as estimated from CCSM (d-f) and MIROC (g-i) climatic simulations. Black dots represent occurrence records used to generate the models.

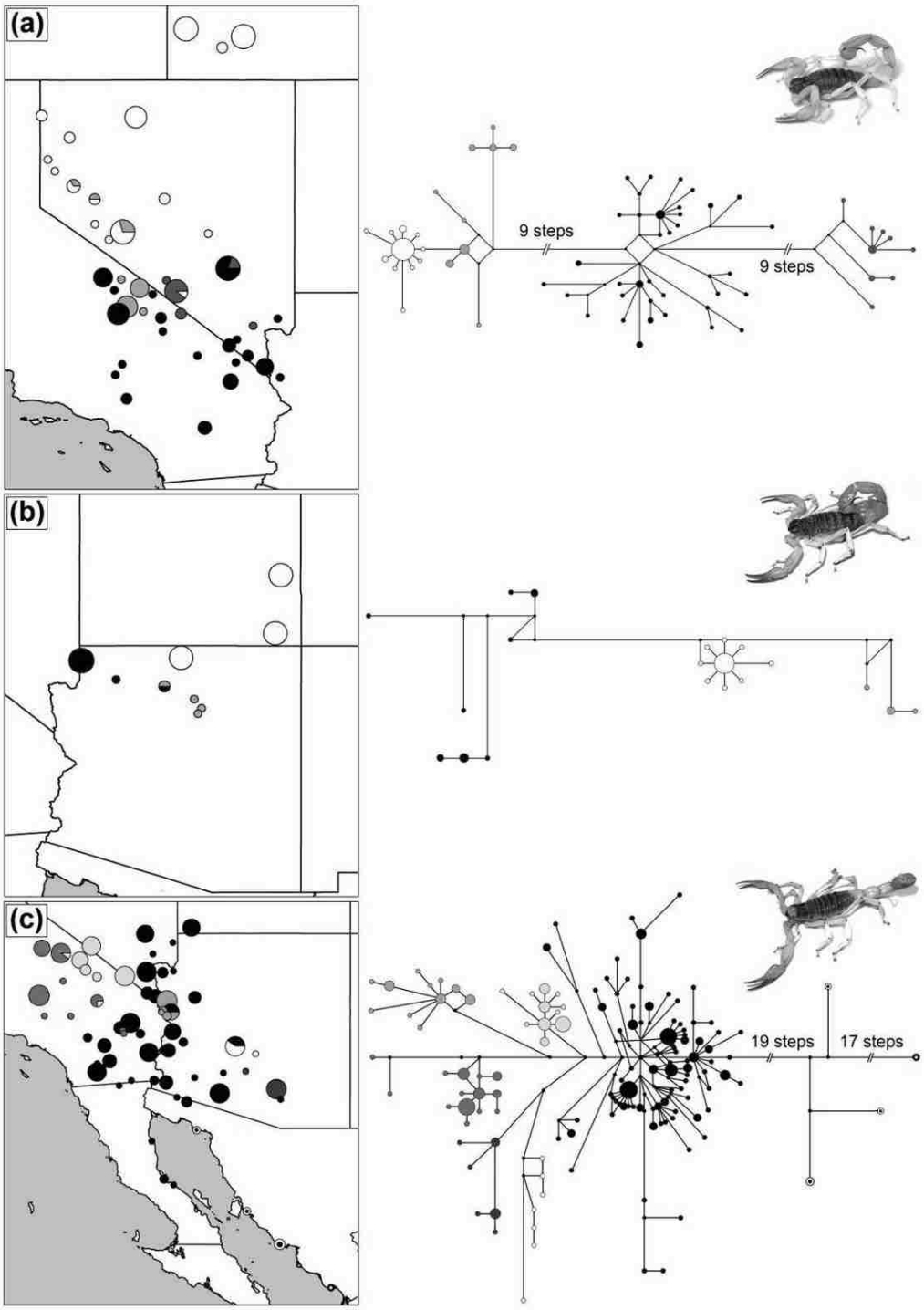

Figure 3.3. Map and network of mtDNA sequence haplotypes for *Hadrurus jedediah* Prendini et al. (in prep) (a), *Hadrurus spadix* Stahnke (b), and *Hadrurus arizonensis* Ewing (c). Each circle in the network represents one haplotype. Circle size in both the map and network are proportional to sample size. Lengths of lines connecting haplotypes in the network are proportional to the number of mutations between the haplotypes, assuming a transition/transversion ratio of 3:1.

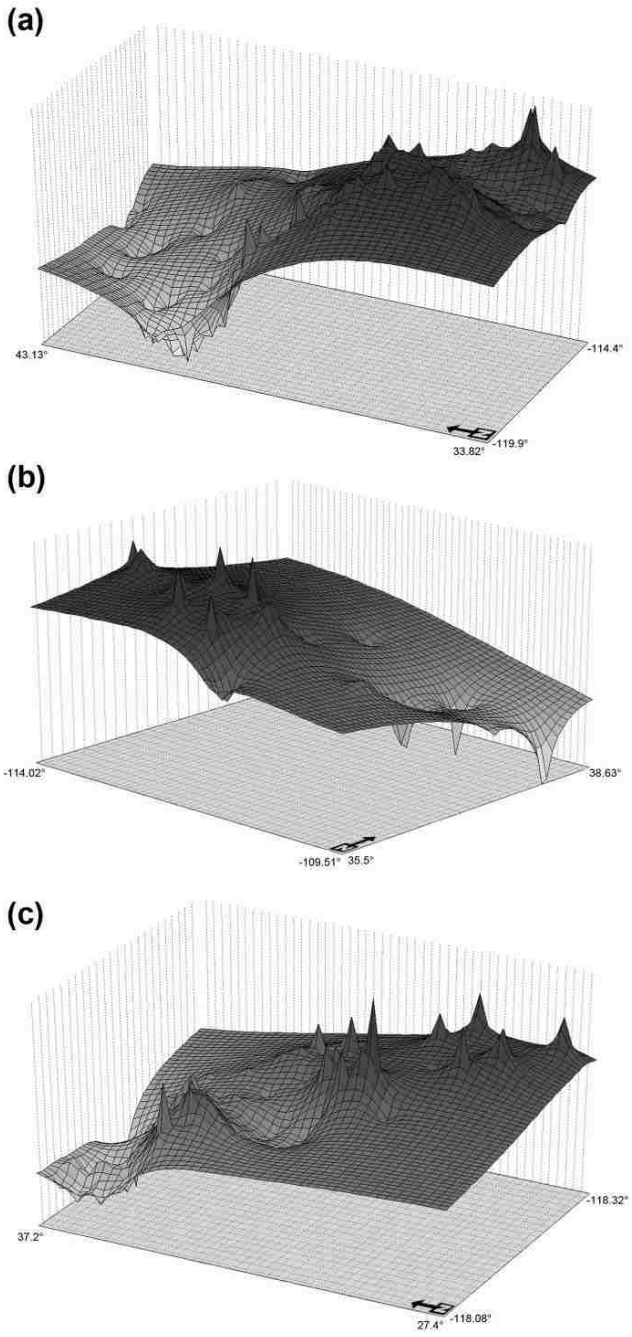

Figure 3.4. Genetic landscape shape analysis (Miller, 2005) for *Hadrurus jedediah* Prendini et al. (in prep) (a), *Hadrurus spadix* Stahnke (b), and *Hadrurus arizonensis* Ewing (c) based on *cox1* data. Surface plots depict genetic distances based on interpolations of geographic midpoints from a Delaunay triangulation network constructed among the sampled populations.

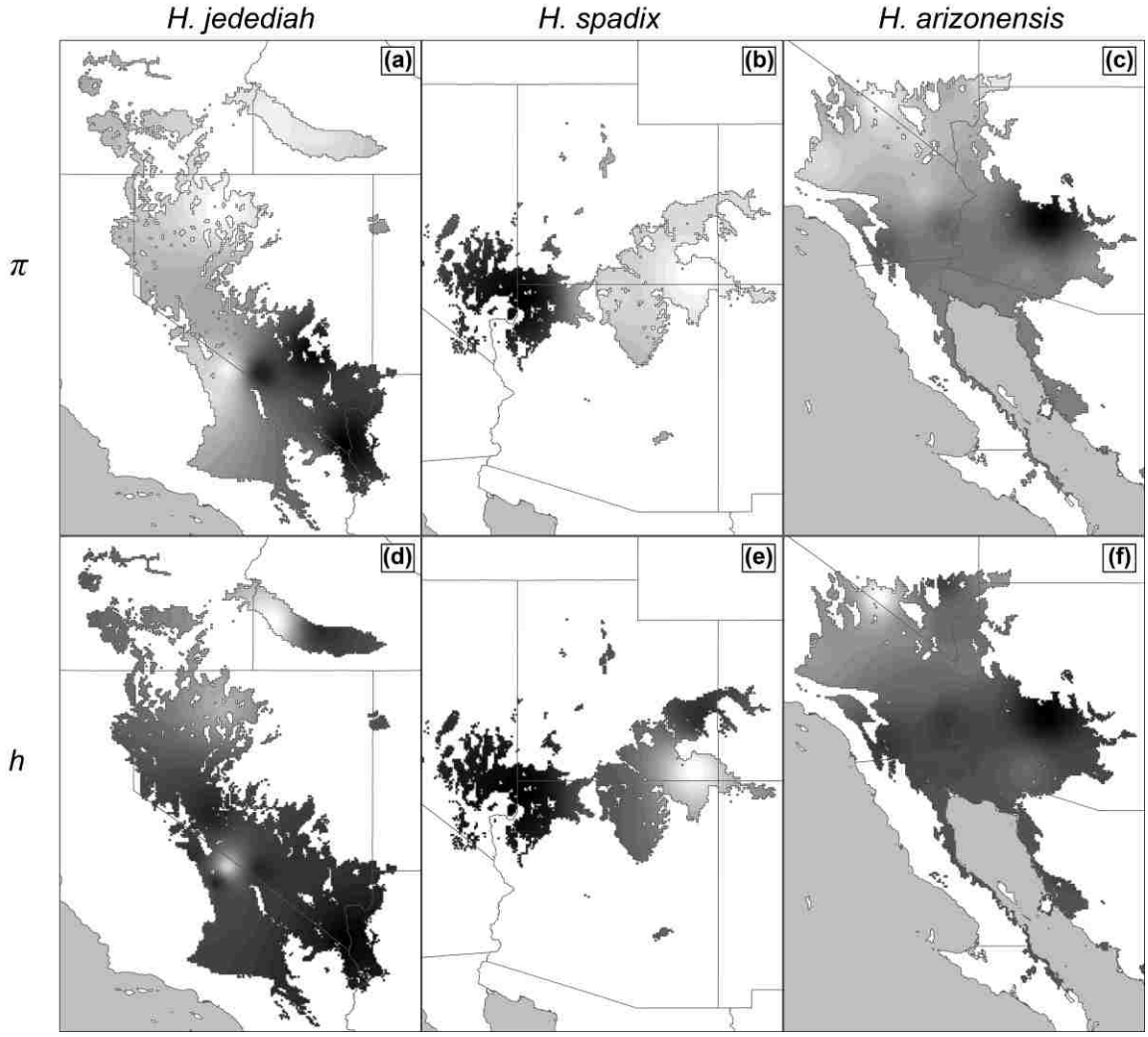

Figure 3.5. Landscape interpolations of nucleotide (a-c) and haplotype (d-f) diversity for *Hadrurus jedediah* Prendini et al. (in prep) (a & d), *Hadrurus spadix* Stahnke (b & e), and *Hadrurus arizonensis* Ewing (c & f). Shading indicates areas predicted to exhibit high (dark) and low (light) values.

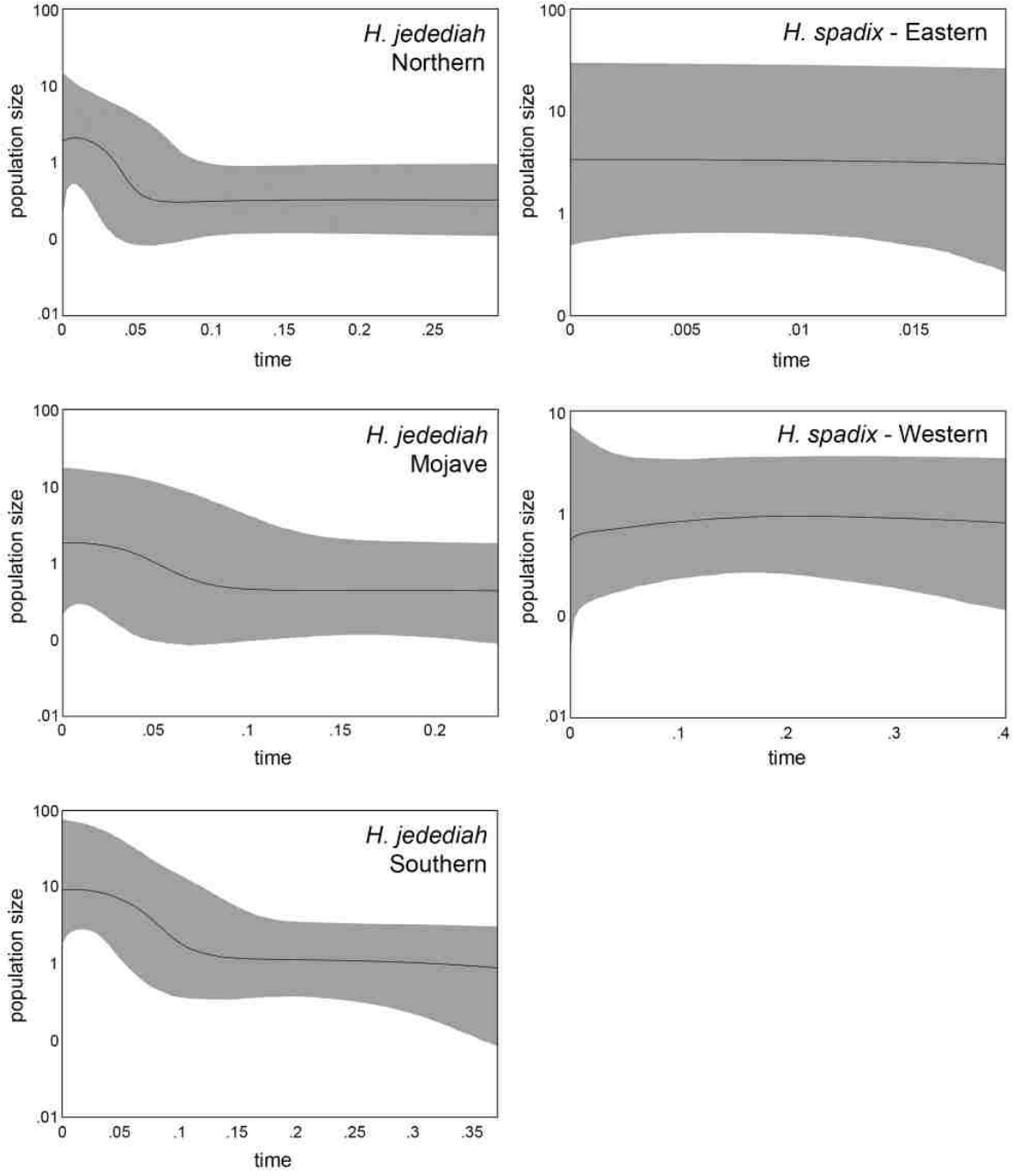

Figure 3.6. Bayesian skyline plots for *Hadrurus jedediah* Prendini et al. (in prep) and *Hadrurus spadix* Stahnke haplogroups.

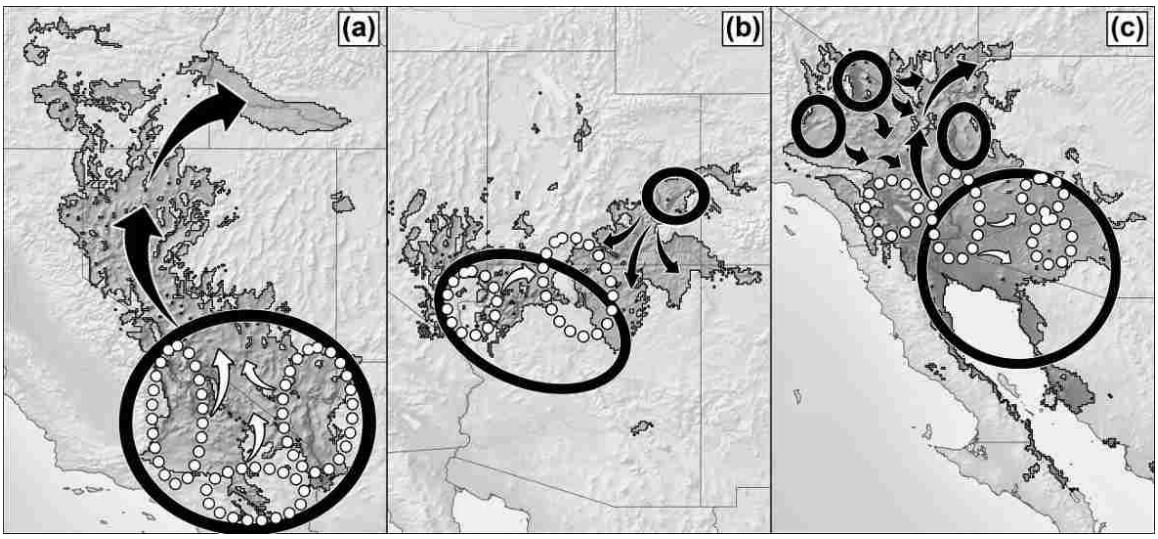

Figure 3.7. Simplified schematics to explain the Quaternary history of *Hadrurus jedediah* Prendini et al. (in prep) (a), *Hadrurus spadix* Stahnke (b), and *Hadrurus arizonensis* Ewing (c). Black circles and arrows indicate supported refugia and post-glacial colonization routes (respectively) that were strongly supported by the analyses. White circles and arrows depict potential but less obvious Quaternary events.

CHAPTER 4

PHYLOGEOGRAPHY OF THE BECK DESERT SCORPION (*PARUROCTONUS BECKI*) REVEALS PLIOCENE DIVERSIFICATION IN THE EASTERN CALIFORNIA SHEAR ZONE AND POSTGLACIAL EXPANSION FROM A GREAT BASIN REFUGIUM

Abstract

The distribution of *Paruroctonus becki* (Scorpiones: Vaejovidae), the Beck desert scorpion, spans the 'warm' Mojave Desert and the western portion of the 'cold' Great Basin Desert. During the late Pleistocene, the Great Basin climate was substantially colder than it is today, which is thought to have caused plant and animal taxa to undergo severe shifts in geographic distributions, especially since the last glacial maximum (LGM). To gain a better understanding of such distributional shifts, I used mitochondrial (*cox1* and 16S) and nuclear (ITS-2) DNA, as well as species distribution modeling, to test whether *P. becki* persisted in the Great Basin Desert during the LGM, or colonized the area as glacial conditions retreated as the climate warmed. Phylogenetic and network analyses uncovered five geographically structured mitochondrial lineages in *P. becki* with varying degrees of statistical support. Molecular clock estimates, and the geographic arrangement of three of the lineages, indicated that Pliocene geologic events in the tectonically dynamic Eastern California Shear Zone may have driven diversification by vicariance. Diversification was estimated to have continued through the Pleistocene, during which a clade endemic to the western Great Basin diverged from related samples in the eastern Mojave Desert and western

Colorado Plateau. Demographic and network analyses indicate that *P. becki* underwent a recent expansion in the Great Basin. According to a landscape interpolation of genetic distances among samples, this expansion probably occurred from the northwest, meaning that *P. becki* could have persisted in a portion of the Great Basin during the LGM. This prediction is supported by species distribution models which suggest that climate was unsuitable throughout the majority of the Great Basin during the LGM, but that small patches of suitable climate may have remained in areas of the Lahontan Trough.

Introduction

Of the currently recognized deserts of North America, the Great Basin Desert is perhaps the most biologically unique (see a review in Hafner and Riddle 2011). Positioned between the Sierra Nevada to the west and the Rocky Mountains to the east, the Great Basin occurs at more northern latitudes and higher elevations than any other North American desert. Together, these factors make the summer climate less severe, but winters longer and colder. Accordingly, the region is sometimes referred to as the only 'cold' or 'temperate' desert in North America (Grayson 1990). During the late Pleistocene, the Great Basin climate was at times even colder, with temperatures fluctuating between cool glacial periods and warm interglacials (Spaulding 1990; Thompson 1990), probably making conditions even more extreme for desert organisms.

Based on macrofossil data from packrat middens, many Great Basin plant taxa are thought to have undergone severe distributional shifts in response to Pleistocene

climate fluctuations, especially since the Last Glacial Maximum (LGM) (Thompson 1990; Thompson and Anderson 2000). Although arid shrub-steppe vegetation was able to persist in some northern areas during at least the most recent Pleistocene glacial-interglacial cycles (Madsen et al. 2001; Wilson and Pitts 2010), phylogeographic data suggest that some arid-adapted taxa may have only recently colonized the Great Basin following the LGM (Norwak et al. 1995; Jezkova 2010; Hornsby and Matocq 2011). Other arid-adapted species, however, appear to have remained in the Great Basin during the Pleistocene in spite of severe habitat changes, potentially enduring fluctuations in climate by shifting their realized niche (within a stable fundamental niche), a phenomenon referred to as 'niche drifting' (Jezkova et al. 2011). Furthermore, genetic data and species distribution models (SDMs) indicate that some montane species in the Great Basin responded to Pleistocene climates by shifting ranges along elevational gradients (Waltari and Guralnick 2008; Galbreath 2009, 2010), colonizing lower elevations during glacial periods and higher elevations when climates were warm. Together, data from fossils, phylogenetics, and SDMs portray a wholesale resorting of plant and animal communities within the Great Basin as climate changed between the LGM and current interglacial.

To the south, a similar but less severe biogeographic history is also beginning to emerge for the Mojave Desert (Bell et al. 2010; Chapter 2). Found at lower latitudes and lower mean elevations, the region experiences more extreme summers but less severe winters (Redmond 2009). The Mojave Desert contains flora and fauna from many of the surrounding regions with few endemics, making it a transitional desert between the

cooler Great Basin to the north and the warmer Peninsular and Sonoran deserts to the south (Bell et al. 2010; Hafner and Riddle 2011). During glacial extremes, the geographic distributions of many arid-adapted organisms in the Mojave Desert are thought to have contracted into areas associated with desert basins and drainages, where some were isolated long enough to form distinct lineages (see review in Bell et al. 2010, and Chapter 2 for an example in scorpions). In the northern Mojave Desert, there is also evidence that some areas harbored arid-adapted taxa that are now primarily distributed throughout the Great Basin (Jezkova et al. 2011)

In this study, I investigated the phylogeography of *Paruroctonus becki* (Gertsch and Allred), commonly known as the Beck desert scorpion, which is found in both the Mojave and Great Basin deserts (Gertsch and Allred). Surprisingly little is known about this often abundant scorpion, but it has been collected from elevations between 343 and 1,798 m and from a variety of plant communities (Gertsch and Allred 1965). Like other members of genus *Paruroctonus* Werner*, P. becki* is fossorial and has setal combs on its tarsi (legs), both of which are thought to be adaptations to life in sandy habitats (Fet et al. 1998). I collected the species in a variety of xeric environments, ranging from sand dunes to Ponderosa Pine forest. Little is published regarding the physiological or ecological factors that limit the distribution of *P. becki*. At higher elevations, *P. becki* may be replaced by *Paruroctonus boreus* (Girard), a related species distributed from northern Arizona to southern Canada, but I did not extensively sample at high elevations. At lower elevations, *P. becki* might face competition from several other small scorpion species and predation from larger species like *Hadrurus arizonensis* Ewing and

Smeringurus mesaensis (Stahnke) that are known to readily prey on other scorpions (Polis 1980; Polis and McCormick 1987). By studying the phylogeographic history of *P. becki*, I hoped to add to our understanding of how organisms with distributions spanning both the Mojave and Great Basin deserts have responded to climatic warming since the LGM. In particular, I set out to test whether *P. becki* persisted in the Great Basin during the LGM, or whether it recently colonized the area as glacial conditions retreated and climates warmed.

To accomplish these objectives, I began by sequencing a mitochondrial gene (*cox1*) from samples collected throughout the species' range. I then sequenced an additional mitochondrial gene (16S) from a subset of samples that characterized the majority of this variation (exemplars from the major *cox1* lineages), and then used these data together (concatenated) in an attempt to resolve poorly supported nodes. I placed the matrilineal genealogy in a temporal context by using a relaxed molecular clock. I then used demographic analyses to compare the genetic data to expectations under models of population expansion. Relying solely on mitochondrial DNA (mtDNA) for evolutionary reconstructions has become controversial (e.g., Zink and Barrowclough 2009; Edwards and Bensch 2009), so I also sequenced a variable nuclear gene (ITS-2) from a subset of individuals for comparison. Finally, I use climate-based species distribution models (SDMs) to examine the potential distribution of suitable climate for *P. becki* during the LGM.

Since phylogeographic studies often expose previously overlooked patterns in morphological variation among populations, sometimes with important taxonomic

implications (e.g. Fouquet et al. 2007; Wood et al. 2008; Köhler and Glaubrecht 2010), I also discuss my results in light of taxonomic hypotheses for *P. becki* currently based on morphology. Specifically, I used the phylogeographic data to address whether *P. becki* represents a monophyletic group with respect to the morphologically similar species *P. variabilis* Hjelle and *Paruroctonus silvestrii* Borelli.

Materials and Methods

Sampling

I collected 89 *P. becki* from 51 locations throughout the Mojave and Great Basin deserts (Table 4.1, Fig. 4.1) using ultraviolet light detection (Stahnke 1972). Legs were removed from the left side of each specimen and stored at -80° in 95% ethanol (Vink et al. 2005). Remaining vouchers were preserved in 70% ethanol and accessioned into the scorpion collections at the San Diego Natural History Museum and the American Museum of Natural History. Four specimens representing three congeneric taxa were also processed as outgroups: *P. boreus*, *P. silvestrii*, and *P. variablis*.

To construct SDMs, I used occurrence records associated with my genetic samples as well as additional records from literature (Gertsch and Soleglad 1966; Haradon 1985). Since the literature records for *P. becki* lacked coordinate data, I used GOOGLE EARTH (http://earth.google.com) to estimate latitude and longitude for specimens from the locality descriptions, and excluded records with errors greater than five kilometers to match the resolution of the modeling rasters (2.5 arc-minutes).

Molecular Techniques

I isolated genomic DNA from leg tissues by standard phenol-chloroform extraction or with a DNeasy Extraction Kit (Qiagen Inc., Valencia, CA, USA). I then sequenced portions of mtDNA coding for cytochrome *c* oxidase I (*cox1*) using the primers LE1r and COImodF (Table 4.2). I chose this gene because it has proven useful in intraspecific studies of arachnids (e.g. Thomas and Hedin 2008; Wang et al. 2008, Graham et al. 2012), and is used in DNA barcoding initiatives (Herbet et al. 2003). Based on a preliminary assessment of the *cox1* dataset (see Results), I selected a subset of samples that represented the majority of the genetic structure in *cox1*. For this subset, I sequenced portions of the mitochondrial 16S ribosomal RNA (16S) using scorpion-specific primers from Gantenbein et al. (1999), and the nuclear internal transcribed spacer region (ITS-2) using primers from Ji et al. (2003). Amplifications were performed via polymerase chain reactions using AmpliTaq Gold (Applied Biosystems, Inc., Foster City, CA, USA). I conducted *cox1* amplifications using annealing temperatures of 50°-54° C for 34 cycles, and amplified 16S at 50° C for 30 cycles. I then conducted fluorescence-based cycle sequencing using BigDye Terminator Cycle Sequencing Ready Reaction Kit v. 3.1 (Qiagen Inc., Valencia, CA, USA) and the associated PCR primers (Table 4.2). Electrophoresis was carried out on an ABI 3130 automated sequencer (Applied Biosystems Inc., Foster City, CA, USA). I aligned sequences using SEQUENCHER v. 4.9 (Gene Codes Corp., Inc., Ann Arbor, MI, USA).

Phylogenetics and Divergence Dating

I assessed phylogenetic patterns using the criterion of Bayesian inference (BI) implemented in MRBAYES v. 3.1.2 (Ronquist and Huelsenbeck 2003) through the Cyberinfrastructure for Phylogenetic Research cluster (CIPRES Gateway v 3.1) at the San Diego Supercomputer Center. For the *cox1* data, I calculated best-fit models of nucleotide substitution for the haplotype data under several codon partitions (separately, positions 1+2 and 3 separate, and unpartitioned) using JMODELTEST v. 0.1.1 under the Akaike information criterion (Posada 2008). For a concatenated mtDNA dataset (*cox1*+ 16S), I also explored substitution models calculated for different gene partitions. I then determined the best-fit partitioning scheme for each dataset using Bayes factors on the harmonic mean marginal likelihood values (Nylander et al. 2004). Final analyses were run for 10 million generations using the appropriate partitioning scheme and substitution models. Trees were sampled every 1,000 generations with the first 2.5 million generations of sampled trees discarded as burn-in after confirming chain stationarity using TRACER v. 1.5 (Rambaut and Drummond 2007) and the web-based program AWTY (Nylander et al. 2008).

I used the program NETWORK v. 4.5.1.6 (Fluxus Technology Ltd 2004) to construct separate median-joining networks of mtDNA and nuclear haplotypes (Bandelt et al. 1999). I limited the mtDNA network to the *cox1* sequences of *P. becki*. For the nuclear network, I included ITS-2 sequences from the *P. becki* exemplars as well as from the *P. variabilis* samples. To remove excessive links within these networks, I selected the

maximum parsimony option (Polzin and Daneshmand 2003). Three individuals contained a heterozygous site in the nuclear data, so I first reconstructed haplotypes using PHASE (Stephens and Donnelly 2003) implemented in DNASP v. 5 (Librado and Rozas 2009).

To estimate diversification times within the *P. becki* phylogeography, I used a relaxed molecular clock implemented in BEAST v. 1.5.4 (Drummond and Rambaut 2007). I chose best-fit substitution models for each gene (no codon partitions) using JMODELTEST, and estimated divergence dates using an uncorrelated lognormal clock model. I selected a scorpion-specific mean mutation rate of 0.007 substitutions/site/million based on *cox1* data (Gantenbein et al. 2005) with a mean standard deviation of 0.003 (see Chapter 2; Gantenbein and Largiadèr 2002). I ran BEAST for 40 million generations with the Yule tree prior and retained samples every 1,000 generations, with Tracer used to confirm stationarity of the MCMC chain, as well as to determine the adequacy of the effective sample sizes (ESS > 200 for each estimated parameter).

Demographic Analyses

I used ARLEQUIN v. 3.11 (Excoffier et al. 2005) to conduct mismatch distribution tests of demographic expansion for four of the geographically structured lineages indentified in the phylogenetic and network analyses (see Results below). These distributions were run with 10,000 bootstrap replicates, with the sum of square

deviations (SSD) between the observed and simulated data used to assess statistical significance. In addition, I used ARLEQUIN to calculate Fu's *F* (Fu 1997) for the same four groups. Groups that underwent recent demographic expansion would be expected to have significantly negative *F* values, indicating deviations from mutation-drift equilibrium.

Species Distribution Modeling

I used MAXENT v. 3.3.2 (Phillips et al. 2006) to construct SDMs from a total of 65 unique occurrence points. Additional input data included bioclimatic layers representing current climatic trends, seasonality, and extremes of temperature and precipitation (Hijmans et al. 2005). For model accuracy and to reduce problems with extrapolation (Pearson et al. 2002; Thuiller et al. 2004; Randin et al. 2006), I masked (clipped) the bioclimatic layers to the ecoregions (Olson et al. 2001) that contained occurrence records (Central Basin and Range, Northern Basin and Range, Mojave Basin and Range, Sonoran Desert). I then assessed correlations among available bioclimatic layers from the values of grid cells containing occurrence records to avoid over-fitting the models and to improve model transferability (Peterson et al. 2007). When the Pearson's correlation coefficient was > 0.75 (Rissler et al. 2006; Rissler and Apodaca 2007), I selected an individual layer among the correlated layers for retention in MAXENT runs. For modeling, I chose 9 bioclimatic layers representing quarter climates rather than monthly climates, precipitation during the driest quarter over precipitation during the

warmest quarter, and temperature annual range instead of mean diurnal range. These bioclimatic layers were: Bio3, isothermality; Bio5, maximum temperature of the warmest month; Bio6, minimum temperature of the coldest month; Bio7, Temperature Annual Range (P5-P6); Bio8, mean temperature of the wettest quarter; Bio9, mean temperature of the driest quarter; Bio15, precipitation seasonality; Bio16, precipitation of the wettest quarter; Bio17, precipitation of the driest quarter.

I ran MAXENT using logistic output with default settings except that I selected random seeding. I used cross-validation to assess model robustness by dividing presence points into five groups and running five iterations with different groups selected for each run; thus, 20% of the presence points were used as test points and 80% were used for model training (Nogués-Bravo 2009). Model performance was evaluated by the area under the receiver operating characteristic curve (AUC). To extrapolate models to LGM climates, I projected the distribution models onto simulated climates for the LGM (c. 21 ka) derived from the Community Climate System Model (CCSM; Otto-Bliesner et al. 2006) and the Model for Interdisciplinary Research on Climate (MIROC; Hasumi and Emori 2004). I displayed climatic suitability in ARCGIS v. 9.2 (ESRI, Redlands, CA, USA) by converting continuous MAXENT outputs into binary grids using the maximum training sensitivity plus specificity threshold (Liu et al. 2005; Jiménez-Valverde 2007).

Landscape Interpolations

To assess genetic diversification across the Great Basin, I created a landscape interpolation of genetic distances; limiting this assessment to data from a genetic clade

identified from this region (see Results). I used the program ALLELES IN SPACE v. 3.11 (Miller 2005) to calculated pairwise genetic distances from the *cox1* sequence data as determined by a Delaunay triangulation-based connectivity network. To correct for spatial autocorrelation among samples, distance values were calculated as residuals from a regression of genetic and geographic distances (Miller et al. 2006). The program then interpolated values onto a 50 x 50 grid representing a minimum convex polygon around the targeted samples. I set the distance weighting parameter to 0.25.

Results

Phylogenetics and Divergence Dating

I successfully sequenced a 747 bp portion of *cox1* for 92 samples, a 484 bp region of 16S for 47 samples, and 241 bp section of ITS-2 for 33 samples. For 45 individuals, I constructed a concatenated dataset by combining *cox1* and 16S sequences. After comparing bayes factors, I ran BI analyses of the *cox1* dataset with sequence data partitioned by codon, and the concatenated mtDNA dataset partitioned by gene and codon.

The *cox1* phylogeny yielded several geographically structured lineages, although not all were strongly supported (Figs. 4.2). Among the outgroups, *P. boreus* and *P. silvestrii* formed a strongly supported basal lineage, but one *P. variabilis* sample appeared more closely aligned with *P. becki* than to the other outgroups, while the other *P. variabilis* sample was paraphyletic with respect to *P. becki* samples from the Providence Mountains and the White-Inyo Mountain Range (see Fig. 4.1). Other

geographically structured lineages comprise individuals from the Great Basin Desert, the western Mojave Desert, and eastern Mojave Desert, with a few samples in the latter group also extending into the highlands of Northern Arizona. Of all the geographically structured lineages, only the Great Basin and White-Inyo Range lineages were strongly supported. In general, individuals collected from the same or nearby sample sites generally grouped together on this tree with strong BI support, although three areas (sites 21, 31, and 40) contain haplotypes from different lineages.

The topology of the concatenated (*cox1* and 16S) tree (Fig. 4.3) was similar to the *cox1* tree, but with a few important differences. In the concatenated tree, the *P. becki* samples from the Providence Mountains that were divergent in the *cox1* tree instead formed the most basal lineage within a weakly supported clade containing all *P. becki* samples, rendering the species tentatively monophyletic. Although Bayesian support was not strong, *P. variabilis* samples from the San Joaquin Valley in California appeared monophyletic in the concatenated tree, and sister to the clade containing *P. becki*. As in the *cox1* tree, samples from the White-Inyo Range were strongly supported as a monophyletic clade (hereafter the White-Inyo Clade). Samples from the western Mojave formed a lineage with low Bayesian support in the *cox1* tree, but strong support in the concatenated tree (hereafter the Western Mojave Clade). In both the *cox1* and concatenated trees, specimens from throughout the eastern Mojave Desert form a weakly supported group together with those from the Great Basin (hereafter the Eastern Group, reserving 'clade' for lineages with high Bayesian support). Within the Eastern Group, most of the widespread samples from the Great Basin form a strongly

supported lineage consisting of very similar haplotypes (hereafter the Great Basin Clade) (Fig. 4.4).

The haplotype network constructed from *cox1* data portrayed a pattern similar to that of the concatenated mtDNA tree (Fig. 4.3). Samples from the Great Basin Clade formed a star-shaped pattern that was 20 mutational steps from the nearest sample within the Eastern Group, which also formed a distinct, though diverse subnet. Of the four samples from the Providence Mountains, two were nested within the Eastern Group and two formed a divergent lineage positioned between the samples from the Western Mojave Clade (37 mutational steps removed) and the Western Mojave Clade (41 steps removed).

Much less genetic structure was recovered in the nuclear haplotype network, with all *P. becki* haplotypes centered within two mutations steps from the most common haplotype consisting of samples from the Eastern Group, and including both mitochondrial lineages from the Providence Mountains (Fig. 4.5b). The only sample successfully sequenced for ITS-2 from the White-Inyo Clade shared a haplotype with samples from the Western Mojave Clade, and this haplotype was only one step removed from the most common haplotype. Both *P. variabilis* samples comprised the most divergent haplotype in the nuclear network, but this haplotype was only two steps from the most similar *P. becki* haplotype.

Results from BEAST analyses of the concatenated mitochondrial data (Fig. 4.6) suggest that divergence between *P. becki* and the most closely related outgroup, *P. variabilis*, took place between the Late Miocene and early Pliocene. Subsequently, initial

diversification within *P. becki* began with the divergence of a linage represented in the Providence Mountains sometime in the Late Miocene to mid Pliocene. The Eastern Group, White-Inyo Clade and Western Mojave Clade were estimated to have diverged during the Pliocene, and the remaining diversification, including that between Great Basin Clade and the other samples in the Eastern Group, was estimated to have occurred during the Pleistocene.

Demographic Analyses

Mismatch analyses of the Western Mojave, and the White-Inyo clades resulted in sum of squared deviation (SSD) values that were nonsignificant, meaning that these data do not deviate from models of demographic expansion (Table 4.3), but significant for the Eastern Group. However, when the Great Basin Clade was analyzed independently, the SSD value was nonsignificant. Furthermore, the Great Basin Clade exhibited unimodal distribution(Fig. 4.7), and was the only grouping that yielded a significantly negative Fu's *F* value, both of which would be expected for a population that has undergone expansion.

Species Distribution Models

The SDMs performed significantly better than random, as AUC scores were high (both > 0.95) for both training and testing data (Fig. 4.8). Under current climatic conditions, the SDM for *P. becki* depicts suitable climate over much of the low and mid-

elevation areas within the Mojave Desert, Great Basin, and the southern Colorado Plateau. Additional areas are also predicted to the north along the Snake River Plain of southern Idaho, in patches of arid regions in southeastern Oregon, and in the northwest portion of the Sonoran Desert in the Anza-Borrego Desert.

Both LGM models (CCSM & MIROC) portrayed suitable climate throughout the Mojave and western Sonoran deserts, as well as along the length of western California and northern Baja California (Fig. 4.5). In contrast, areas of suitable climate extended further south along the coast of Sonora, Mexico in the MIROC model, but not as far north in California. The MIROC model also suggested that climate was generally not suitable throughout the higher elevations of southern California. The CCSM model predicted suitable climate in all but the highest elevations in southern California. Both models suggested that climate in the Great Basin was not suitable during the LGM, except for very small patches in the western Great Basin Desert (the Lahontan Basin). Neither model predicted suitable climate in the Colorado Plateau during the LGM.

Landscape Interpolation

The interpolation of residual genetic distances for the *cox1* data from the Great Basin Clade (Fig. 4.4b) displays a pattern of decreasing genetic diversity from the northwest to the southeast. The highest diversity occurs in the extreme northwest portion of the current distribution of *P. becki* in an area within the Lahontan Basin.

Discussion

Postglacial Colonization of the Great Basin

The main purpose of this study was to determine whether *P. becki* persisted throughout its current distribution in the Great Basin Desert during the LGM, or whether the species recently colonized the area as glacial conditions retreated and climates warmed. Phylogenetic and demographic analyses of mtDNA provide convincing evidence of the latter, as *P. becki* appears to have recently colonized a large part of the western Great Basin following the LGM. The pattern, however, was not as expected since the SDMs and genetic data suggest that *P. becki* persisted in part of the Great Basin during the LGM and then expanded its range from this refugial area when the climate warmed.

The SDMs projected onto LGM conditions predicted that climate throughout most of the Great Basin was unsuitable; but suitable climate remained available in much of the Mojave Desert and importantly in small low-elevation subbasins in the western Great Basin (Fig. 4.8). In the CCSM model, the predicted area encompasses Walker Lake (Fig. 4.8b), whereas the MIROC model predicted subbasins further north that include Pyramid Lake and the Smoke Creek Desert (Fig. 4.8c). These subbasins occur within the Lahontan Trough, which filled with water and coalesced to form Lake Lahontan during pluvial maxima (Fig. 4.4; Bensen 1991). Therefore, at times most if not all of the area identified as suitable during the LGM was enveloped by lake waters. Persistence of *P. becki* in this region, perhaps only along slopes adjacent to the lake, would likely have

resulted in a bottleneck at that time which may explain the low genetic diversity within the Great Basin Clade.

Genetic analyses support the prediction that *P. becki* persisted in the western Great Basin. In the *cox1* haplotype network, the samples from this region formed a star-shaped pattern (Fig. 4.4b), which is usually indicative of recent range expansion (Avise 2000). Furthermore, demographic analyses lend support to a pattern of expansion by the Great Basin Clade (Table 4.2). The foremost models of colonization, the gradual expansion model (reviewed in Koizumi et al. 2012) and the leading edge model (reviewed in Jezkova et al. 2011), both predict that genetic differentiation should be higher among older populations than between populations from recently colonized regions. Under this prediction, the landscape interpolation of genetic distances within the Great Basin Clade (Fig. 4.4b) indicates that *P. becki* probably expanded its Great Basin distribution from one or more glacial refugia within the region.

This geographic expansion appears to have been to the east and southeast. Westward expansion was probably inhibited by the Sierra Nevada, but no obvious biogeographic barriers occur to the north. I conducted several searches in northern areas predicted to be currently suitable for *P. becki*, but did not find any of these scorpions. I suspect that the species is absent from more northern areas and speculate that this could reflect physiological or ecological limitations associated with higher latitudes that were not accurately portrayed by the SDMs. Provocatively, individuals from the Great Basin Clade in the south were found within close proximity to individuals from several other lineages, but never in sympatry (Fig. 4.4), so I suspect that there

might be some degree of high density blocking (Waters 2011), or even potential competition, among *P. becki* lineages.

Pre-Pleistocene Diversification

Divergence between *P. becki* and *P. variabilis* (putative sister species) was estimated to have occurred during the Late Miocene, a timeframe that corresponds with that of a marine embayment of the San Joaquin Valley (Hall 2002). *Paruroctonus variabilis* is endemic to the eastern flanks of the California coastal ranges that boarder the San Joaquin Valley (Hjelle 1982), so divergence between these species could have occurred when marine waters isolated the Coastal Ranges from adjacent arid regions (Fig. 4.4). Intriguingly, subsequent nodes representing diversification among the Western Mojave Clade, Eastern Group, and White-Inyo Clade have mean estimates within the Pliocene. These clades meet in the eastern California Shear Zone, a geologically active region of predominantly right-lateral strike-slip faults (Fig. 4.1). The faults are thought to accommodate motion between the Pacific and North America plates (Frankel et al. 2010). This region experienced intense extensional tectonics (stretching of the earth's crust) during the Pliocene (Phillips 2008). Extensional faulting is thought to have first begun along the east side of the White-Inyo Range at the Fish Lake Valley fault zone (6.9–4 Ma), forming deep desert valleys (Reheis and Sawyer 1997). Subsequent faulting on the west side of the White-Inyo Range then took place during the late Pliocene, causing a rapid deepening of a preexisting valley and forming the modern low-laying Owens Valley along the White Mountains and Owens faults

(Stockli et al. 2003; Phillips, 2008). The location (Figs. 4.1 & 4.4) and timing (Fig. 4.6) of these events match the placement and estimated divergence times between the three clades, and populations of *P. becki* may have become divided on each side of the expanding low-elevation valleys east of the White-Inyo Range. Formation of the Owens Valley in the Late Pliocene could have then further sundered *P. becki* populations within the region, facilitating the formation of the Western Mojave and White-Inyo clades.

The divergent mtDNA haplotypes recovered from the Providence Mountains are curious (Figs. 4.1–4.4, Vulcan Mine). Out of four samples from this site (Fig. 4.1), two grouped with other eastern Mojave samples, while the other two formed a lineage basal to all other *P. becki* samples (Figs. 4.2 & 4.3). The nuclear haplotypes of these latter samples, however, were identical to the haplotypes recovered in samples from the Eastern Group, and I found no obvious differences in their morphology. Assessment of the sequence data revealed no evidence of pseudogenes (numts), such as double peaks, indels, frameshifts, or premature stop codons (Bertheau et al. 2011). Other potential explanations include incomplete lineage sorting (retention of ancestral polymorphism) or mitochondrial introgression from a divergent population or related species not represented in my sampling. Of these, the latter explanation may be more likely. The southernmost record for *P. becki* is from the Coachella Valley area of the Colorado Desert region (Gertsch and Soleglad 1966) of the Sonoran Desert. Although I searched the area twice in seemingly suitable habitat and at various elevations between the Coachella Valley and the Providence Mountains, I was unable to find *P. becki*. If

populations do exist in these areas, then perhaps these animals hold the answer to the patterns I found in samples from the Providence Mountains.

Taxonomic Considerations

Although a thorough morphological assessment was beyond the scope of this project, I did notice a few morphological points of interest among the voucher specimens. First, I noted a conspicuous morphological similarity between *P. becki* and its likely sister species *P. variabilis.* I find this surprising because *P. variabilis* was at first considered to be a "light race" of *P. silvestrii*, a species distributed throughout southern California and adjacent areas in northern Baja California (Gertsch and Soleglad 1966; Hjelle 1982). The original description of *P. variabilis*, however, compares it to *P. silvestrii* and *P. becki,* distinguishing *P. variabilis* from the latter by a combination of the following characters: distinct denticles opposite biscuspid tooth on the ventral margin of the cheliceral fixed finger, more dorsal marbling, and different electrophoretic patterns of venom proteins. This last character was of little use as venom is not typically used to diagnose scorpion species, and the degree to which venom proteomes vary within scorpion species has not yet be adequately assessed. I found that dorsal marbling also was an unreliable diagnostic character. Although most *P. becki* are superficially similar in color and degree of marbling of the dorsum, some populations (e.g. Site 32 - Ash Meadows) contained phenotypes with darker marbling than that of *P. variabilis.* This left only the cheliceral denticles, and I screened several *P. becki* specimens representing each major lineage, but none had these structures. Consequently, the presence of

cheliceral denticles on *P. variabilis* seems to remain a diagnostic character between these species. Because *P. variabilis* forms a monophyletic group slightly differentiated from *P. becki* in my analyses of both nuclear and mtDNA data (Fig. 4.3), I suggest retaining their current status as independent species.

Both species, however, would clearly benefit from more rigorous morphological evaluations and detailed redescriptions, which would perhaps uncover additional distinguishing traits. This would be particularly valuable as I found that several characters typically used to identify *P. becki* are actually highly variable. Specimens are often identified by chelae morphology, for example, but I found that some populations of *P. becki* possessed more robust chelae with strong carination, while others contained slender chelae with little carination. In addition, *P. becki* are commonly thought to be easily identified in the field by the presence of a crescent shaped area of infuscation between the lateral and median eyes, but I discovered several specimens that completely lacked this pattern.

Conclusions

Due to the wealth of data that have been extracted from packrat middens throughout southwestern North America (Betancourt 1990), floristic responses to late Pleistocene climate fluctuations are relatively well characterized for the Great Basin. The geographic ranges of Great Basin plant species are thought to have responded in two ways; they were either relatively insensitive to climate change and experienced very little changes to their geographic ranges, termed ‘orthoselective’ (i.e. species that

shifted along elevational gradients but did not undergo large geographic changes), or they shifted to new areas, following a 'migration' model (Nowak et al. 1994). Using this logic, we can begin to develop a model of late Pleistocene distributional response for the Great Basin terrestrial fauna.

Rodent species that occupy basins within the region appear to fall under both categories. Recent phylogeographic assessments of the chisel-toothed kangaroo rat, *Dipodomys microps* Merriam (Jezkova et al. 2011), and the pallid kangaroo mouse, *Microdipodops pallidus* Merriam (Hafner et al. 2008), suggest that both species remained in the Great Basin during the LGM (rendering them orthoselective). Phylogeography of the bushy-tailed woodrat, *Neotoma cinerea* (Ord), indicates that it followed the migration model, as the LGM distribution of this species appears to have shifted to the south (Hornsby and Matocq 2011). Other recent studies of arid-adapted reptile species – the desert horned lizard, *Phrynosoma platyrhinos* Girard (Jezkova 2010) and the western North American nightsnake, *Hypsiglena torquata* (Günther) (Mulcahy 2008) – suggest that both species likely followed the migration model. Data from *P. becki* provide multiple lines of evidence that this scorpion persisted within limited areas of the western Great Basin, and then recently expanded to occupy a larger portion of the region, fitting a migration model.

The phylogeography of *P. becki* also uncovered an unexpected degree of phylogeographic structure across the Mojave Desert. Given that mitochondrial lineages were not strongly supported by nuclear data, and the fact that no obvious morphological divergences were discerned from samples collected throughout the

species' range, I conclude that *P. becki* probably represents a single species. Such patterns underscore the need for integrative and modern approaches to delimit species and assess relationships among little-known terrestrial invertebrates like scorpions.

Table 4.1. Location and voucher information for genetic samples used in this study. Site numbers correspond with localities portrayed in Fig. 4.1. Coordinates only represent the general sample area.

Site	State	Locality	Latitude	Longitude	Voucher Numbers
1	NV	WINNEMUCCA	41.12564	-117.76308	MG0397, MG0398
2	NV	GERLACH	40.64307	-119.31268	MG0350, MG0351
3	NV	FLAT TIRE	40.601367	-117.91349	L10560
4	NV	BEOWAWE	40.52007	-116.51368	MG0015, MG0018
5	NV	HONEY LAKE VALLEY	40.12901	-119.82145	MG0516, MG0517
6	NV	SPARKS NORTH	39.855278	-119.655889	LP6289
7	NV	HOT SPRINGS MT	39.76	-118.87	MG0164
8	NV	SPARKS SOUTH	39.735998	-119.686388	LP6290
9	NV	WADSWORTH	39.633801	-119.285448	MG0514
10	NV	BLOW SAND MTS	39.19902	-118.72205	MG0528, MG0529
11	NV	BIG SMOKEY VALLEY	39.239123	-117.000493	MG0879, MG0080
12	NV	HAWTHORNE	38.586683	-118.604542	LP6291
13	NV	MINA	38.429296	-118.065709	MG0837, MG0838
14	NV	MURIETTA	38.252972	-118.350441	MG0504, MG0505, MG0506
15	NV	TEMPIUTE	37.654021	-115.640362	MG0918, MG0919, MG0920
16	NV	GOLDFIELD	37.61572	-117.226262	MG1080, MG1081
17	CA	MILLPOND	37.37903	-118.48391	MG0385, MG0386, MG0387
18	CA	TUNGSTON	37.3424	-118.52415	LP5007
19	CA	DEEP SPRINGS VALLEY	37.31298	-118.10313	MG0375, MG0376, MG0378
20	NV	SARCOBATUS FLAT	37.040003	-116.815702	MG0949, MG0950, MG951
21	CA	SALINE VALLEY	36.753133	-117.86325	LP4984, LP4992
22	CA	TUTTLE CREEK	36.596765	-118.188562	MG0541, MG0542
23	CA	ALABAMA HILLS	36.59985	-118.183417	LP4991
24	CA	LONG JOHN CYN	36.63608	-118.00033	MG0361, MG0362, MG0363
25	CA	PANAMINT RANGE	36.40923	-117.17596	MG0475, MG0476, MG0477
26	CA	CHINA LAKE, MT SPRINGS CYN	35.944983	-117.543652	LP4373
27	CA	TRONA PINNACLES	35.617533	-117.370104	LP4369
28	CA	MOJAVE	35.069529	-118.220224	MG0713
29	CA	PALMDALE	34.508208	-117.978967	MG1112, MG1113, MG1155
30	CA	DANTE'S VIEW	36.21697	-116.72399	MG0451, MG0542
31	CA	AMARGOSA DUNES	36.432483	-116.421417	LP4995
32	NV	ASH MEADOWS	36.466013	-116.377554	L10450

Table 4.1. Location and voucher information continued.

Site	State	Locality	Latitude	Longitude	Voucher Numbers
33	CA	AVAWATZ MTS	35.510409	-116.309343	LP4384
34	CA	HALLORAN SUMMIT	35.412699	-115.802629	MG1042, MG1043, MG1044
35	CA	VULCAN MINE	34.914776	-115.545667	MG1131, MG1132, MG1153, MG1154
36	NV	SPRING MTS NORTH	36.2458	-115.54299	MG0012
37	NV	SPRING MTS SOUTH	35.95397	-115.43804	MG0136
38	NV	MT POTOSI	35.9149	-115.55276	MG0060
39	CA	MORNING STAR MINE	35.362694	-115.422928	LP8502
40	NV	NIPTON ROAD	35.5197	-115.14	MG0224, MG0225, MG0226
41	NV	CHRISTMAS TREE PASS	35.261226	-114.743965	MG1060, MG1061, MG0162
42	NV	BLUE POINT	36.399938	-114.446469	MG0127, MG0128, MG0129
43	AZ	VIRGIN MTS	36.639712	-114.014165	MG0157, MG0158, MG0159
44	UT	WARNER VALLEY	37.042092	-113.453533	LP7250
45	AZ	HUALAPAI MTS	35.076556	-113.882472	MG1151, MG1152
46	AZ	SOAP CREEK CYN	36.72607	-111.75808	MG0183, MG0184
47	AZ	CLIFF DWELLERS LODGE	36.74677	-111.751569	LP7698

Table 4.2. Primers used in this study to amplify and sequence portions of mitochondrial and nuclear DNA.

Primer name	Sequence	Source
COImodF	5'-ATCATAAGGATATTGGGACTATGT-3'	Bryson et al. (in review)
LE1r	5'-GTAGCAGCAGTAAARTARGCYCGAGTATC-3'	Bryson et al. (in review)
16SmodF	5'-CACCGRTTTGAACTCAGATCA-3'	Gantenbein et al. (1999)
16SnewR	5'-ACCTTTTGTATCAGGGATT-3'	Gantenbein et al. (1999)
CAS28sB1d	5'-TTCTTTTCCTCCGCTTATTTATATGCTTAA-3'	Ji et al. (2003)
CAS5p8sFc	5'-TGAACATCGACATTTYGAACGCACAT-3'	Ji et al. (2003)

Table 4.3. Results from goodness-of-fit tests of population expansion based on mismatch distributions and Fu's *F* for geographically structured lineages in *Paruroctonus becki* (Gertsch and Allred) identified by phylogenetic (Figs. 4.2 & 4.3) and network (Fig. 4.4) analyses. Asterisks indicate nonsignificant SSD values (>0.05) and significant *F* values (<0.02) which both mean the data do not differ from expectations under models of expansion.

	Western Mojave Clade	**White-Inyo Clade**	**Eastern Group**	**Great Basin Clade**
Goodness-of-fit test				
Distribution curve	multimodal	multimodal	multimodal	unimodal
SSD	0.016072	0.081827	0.0173	0.000059
P	0.134*	0.134*	0.012	1.0*
Fu's *F*	-0.27583	0.1211	-5.41313	-5.47584
P	0.432	0.488	0.087	<0.001*

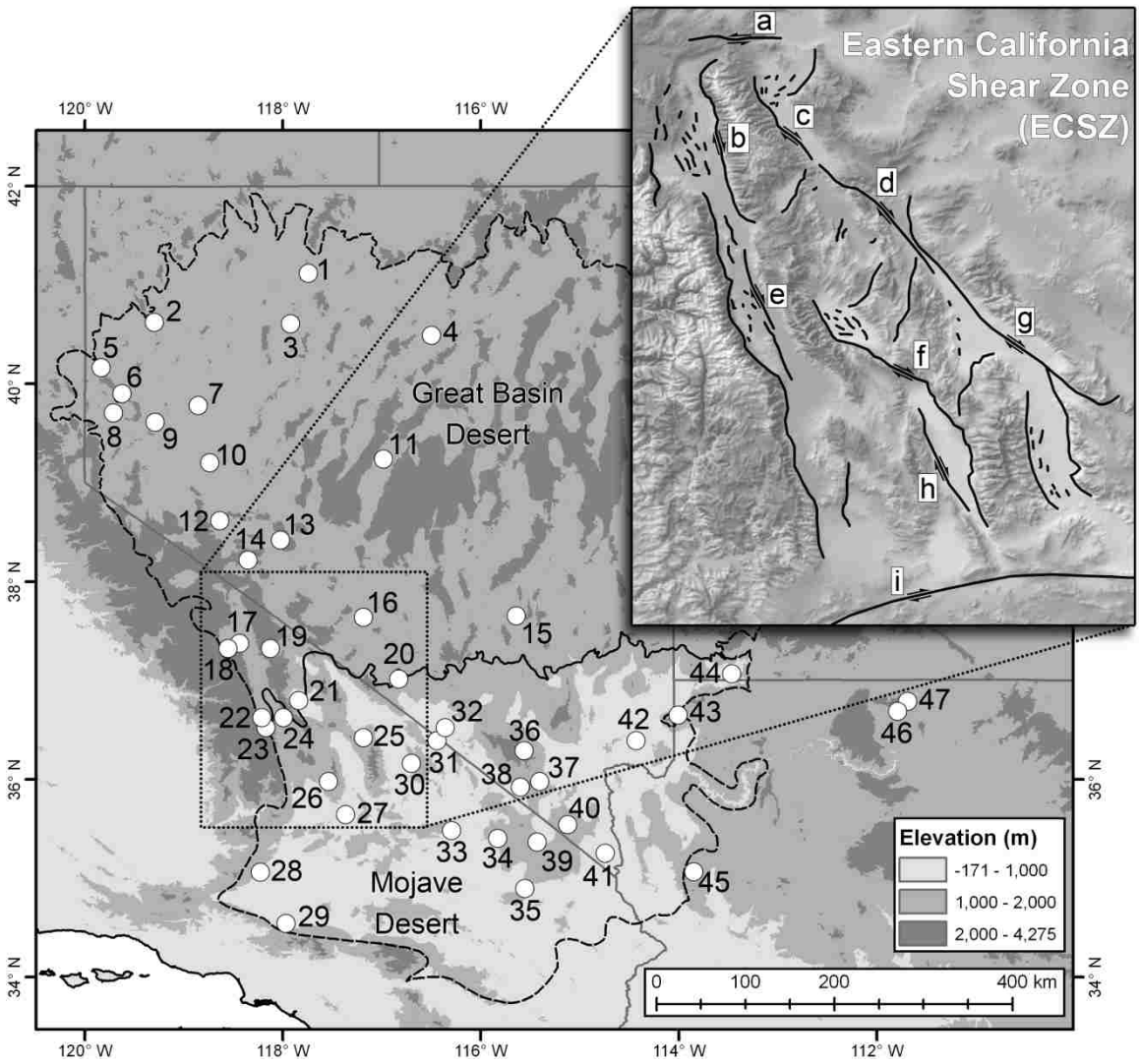

Figure 4.1. Map of the study area showing sample locations for *Paruroctonus becki* (Gertsch and Allred), with numbers corresponding to sites identified in Table 4.1. Dashed lines outline the Mojave and Great Basin Deserts. Inset indicates major faults within the Eastern California Shear Zone. Strike-slip faults are identified by dark lines with arrows and letters as follows: a = Coaldale Fault, b = White Mountains Fault zone, c = Fish Lake Valley Fault zone, d = Furnace Creek Fault, e = Owens Valley Fault, f = Hunter Mountain Fault, g = Death Valley Fault, h = Panamint Valley Fault, i = Garlock Fault. Dark lines without arrows indicate normal faults.

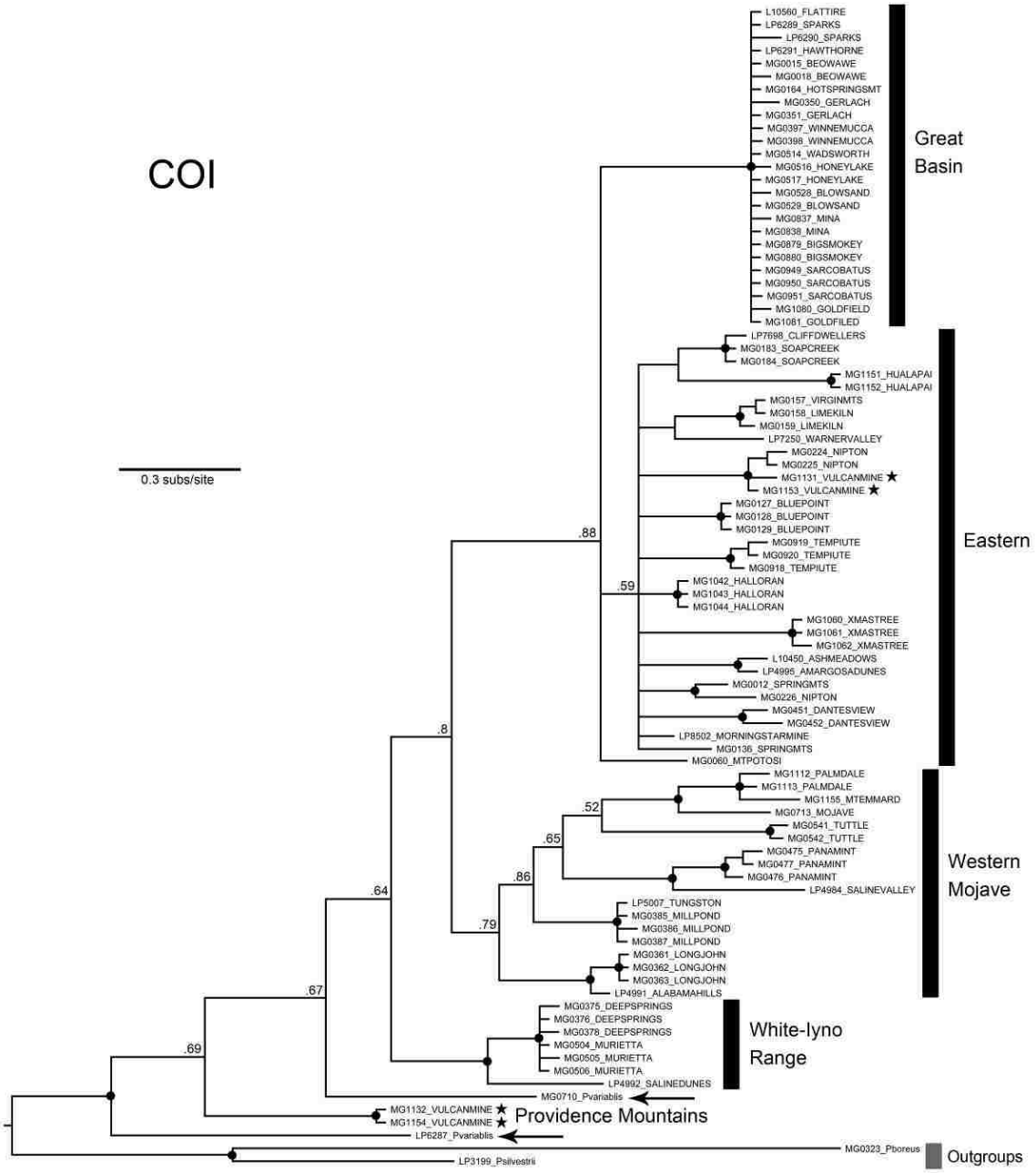

Figure 4.2. Majority rule (50%) consensus tree depicting results of Bayesian phylogenetic analysis of *Paruroctonus becki* (Gertsch and Allred) using *cox1* mtDNA. Vertically arranged bars indicate geographically structured lineages. Arrows point to two *Paruroctonus variabilis* Hjelle sequences. Stars indicate individuals from the Providence Mountains. Nodes with Bayesian posterior probability values indicating strong support (PP > 0.9) are represented by black dots, otherwise actual values are indicated above nodes.

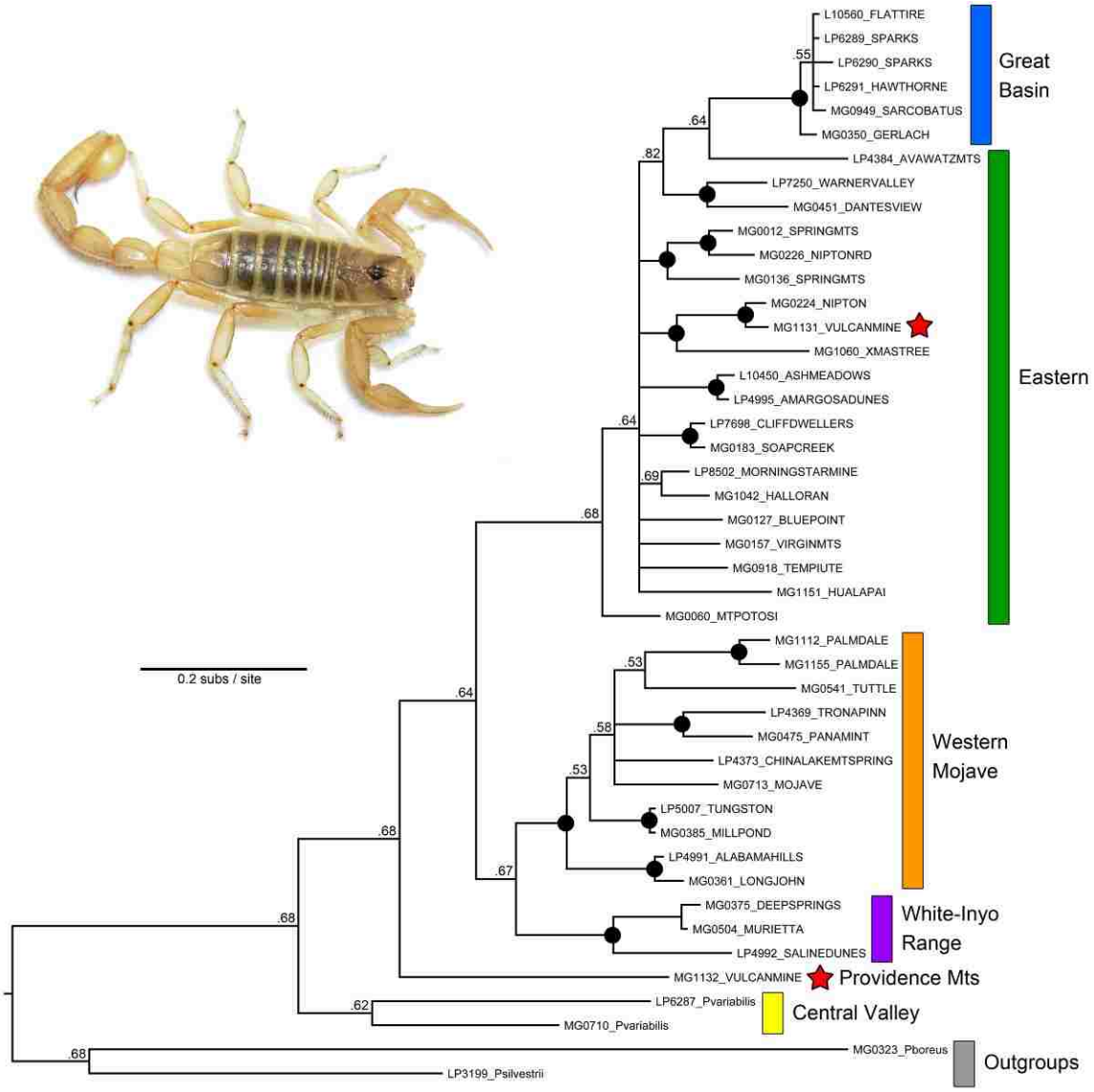

Figure 4.3. Combined *cox1* and 16S phylogenetic estimate based on Bayesian inference. Vertically arranged bars indicate geographically structured lineages. Nodes with Bayesian posterior probability values indicating strong support (PP > 0.9) are represented by black dots, otherwise actual values are indicated above nodes.

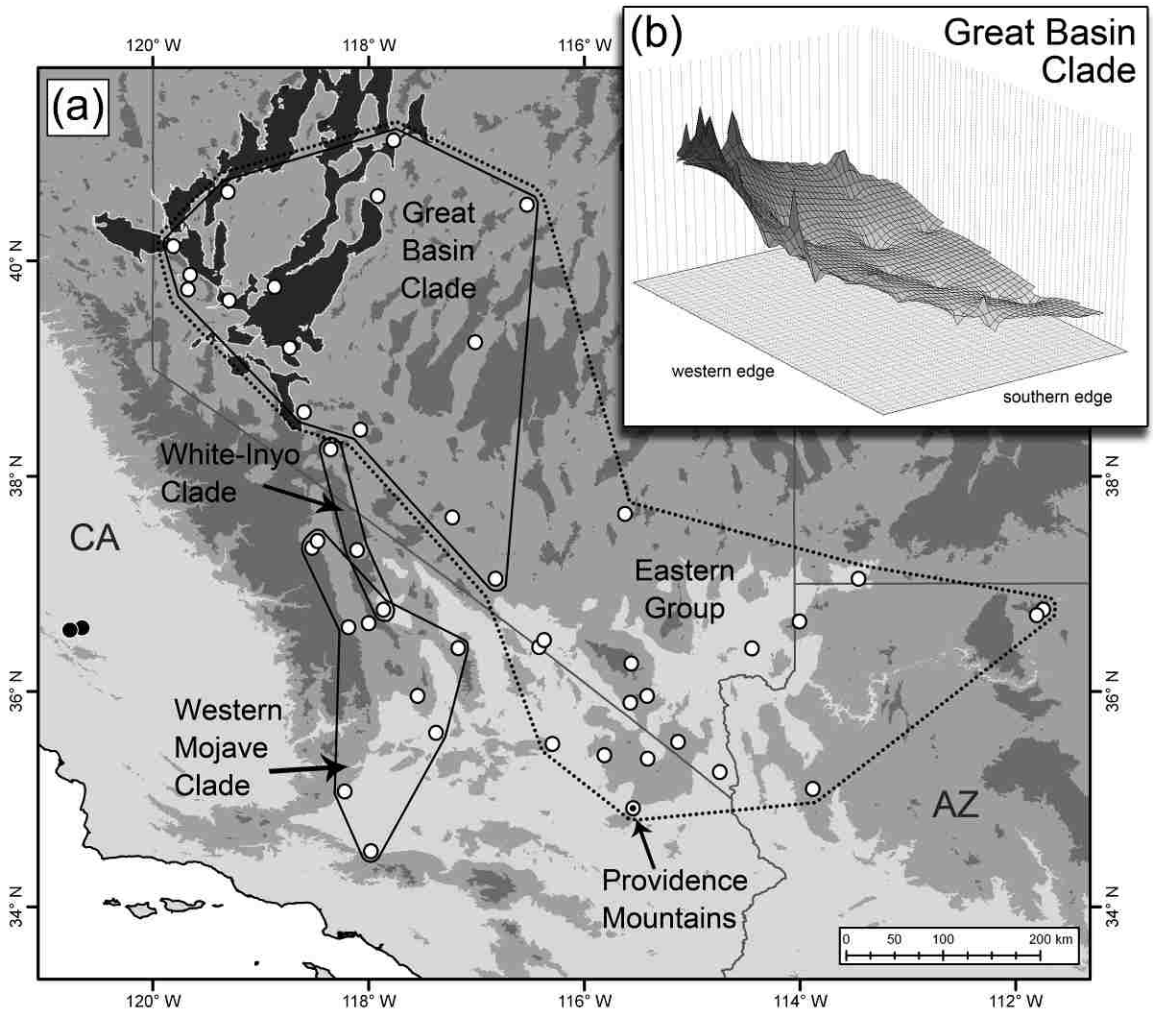

Figure 4.4. Map depicting the distribution of major lineages within the phylogeography of *Paruroctonus becki* (Gertsch and Allred) discussed in the text. Sample sites used for genetic analyses are indicated by white dots. The dark shading with the white outline portrays Lake Lahontan at its pluvial maximum. Solid lines indicate strongly supported clades, whereas the dotted line outlines the weakly supported Eastern Group.

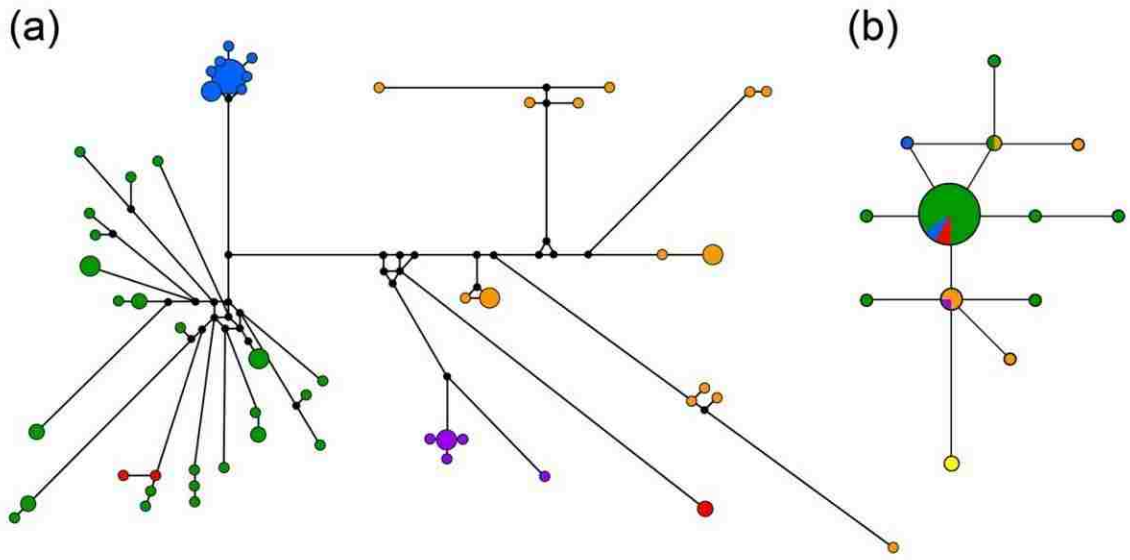

Figure 4.5. Haplotype networks for *Paruroctonus becki* (Gertsch & Allred) based on mitochondrial *cox1* (a) and nuclear ITS-2 (b) sequence data. Circle sizes are proportional to haplotype frequencies. Color indicates geographic groups identified in Fig. 4. The yellow circle in the nuclear network (b) represents *Paruroctonus variabilis* Hjelle.

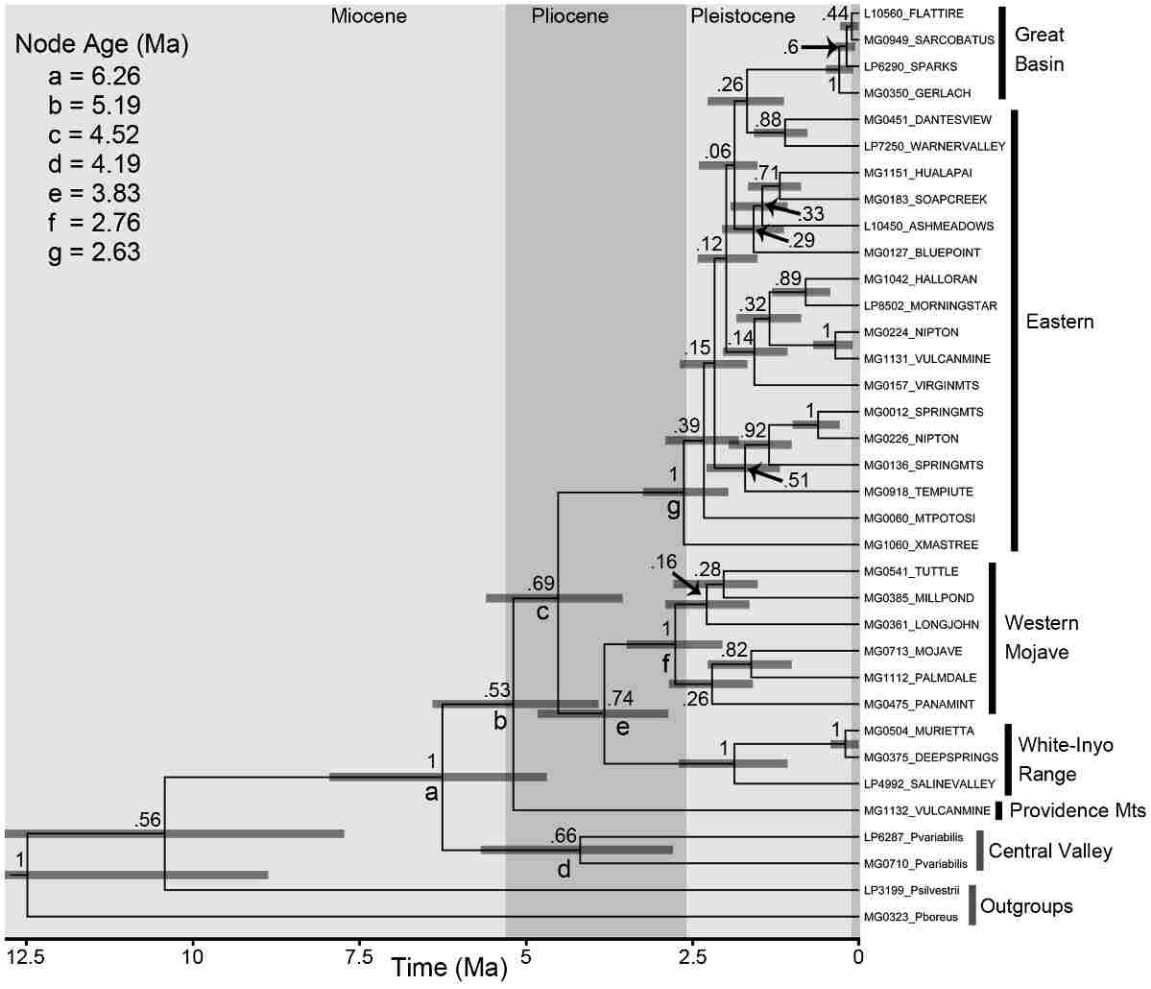

Figure 4.6. Rate-calibrated chronogram for *Paruroctonus becki* (Gertsch and Allred). Posterior probabilities are indicated for nodes. Letters below nodes identify mean divergence date estimates within the Miocene or Pliocene. Bars represent highest posterior densities (95%) around mean date estimates.

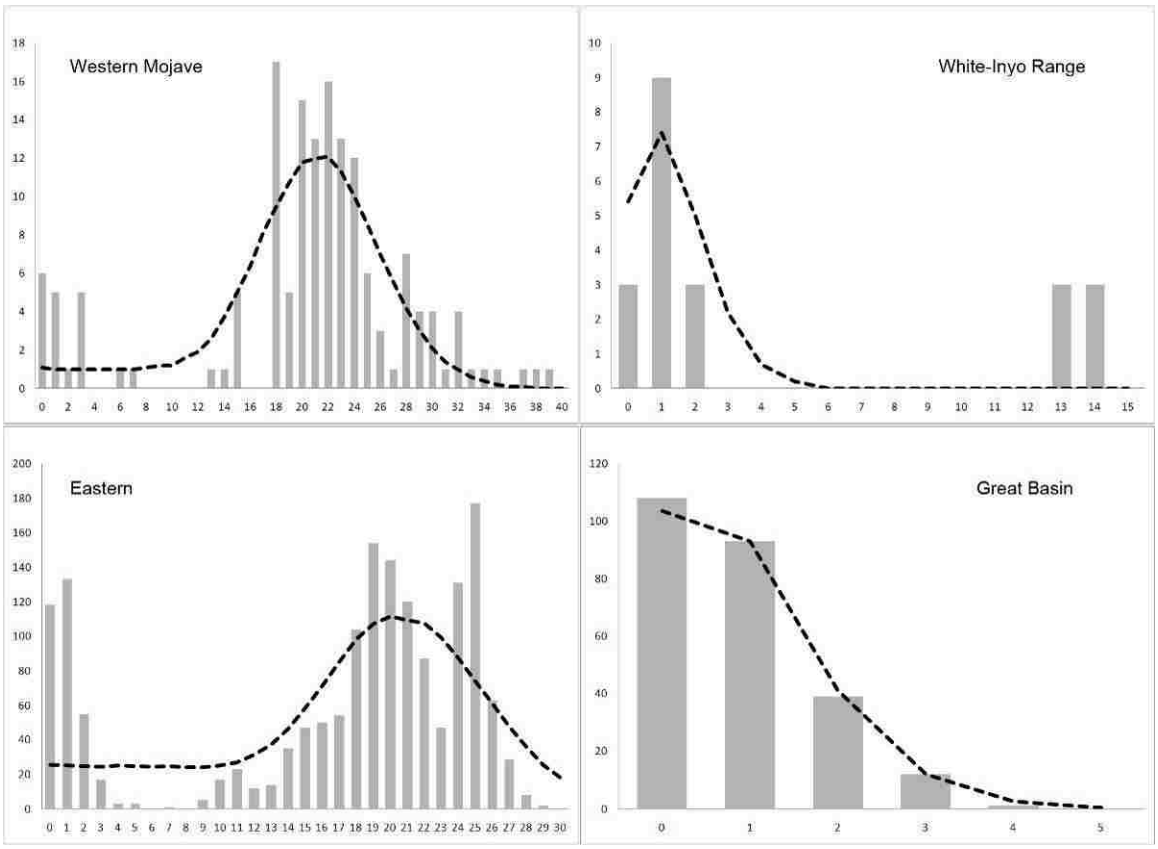

Figure 4.7. Mismatch distributions based on *cox1* data for four mtDNA groups of *Paruroctonus becki* (Gertsch and Allred) recovered in phylogenetic analyses. Dashed lines represent the expected distribution if populations underwent demographic expansion, whereas bars indicate the observed frequency (y-axis) of pairwise differences (x-axis).

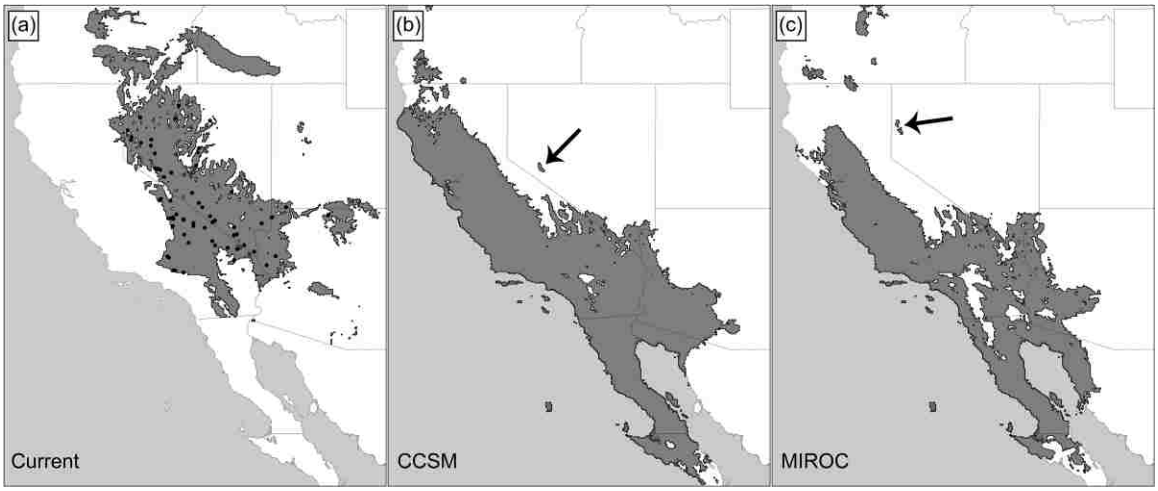

Figure 4.8. Graphical results from species distribution models of *Paruroctonus becki* (Gertsch and Allred) generated using MAXENT and displayed using the maximum training sensitivity plus specificity threshold. Models represent climate predicted as suitable (dark shading) during current conditions (a) and LGM conditions estimated from CCSM (b) and MIROC (c) climatic simulations. Black dots represent occurrence records used to generate the models. Arrows indicate potential northern refugia within the Great Basin Desert

BIBLIOGRAPHY

Althoff, D. M. and O. Pellmyr. 2002. Examining genetic structure in a bogus yucca moth: a sequential approach to phylogeography. Evolution 56:1632–1643.

Anderson, R. C. 1975. Scorpions of Idaho. Tebiwa (Miscellaneous Papers of the Idaho State University Museum of Natural History) 18:1–17.

Anderson D. E. and S.G. Wells S.G. 2003. Latest Pleistocene lake highstands in Death Valley, California. *In* Y. Enzel, S. G. Wells and N. Lancaster, eds., Paleoenvironments and paleohydrology of the Mojave and southern Great Basin Deserts: Boulder, Colorado, Geological Society of America Special Paper 368, pp. 115–128.

Ashton, K. G. and A. de Queiroz. 2001. Molecular systematics of the western rattlesnake, *Crotalus viridis* (Viperidae), with comments on the utility of the d-loop in phylogenetic studies of snakes. Molecular Phylogenetics and Evolution 21:176–189.

Avise, J. 2000. Phylogeography: The History and Formation of Species. Harvard University Press, Cambridge.

Axelrod, D. I. 1979. Age and origin of Sonoran Desert vegetation. Occasional Papers of the California Academy of Sciences 132:1–74.

Bandelt, H. J., P. Forster and A. Rohl. 1999. Median-joining networks for inferring intraspecific phylogenies. Molecular Biology and Evolution 16:37–48.

Bell, K. C., D. J. Hafner, P. Leitner and M. D. Matocq. 2010. Phylogeography of the ground squirrel subgenus *Xerospermophilus* and assembly of the Mojave Desert biota. Journal of Biogeography 37:363–378.

Bertheau, C., H. Schuler, S. Krumböck, W. Arthofer and C. Stauffer. 2011. Hit or miss in phylogeographic analyses: the case of the cryptic NUMTs. Molecular Ecology Resources 11:1056–1059.

Bentancourt, J. L., T. R. Van Devender and P. S. Martin. 1990. Introduction. In: Bentancourt, J. L., T. R. Van Devender and P. S. Martin, (eds), Packrat Middens: The Last 40 000 Years of Biotic Change. University of Arizona Press, Tucson, AZ pp. 2–11.

Bertheau, C., H. Schuler, S. Krumböck, W. Arthofer and C. Stauffer. 2011 Hit or miss in phylogeographic analyses: the case of the cryptic NUMTs. Molecular Ecology Resources 11:1056–1059.

Bintanja, R., R. S. W. van de Wal and J. Oerlemans. 2005. Modelled atmospheric temperatures and global sea levels over the past million years. Nature 437:125–128.

Blomberg, S. P. and T. Garland. 2002. Tempo and mode in evolution: phylogenetic inertia, adaptation and comparative methods. Journal of Evolutionary Biology 15:899–910.

Borges, A., E. Bermingham, N. Herrera, M. Alfonzo and O. Sanjur. 2010. Molecular systematics of the neotropical scorpion genus *Tityus* (Buthidae): The historical biogeography and venom antigenis diversity of toxic Venezuela species. Toxicon 55:436–454.

Brouns, G., A. De Wulf and D. Constales. 2003. Delaunay triangulation algorithms useful for multibeam echosounding. Journal of Surveying Engineering 129:79–84.

Bryson, R. W., B. R. Riddle, M. R. Graham, B. T. Smith and L. Prendini. As old as the hills: Montane scorpions in southwestern North America reveal an ancient association between biotic diversification and landscape history. (in review)

Burt, A. 1989. Comparative methods using phylogenetically independent contrasts. Oxford Surveys in Evolutionary Biology 6:33–53.

Coddington, J. A., G. Giribet, M. S. Harvey, L. Prendini and D. E. Walter. 2004. Arachnida. In: Cracraft, J., M. Donoghue, (eds), Assembling the Tree of Life. Oxford University Press, pp. 296–318.

Cole, K. L. 1990. Reconstruction of past desert vegetation along the Colorado River using packrat middens. Palaeogeography, Palaeoclimatology, Palaeoecology 76:349–366.

Cox, B. F., J. W. Hillhouse and L. A. Owen. 2003. Pliocene and Pleistocene evolution of the Mojave River, and associated tectonic development of the Transverse Ranges and Mojave Desert, based on borehole stratigraphy studies and mapping of landforms and sediments near Victorville, California. *in* Y. Enzel, S. G. Wells and N. Lancaster, eds., Paleoenvironments and paleohydrology of the Mojave and southern Great Basin Deserts: Boulder, Colorado, Geological Society of America Special Paper 368, p. 1–42.

Crandall, K. A. and A. R. Templeton. 1996. Applications of intraspecific phylogenetics. In: Harvey, P. H., A. J. Leigh Brown, J. Maynard Smith and S. Nee, (eds), New uses for new phylogenies. Oxford University Press, pp. 81–99.

Darwin, C. 1859. On the Origin of Species. John Murray, London, UK.

Drummond, A. J. and A. Rambaut. 2007. BEAST: Bayesian evolutionary analysis by sampling trees. BMC Evolutionary Biology 7:214.

Dupanloup, I., S. Schneider and L. Excoffier. 2002. A simulated annealing approach to define the genetic structure of populations. Molecular Ecology 11:2571–2581.

Edwards, S. and S. Bensch. 2009. Looking forwards or looking backwards in avian phylogeography? A comment on Zink and Barrowclough 2008. Molecular Ecology 18:2930–2933.

Elith, J. et al. 2006. Novel methods improve prediction of species' distributions from occurrence data. Ecography 29:129–151.

Elith, J. and J. R. Leathwick. 2009. Species distribution models: ecological explanation and prediction across space and time. Annual Review of Ecology, Evolution, and Systematics 40:677–697.

Elith, J., M. Kearney and S. J. Phillips. 2010. The art of modelling range-shifting species. Methods in Ecology and Evolution 1:330–342.

Excoffier L., G. Laval and S. Schneider. 2005. ARLEQUIN ver. 3.0: an integrated software package for population genetics data analysis. Evolutionary Bioinformatics Online 1:47–50.

Excoffier, L., M. Foll and R. J. Petit. 2009. Genetic consequences of range expansions. Annual Review of Ecology and Systematics 40:481–501.

Felsenstein, J. 1985. Phylogenies and the comparative method. American Naturalist 125:1–15.

Fet, V., G. A. Polis and W. D. Sissom. 1998. Life in sandy deserts: the scorpion model. Journal of Arid Environments 39:609–622.

Fet, V., M. E. Soleglad and M. D. Barker. 2001. Phylogenetic analysis of the "hirsutus" group of the genus Hadrurus Thorell (Scorpiones: Iuridae) based on morphology and mitochondrial DNA. Pp. 139–160 *in* Fet, V. and P. A. Selden (eds). Scorpions

2001. In Memoriam Gary A. Polis. Burnham Beeches, Bucks: British Arachnological Society.

Fet, V. and M. E. Soleglad. 2008. Cladistic analysis of superfamily Iuroidea, with emphasis on subfamily Hadrurinae (Scorpiones: Iurida). Boletín de la Sociedad Entomológica Aragonesa 43:255–281.

Flesch, L. M., W. E. Holt, A. J. Haines and B. Shen-Tu. 2000. Dynamics of the Pacific–North American plate boundary in the Western United States. Science 287:834–836.

Fouquet, A., M. Vences, M. D. Salducci, A. Meyer, C. Marty, M. Blanc and A. Gilles. 2007. Revealing cryptic diversity using molecular phylogenetics and phylogeography in frogs of the *Scinax ruber* and *Rhinella margaritifera* species groups. Molecular Phylogenetics and Evolution 43:567–582.

Francke, O.F. and L. Prendini. 2008. Phylogeny and classification of the giant hairy scorpions, *Hadrurus* Thorell (Iuridae Thorell): A reappraisal. Systematics and Biodiversity 6(2): 205–223.

Frankel, K. L., J. Lee, K. Bishop, N. Dawers, P. Ganev, J. Unruh and L. Owen. 2010. Miocene–Quaternary tectonic evolution of the northern eastern California shear zone. In: Clifton, H. E. and R. V. Ingersoll, (eds.) Geologic Excursions in California and Nevada: Tectonics, Stratigraphy, and Hydrogeology: Pacific Section, SEPM (Society for Sedimentary Geology), pp. 173–231.

Fu, Y. X. 1997. Statistical tests of neutrality of mutations against population growth, hitchhiking and background selection. Genetics 147:915–925.

Galbreath, K. E., D. J. Hafner and K. R. Zamudio. 2009. When cold is better: climate-driven elevation shifts yield complex patterns of diversification and demography in an alpine specialist (American pika, *Ochotona princeps*). Evolution 63:2848–2863.

Galbreath, K. E., D. J. Hafner, K. R. Zamudio and K. Agnew. 2010. Isolation and introgression in the Intermountain West: contrasting gene genealogies reveal the complex biogeographic history of the American pika (*Ochotona princeps*). Journal of Biogeography 37:344–362.

Gantenbein, B., V. Fet, C. R. Largiadèr and A. Scholl. 1999. First DNA phylogeny of *Euscorpius* Thorell, 1876 (Scorpiones: Euscorpiidae) and its bearing on taxonomy and biogeography of this genus. Biogeographica 75(2):49–65.

Gantenbein, B. and C. R. Largiadér. 2002. *Mesobuthus gibbosus* (Scorpiones: Buthidae) on the island of Rhodes – hybridization between Ulysses' stowaways and native scorpions? Molecular Ecology 11:925–938.

Gantenbein, B., V. Fet, I. A. Gantenbein-Ritter and F. Balloux. 2005. Evidence for recombination in scorpion mitochondrial DNA (Scorpiones: Buthidae). Proceedings of the Royal Society B-Biological Sciences 272:697–704.

Gertsch, W. J. and D. M. Allred. 1965. Scorpions of the Nevada test site. Brigham Young University Science Bulletin 6(4):1–15.

Gertsch, W. J. and M. E. Soleglad. 1966. Scorpions of the *Vejovis boreus* group (genus *Paruroctonus*) in North America. American Museum Novitates 2278:1–54.

Graham, M. R., V. Oláh-Hemmings and V. Fet. 2012. Phylogeography of co-distributed dune scorpions identifies the Amu Darya River as a long-standing component of Central Asian biogeography. Zoology in the Middle East 55:95–110.

Grant, W. S. and B. W. Bowen. 1998. Shallow population histories in deep evolutionary lineages of marine fishes: insights from sardines and anchovies and lessons for conservation. The Journal of Heredity 89:415–426.

Grayson, D. K. 1993. The desert's past: a natural prehistory of the Great Basin. Smithsonian Institution Press, Washington D.C.

Gutiérrez-García, T. A. and E. Vázquez-Domínguez. 2011. Comparative Phylogeography: Designing Studies while Surviving the Process. BioScience 61(11):857–868.

Hafner, D. J. and B. R. Riddle. 2011. Boundaries and barriers of North American warm deserts: an evolutionary perspective. Palaeogeography and Palaeobiogeography: Biodiversity in Space and Time. (ed. by P. Upchurch, A. McGowan, and C. Slater), pp. 75–114. CRC Press, Boca Raton U.S.A.

Hafner, J. C. and N. S. Upham. 2011. Phylogeography of the dark kangaroo mouse, *Microdipodops megacephalus*: cryptic lineages and dispersal routes in North America's Great Basin. Journal of Biogeography 38:1077–1097.

Hall, C. A. 2002. Nearshore marine paleoclimatic regions, increasing zoogeographic provinciality, mollsucan extinctions, and paleoshorelines, California: Late Oligocene (27 Ma) to Late Pliocene (2.5 Ma). Geological Society of America Special Papers 357.

Haradon, R. M. 1985. New groups and species belonging to the nominate subgroup *Paruroctonus* (Scorpiones, Vaejovidae). Journal of Arachnology 13:19–42.

Harvey, P. H. and M. D. Pagel. 1991. The comparative method in evolutionary biology. Oxford University Press, Oxford, UK.

Hasumi, H. and S. Emori. 2004. K-1 coupled model (MIROC) description. K-1 Technical Report 1. Center for Climate System Research, University of Tokyo, Tokyo.

Henry, C. D. 2009. Uplift of the Sierra Nevada, California. Geology 37:575–576.

Hewitt, G. M. 1996. Some genetic consequences of ice ages, and their role in divergence and speciation. Biological Journal of the Linnean Society 58:247–276.

Hewitt, G. 2000. The genetic legacy of the Quaternary ice ages. Nature 405:907–913.

Hijmans, R. J., S. E. Cameron, J. L. Parra, P. G. Jones and A. Jarvis. 2005. Very high resolution interpolated climate surfaces for global land areas. International Journal of Climatology 25:1965–1978.

Hjelle, J. T. 1982. *Paruroctonus variabilis*, a new species of scorpion from California (Scorpionida: Vaejovidae). Wasmann Journal of Biology 40:98–101.

Hornsby, A. D. and M. D. Matocq. 2011. Differential regional response of the bushy-tailed woodrat (*Neotoma cinerea*) to late Quaternary climate change. Journal of Biogeography 39:289–305.

Jaeger, J. R., B. R. Riddle and D. F. Bradford. 2005. Cryptic Neogene vicariance and Quaternary dispersal of the red-spotted toad (*Bufo punctatus*): Insights on the evolution of North American warm desert biotas. Molecular Ecology 14(10):3033–3048.

Jeram, A. 1994. Carboniferous Orthosterni and their relationship to living scorpions. Palaeontology 37:513–550.

Jezkova, T., J. R. Jaeger, Z. L. Marshall and B. R. Riddle. 2009. Pleistocene impacts on the phylogeography of the desert pocket mouse (*Chaetodipus penicillatus*). Journal of Mammalogy 90:306–320.

Jezkova, T. 2010. Reconstructing species responses to past climatic changes using niche modeling and genetic data. Unpublished PhD Dissertation, University of Nevada Las Vegas, Las Vegas, U.S.A.

Jezkova, T., V. Olah-Hemmings and B. R. Riddle. 2011. Niche shifting in response to warming climate after the last glacial maximum: inference from genetic data and niche assessments in the chisel-toothed kangaroo rat (*Dipodomys microps*). Global Change Biology 17(11):3486–3502.

Ji, Y-J., D.-X. Zhang and L.-J. He. 2003. Evolutionary conservation and versatility of a new set of primers for amplifying the ribosomal internal transcribed spacer regions in insects and other invertebrates. Molecular Ecology Notes 3:581–585.

Jiménez-Valverde, A. and J. M. Lobo. 2007. Threshold criteria for conversion of probability of species presence to either-or presence-absence. Acta Oecologica – International Journal of Ecology 31:361–369.

Jones, K. B. 1995. Phylogeography of the desert horned lizard (*Phrynosoma platyrhinos*) and the short-horned lizard (*Phrynosoma douglassi*): patterns of divergence and diversity. PhD Thesis, University of Nevada, Las Vegas, U.S.A.

Jones, C. H., G. L. Farmer and J. Unruh. 2004. Tectonics of Pliocene removal of lithosphere of the Sierra Nevada, California: Geological Society of America Bulletin 116:1408–1422.

Kerdelhue, C., L. Zane, M. Simonato, P. Salvato, J. Rousselet, A. Roques and A. Battisti. 2009. Quaternary history and contemporary patterns in a currently expanding species. BMC Evolutionary Biology 9:14.

Koizumi, I., N. Usio, T. Kawai, N. Azuma and R. Masuda. 2012. Loss of Genetic Diversity Means Loss of Geological Information: The Endangered Japanese Crayfish Exhibits Remarkable Historical Footprints. PLoS ONE 7(3): e33986. doi:10.1371/journal.pone.0033986

Köhler, F. and M. Glaubrecht. 2010. Uncovering an overlooked radiation: molecular phylogeny and biogeography of Madagascar's endemic river snails (Caenogastropoda: Pachychilidae: *Madagasikara* gen. nov.). Biological Journal of the Linnean Society 99:867–894.

Leaché, A. D. and D. G. Mulcahy. 2007. Phylogeny, divergence times and species limits of spiny lizards (*Sceloporus magister* species group) in western North American deserts and Baja California. Molecular Ecology 16:5216–5233.

Librado, P. and J. Rozas. 2009. DnaSP v5: a software for comprehensive analysis of DNA polymorphism data. Bioinformatics 25:1451–1452.

Liu, C. R., P. M. Berry, T. P. Dawson and R. G. Pearson. 2005. Selecting thresholds of occurrence in the prediction of species distributions. Ecography 28:385–393.

Losos, J. B. 2008. Phylogenetic niche conservatism, phylogenetic signal and the relationship between phylogenetic relatedness and ecological similarity among species. Ecology Letters 11:995–1003.

MacDougall-Shackleton, S. A. and G. F. Ball. 1999. Comparative studies of sex differences in the song control system of songbirds. Trends in Neurosciences 22:432–436.

Madsen, D. B., D. Rhode, D. K. Grayson, J. M. Broughton, S. D. Livingston, J. Hunt, J. Quade, D. N. Schmitt and M. W. Shaver III. 2001. Late Quaternary environmental change in the Bonneville basin, western USA. Palaeogeography, Palaeoclimatology, Palaeoecology 167:243–271.

Mantel, N. A. 1967. The detection of disease clustering and a generalized regression approach. Cancer Research 27:209–220.

Miller, M. P. 2005. Alleles In Space (AIS): computer software for the joint analysis of interindividual spatial and genetic information. Journal of Heredity 96:722–724.

Miller, M. P., M. R. Bellinger, E. D. Forsman and S. M. Haig. 2006. Effects of historical climate change, habitat connectivity, and vicariance on genetic structure and diversity across the range of the red tree vole (*Phenacomys longicaudus*) in the Pacific Northwestern United States. Molecular Ecology 15:145–159.

Mittermeier, R. A., C. G. Mittermeier, T. M. Brooks, J. D. Pilgrim, W. R. Konstant, G. A. B. de Fonseca et al. 2003. Wilderness and biodiversity conservation. Proceedings of the National Academy of Sciences USA 100:10309–10313.

Mulcahy, D. G. 2008. Phylogeography and species boundaries of the western North American Nightsnake (*Hypsiglena torquata*): revisiting the subspecies concept. Molecular Phylogenetics and Evolution 46:1095–1115.

Mulcahy, D. G., A. W. Spaulding, R. Mendelson, III and E. D. Brodie, Jr. 2006. Phylogeography of the flat-tailed horned lizard (*Phrynosoma mcallii*) and systematics of the *P. mcallii–platyrhinos* mtDNA complex. Molecular Ecology 15:1807–1826.

Murphy, R. W., T. L. Trépanier and D. J. Morafka. 2006. Conservation genetics, evolution and distinct population segments of the Mojave fringe-toed lizard, *Uma scoparia*. Journal of Arid Environments 67:226–247.

Neiswenter, S. A. and B. R. Riddle. 2011. Landscape and climatic effects on the evolutionary diversification of the *Perognathus fasciatus* species group. Journal of Mammalogy 95(5):982–993.

Nogués-Bravo, D. 2009. Predicting the past distribution of species climatic niches. Global Ecology and Biogeography 18:521–531.

Nowak, C. L., R. S. Nowak, R. J. Tausch and P. E. Wigand. 1994. Tree and shrub dynamics in the northwestern Great Basin woodland and shrubland steppe during the late Pleistocene and Holocene. American Journal of Botany 81:265–277.

Nylander, J. A. A., F. Ronquist, J. P. Huelsenbeck and J. L. Nieves-Aldrey. 2004. Bayesian phylogenetic analysis of combined data. Systematic Biology 53:47–67.

Nylander, J. A. A., J. C. Wilgenbusch, D. L. Warren and D. L. Swofford. 2008. AWTY (are we there yet?): a system for graphical exploration of MCMC convergence in Bayesian phylogenetic inference. Bioinformatics 24:581–583.

Oláh-Hemmings, V., J. R. Jaeger, M. J. Sredl, M. A. Schlaepfer, R. D. Jennings, C. A. Drost, D. F. Bradford and B. R. Riddle. 2010. Phylogeography of declining relict and lowland leopard frogs in the desert Southwest of North America. Journal of Zoology 280:343–354.

Olson, D. M. et al. 2001. Terrestrial ecoregions of the World: A new map of life on Earth. BioScience 51:1–6.

Orange, D. I. 1997. Comparative biogeography within and among four species of lizards in western North American deserts. PhD thesis, University of Nevada, Reno, NV.

Otto-Bliesner, B. L., E. C. Brady, G. Clauzet, R. Tomas, S. Levis and Z. Kothavala. 2006. Last Glacial Maximum and Holocene climate in CCSM3. Journal of Climatology 19:2526–2544.

Pearson, R. G., T. P. Dawson, P. M. Berry and P. A. Harrison. 2002. SPECIES: a spatial evaluation of climate impact on the envelope of species. Ecological Modelling 154:289–300.

Peterson, A. T., M. Papes and M. Eaton. 2007. Transferability and model evaluation in ecological niche modeling: a comparison of GARP and Maxent. Ecography 30:550–560.

Phillips, S. J., R. P. Anderson and R. E. Schapire. 2006. Maximum entropy modeling of species geographic distributions. Ecological Modelling 190:231–259.

Phillips, F. M. 2008. Geological and hydrological history of the paleo-Owens drainage since the late Miocene, In: Reheis, M. C. and R. Hershler, (eds.), Late Cenozoic Drainage History of the Southwestern Great Basin and Lower Colorado River Region: Geologic and Biotic Perspectives: Geological Society of America Special Paper 439, pp. 115–150.

Polzin, T. and S. V. Daneshmand. 2003. On Steiner trees and minimum spanning trees in hypergraphs. Operations Research Letters 31:12–20.

Polis, G. A. 1980. The effect of cannibalism on the demography and activity of a natural population of desert scorpions. Behavioral Biology and Sociobiology 7:25–35.

Polis, G. A. and S. J. McCormick. 1987. Intraguild predation and competition among desert scorpions. Ecology 68(2):332–343.

Polzin, T. and S. V. Daneshmand. 2003. On Steiner trees and minimum spanning trees in hypergraphs. Operations Research Letters 31:12–20.

Pook, C. E., W. Wuèster and R. S. Thorpe. 2000. Historical biogeography of the western rattlesnake (Serpentes: Viperidae: *Crotalus viridis*), inferred from mitochondrial DNA sequence information. Molecular Phylogenetics and Evolution 15:269–282.

Posada, D. 2008. jModelTest: phylogenetic model averaging. Molecular Biology and Evolution 25:1253–1256.

Prendini, L. 2001. Substratum specialization and speciation in southern African scorpions: the Effect Hypothesis revisited. In: Fet, V. and P. A. Selden, (eds), Scorpions 2001. In Memoriam Gary A. Polis, British Arachnological Society, Burnham Beeches, Bucks, UK, pp. 113–138.

Prendini, L., T. M. Crowe and W. C. Wheeler. 2003. Systematics and biogeography of the family Scorpionidae Latreille, with a discussion of phylogenetic methods. Invertebrate Systematics 17:185–259.

Prendini, L., P. Weygoldt and W. C. Wheeler. 2005. Systematics of the *Damon variegatus* group of African whip spiders (Chelicerata: Amblypygi): Evidence from behaviour, morphology and DNA. Organisms, Diversity and Evolution 5:203–236.

Raes, N and H. ter Steege. 2007. A null-model for significance testing of presence-only species distribution models. Ecography 30:231–259.

Randin, C. F., T. Dirnbock, S. Dullinger, N. E. Zimmermann, M. Zappa and A. Guisan. 2006. Are niche-based species distribution models transferable in space? Journal of Biogeography 33:1689–1703.

Rambaut, A. and A. J. Drummond. 2007. Tracer v1.4. Available at: http://beast.bio.ed.ac.uk/Tracer

Randin, C. F., T. Dirnbock, S. Dullinger, N. E. Zimmermann, M. Zappa and A. Guisan. 2006. Are niche-based species distribution models transferable in space? Journal of Biogeography 33:1689–1703.

Raes, N. and H. ter Steege. 2007. A null-model for significance testing of presence-only species distribution models. Ecography 30:231–259.

Redmond, K. T. 2009. Historic climate variability in the Mojave Desert. In: Webb, R. H., L. F. Fenstermaker, J. S. Heaton, D. L. Hughson, E. V. McDonald and D. M. Miller, (eds.), The Mojave Desert: Ecosystem Processes and Sustainability: University of Nevada Press.

Reheis, M.C. and T. L. Sawyer. 1997. Late Cenozoic History and Slip Rates of the Fish Lake Valley, Emigrant Peak, and Deep Springs Fault Zones, Nevada and California. Geological Society of America Bulletin 109(3):280–299.

Ricklefs, R. E. and J. M. Starck. 1996. Applications of phylogenetically independent contrasts: a mixed progress report. Oikos 77:167–172.

Riddle, B. R. and R. L. Honeycutt. 1990. Historical biogeography in North American arid regions: an approach using mitochondrial DNA phylogeny in grasshopper mice (genus *Onychomys*). Evolution 44:1–15.

Riddle, B. R. 1995. Molecular biogeography in the pocket mice (*Perognathus* and *Chaetodipus*) and grasshopper mice (*Onychomys*): the Late Cenozoic development of a North American aridlands rodent guild. Journal of Mammalogy 76:283–301.

Riddle, B. R., D. J. Hafner, L. F. Alexander and J. R. Jaeger. 2000. Cryptic vicariance in the historical assembly of a Baja California Peninsular Desert biota. Proceedings of the National Academy of Sciences 97(26):14438–14443.

Riddle, B. R. and D. J. Hafner. 2006. A step-wise approach to integrating phylogeographic and phylogenetic biogeographic perspectives on the history of a core North American warm deserts biota. Journal of Arid Environments 66:435–461.

Rissler, L. J., R. J. Hijmans, C. H. Graham, C. Moritz and D. B. Wake. 2006. Phylogeographic lineages and species comparisons in conservation analyses: a case study of the California herpetofauna. American Naturalist 167:655–666.

Rissler, L. J. and J. J. Apodaca. 2007. Adding more ecology into species delimitation: Ecological niche models and phylogeography help define cryptic species in the black salamander (*Aneides flavipunctatus*). Systematic Biology 56:924–942.

Rogers, A. R. and H. Harpending. 1992. Population growth makes waves in the distribution of pairwise genetic differences. Molecular Biology and Evolution 9:552–569.

Rogers, A. R. 1995. Genetic evidence for a Pleistocene population explosion. Evolution 49:608–615.

Rogers, A. R. and H. Harpending. 1992. Population growth makes waves in the distribution of pairwise genetic differences. Molecular Biology and Evolution 9:552–569.

Ronquist, F. and J. P. Huelsenbeck. 2003. MrBayes 3: Bayesian phylogenetic inference under mixed models. Bioinformatics 19:1572–1574.

Schulte, J. A., J. R. Macey and T. J. Papenfuss. 2006. A genetic perspective on the geographic association of taxa among arid North American lizards of the *Sceloporus magister* (squamata: iguanidae: phrynosomatidae). Molecular Phylognetics and Evolution 39:873–880.

Sinclair, E. A., R. L. Bezy, K. Bolles, J. L. Camarillo, K. A. Crandall and J. W. Sites. 2004. Testing species boundaries in an ancient species complex with deep phylogeographic history: genus *Xantusia* (Squamata: Xantusiidae). American Naturalist 164:396–414.

Soleglad, M.E. 1976. The taxonomy of the genus *Hadrurus* based on chela trichobothria (Scorpionida: Vejovidae). Journal of Arachnology 3:113–134.

Spaulding, A. W. 1990. Vegetational and climatic development of the Mojave Desert: The last glacial maximum to the Present. In: Packrat middens: The last 40,000 years of biotic change (eds. Betancourt, J. L., T. T. Van Devender and P. S. Martin), pp. 200–239. The University of Arizona Press, Tucson, AZ, USA.

Stahnke, H. L. 1966. Some aspects of scorpion behavior. Bulletin of the Southern California Academy of Sciences 65:65–80.

Stahnke, H. L. 1972. UV light, a useful field tool. Bioscience 22:604–607.

Stephens, M., N. J. Smith and P. Donnelly. 2001. A new statistical method for haplotype reconstruction from population data. American Journal of Human Genetics 68:978–989.

Stephens, M. and P. Donnelly. 2003. A comparison of Bayesian methods for haplotype reconstruction from population genotype data. American Journal of Human Genetics 73:1162–1169.

Stockli, D. F., T. A. Dumitru, M. O. McWilliams and K. A. Farley. 2003. Cenozoic tectonic evolution of the White Mountains, California and Nevada. Geological Society of America Bulletin 115:788–816.

Thomas, S. M. and M. Hedin. 2008. Multigenic phylogeographic divergence in the paleoendemic southern Appalachian opilionid *Fumontana deprehendor* Shear (Opiliones, Laniatores, Triaenonychidae). Molecular Phylogenetics and Evolution 46:645–658.

Thompson, R. S. 1990. Late Quaternary vegetation and climate in the Great Basin. In: Betancourt, J. L., T. R. Van Devender and P. S. Martin, (Eds.), Packrat middens: the last 40,000 years of biotic change, Tucson, AZ: University of Arizona Press, AZ, pp. 167–199.

Thompson, R. S. and K. H. Anderson. 2000. Biomes of western North America at 18 000, 6000 and 0 14C yr bp reconstructed from pollen and packrat midden data. Journal of Biogeography 27:555–584.

Thuiller, W., L. Brotons, M. B. Araujo and S. Lavorel. 2004. Effects of restricting environmental range of data to project current and future species distributions. Ecography 27:165–172.

Vink, C. J., S.M. Thomas, P. Paquin, C. Hayashi and M. Hedin. 2005. The effects of preservatives and temperatures on arachnid DNA. Invertebrate Systematics 19:99–104.

Wakabayashi, J. and T. L. Sawyer. 2001. Stream incision, tectonics, uplift, and evolution of topography of the Sierra Nevada, California: The Journal of Geology, v. 109:539–562.

Walteri, E. and R. P. Guralnick. 2008. Ecological niche modelling of montane mammals in the Great Basin, North America: examining past and present connectivity of species across basins and ranges. Journal of Biogeography 36(1):148–161.

Wang, Q., S. Li,R. Wang and P. Paquin. 2008. Phylogeographic analysis of Pimoidae (Arachnida: Araneae) inferred from mitochondrial cytochrome c oxidase subunit I and nuclear 28S rRNA gene regions. Journal of Zoological Systematics and Evolutionary Research 46:96–104.

Warrick, J. A. and L. A. Mertes, L. A. K. 2009. Sediment yield from the tectonically active semiarid western transverse ranges of California. Geological Society of America Bulletin 121:1054–1070.

Waters, J. M. 2011. Competitive exclusion: phylogeography's 'elephant in the room'? Molecular Ecology 20:4388–4394.

Watson, D. F. and G. M. Philip. 1985. A refinement of inverse distance weighted interpolation. Geo-Processing 2:315–327.

Watson, D. F. 1992. Contouring: a guide to the analysis and display of spatial data. Pergamon Press, New York, NY.

Webb, T. III and P. J. Bartlein. 1992. Global changes during the last three million years: climate controls and biotic responses. Annual Review of Ecology and Systematics 23:141–173.

Williams, S. C. 1970. A systematic revision of the giant hairy scorpion genus *Hadrurus*. Occasional Papers of the California Academy of Sciences 87:1–62.

Wilson, J. S. and J. P. Pitts. 2010. Illuminating the lack of consensus among descriptions of earth history data in the North American deserts: a resource for biologists. Progress in Physical Geography 34(4):419–441.

Wood, D. A., R. N. Fisher and T. W. Reeder. 2008. Novel patterns of historical isolation, dispersal, and secondary contact across Baja California in the Rosy Boa (*Lichanura trivirgata*). Molecular Phylogenetics and Evolution 46:484–502.

Zhang, D.-X. and G. M. Hewitt. 1997. Assessment of the universality and utility of a set of conserved mitochondrial primers in insects. Insect Molecular Biology 6:143–150.

Zink, R. M. and G. F. Barrowclough. 2008. Mitochondrial DNA under siege in avian phylogeography. Molecular Ecology 17:2107–2121.

VITA

Graduate College
University of Nevada, Las Vegas

Matthew R. Graham

Degrees:

Bachelor of Science, Biological Sciences 2002
Marshall University

Master of Science, Biological Sciences 2005
Marshall University

Select Publications in Scorpiology:

Graham, M. R., R. F. Ayrey and R. B. Bryson (in press) Multivariate methods support the distinction of a new highland *Vaejovis* (Scorpiones: Vaejovidae) from the Sierra de los Ajos, Mexico. Journal of Arachnology

Webber, M. M., M. R. Graham and J. R. Jaeger. 2012. *Wernerius inyoensis*, an elusive new scorpion from the Inyo Mountains of California (Scorpiones: Vaejovidae). ZooKeys 177:1–13.

Graham, M. R., V. Oláh-Hemmings and V. Fet. 2012. Phylogeography of co-distributed dune scorpions identifies the Amu Darya River as a long-standing component of Central Asian biogeography. Zoology in the Middle East 55:95–110.

Graham, M. R. and R. W. Bryson. 2010. *Vaejovis montanus* (Scorpiones: Vaejovidae), a new species from the Sierra Madre Occidental of Mexico. Journal of Arachnology 38:285–293.

Graham, M. R. and M. E. Soleglad. 2007. A new scorpion genus representing a primitive taxon of tribe Stahnkeini, with a description of a new species from Sonora, Mexico (Scorpiones: Vaejovidae). Euscorpius 57:1–13.

Graham, M. R. 2007. Sky Island *Vaejovis*: two new species and a redescription of *V. vorhiesi* Stahnke (Scorpiones: Vaejovidae). Euscorpius 51:1–14.

Teruel, R., V. Fet and M. R. Graham. 2006. The first mitochondrial DNA phylogeny of Cuban Buthidae (Scorpiones: Buthoidea). Boletín de la S.E.A., 39:219–226.

Fet, E. V., D. Neff, M. R. Graham and V. Fet. 2003. Metasoma of *Orthochirus* (Scorpiones: Buthidae): are scorpions evolving a new sensory organ? Revista Ibérica de Aracnologia 8:69–72.

Dissertation Title: Scorpion Phylogeography in the North American Aridlands

Dissertation Examination Committee:

Co-chair, Brett R. Riddle, Ph.D.
Co-chair, Jef R. Jaeger, Ph.D.
Committee Member, Allen Gibbs, Ph.D.
Graduate Faculty Representative, Matthew Lachniet, Ph.D.